Electronic Supplementary Material (ESI) for Physical Chemistry Chemical Physics.

Supplementary Information for Characterisation of magnetic relaxation on extremely long timescales

William J. A. Blackmore, Gemma K. Gransbury, Peter Evans, Jon G. C. Kragskow, David P. Mills,* and Nicholas F. Chilton*

Department of Chemistry, School of Natural Sciences, University of Manchester, Oxford Road, Manchester, M13 9PL, UK

E-mail: david.mills@manchester.ac.uk; nicholas.chilton@manchester.ac.uk

S1 Waveform Analysis

S1.1 2 K Data

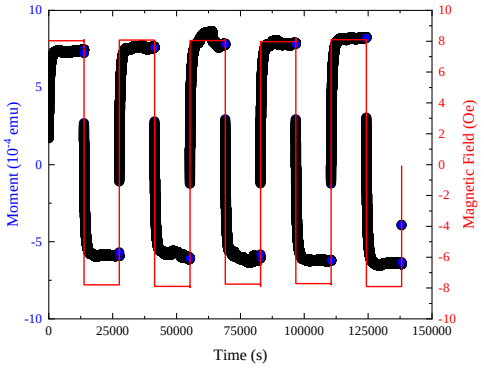

(a) 36 μHz $M(t)$ data

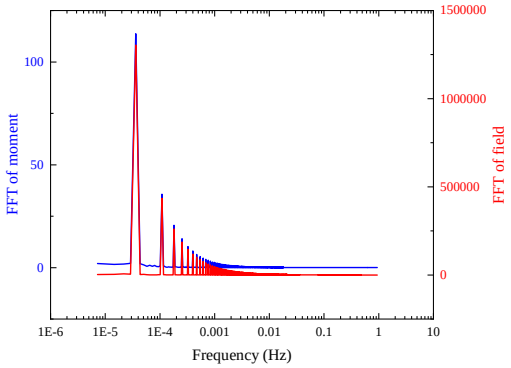

(b) 36 μHz FFT

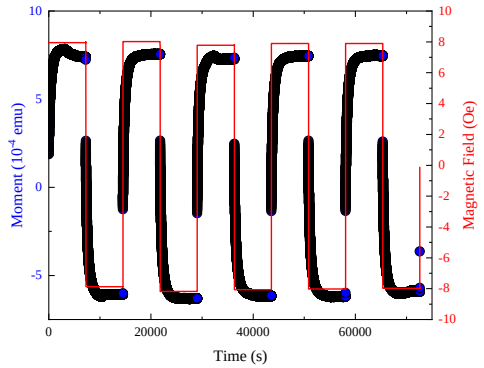

(c) 69 μHz $M(t)$ data

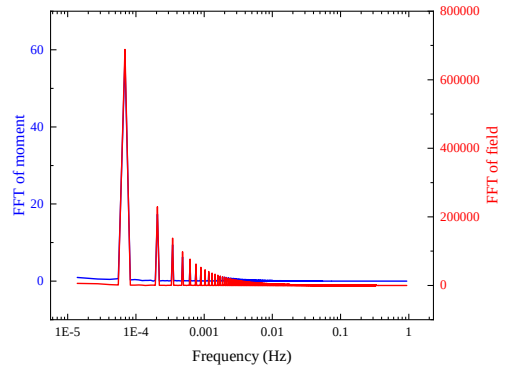

(d) 69 μHz FFT

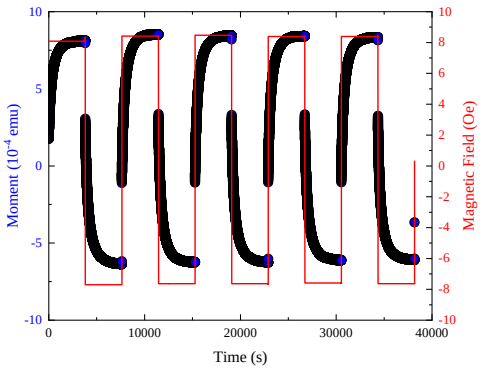

(e) 0.13 mHz $M(t)$ data

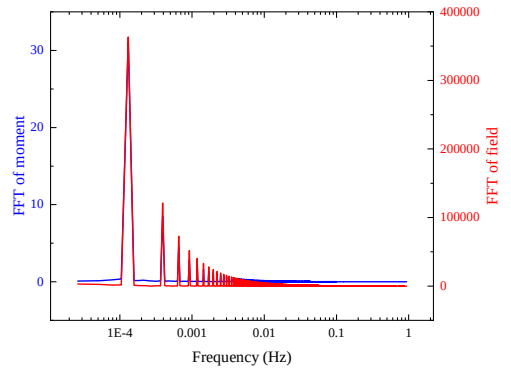

(f) 0.13 mHz FFT

Figure S1: Waveform measurements performed in zero-field at 2 K (left column) with associated Fast Fourier Transforms (FFT - right column)

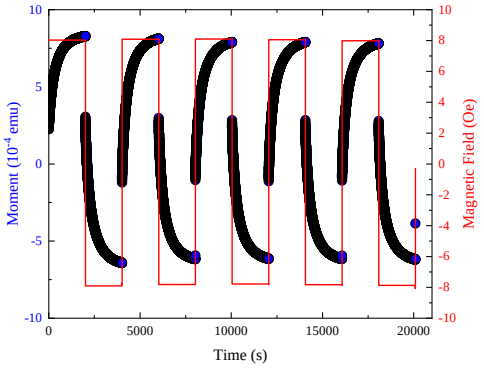

(a) 0.25 mHz $M(t)$ data

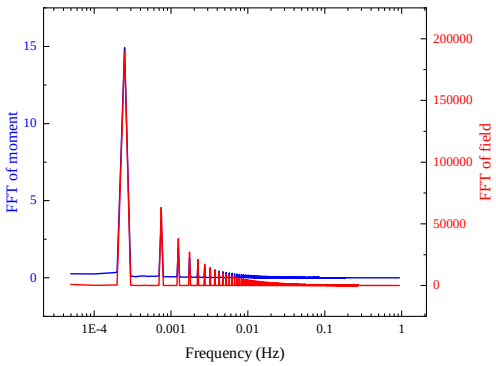

(b) 0.25 mHz FFT

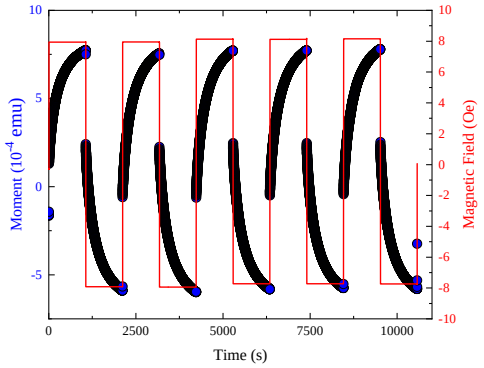

(c) 0.48 mHz $M(t)$ data

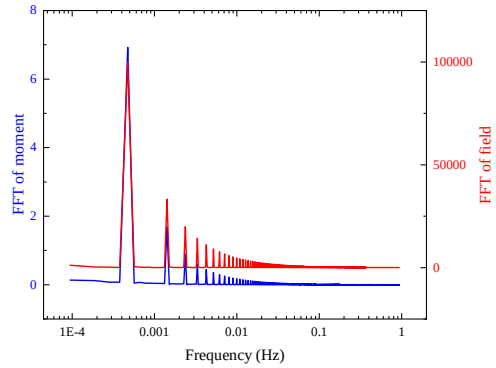

(d) 0.48 mHz FFT

Figure S2: Waveform measurements performed in zero-field at 2 K (left column) with associated Fast Fourier Transforms (FFT - right column)

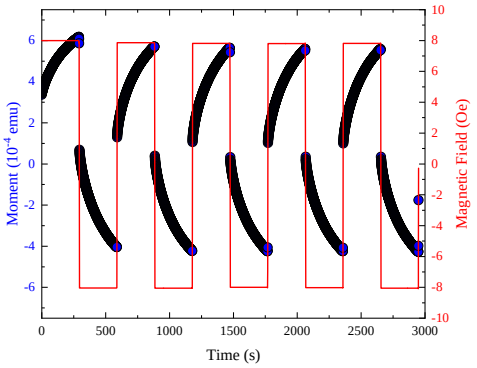

(a) 1p7 mHz $M(t)$ data

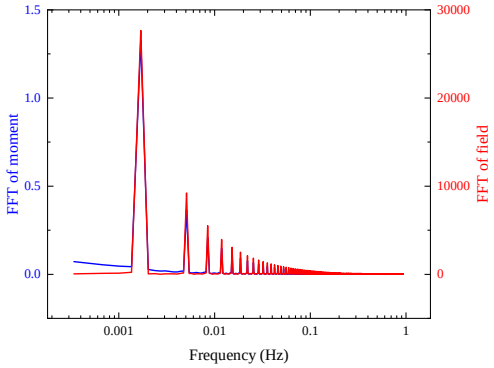

(b) 1.7 mHz FFT

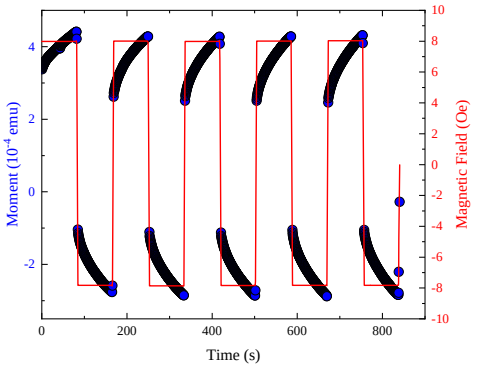

(c) 6 mHz $M(t)$ data

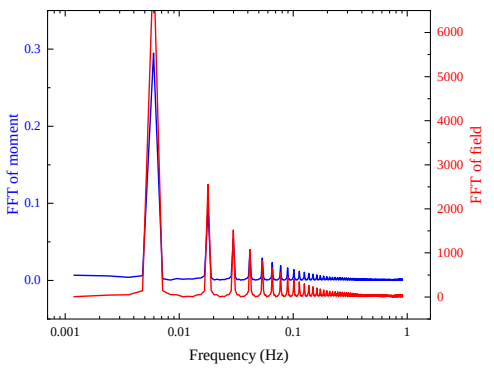

(d) 6 mHz FFT

Figure S3: Waveform measurements performed in zero-field at 2 K (left column) with associated Fast Fourier Transforms (FFT - right column)

S1.2 4 K Data

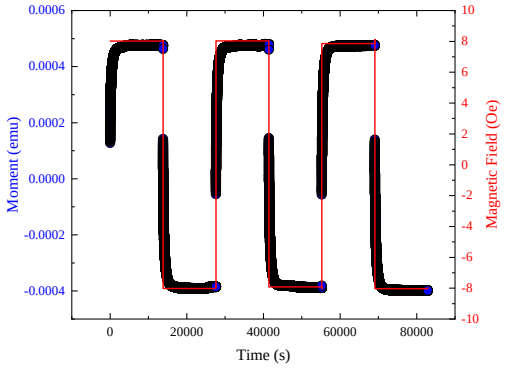

(a) 36 μHz $M(t)$ data

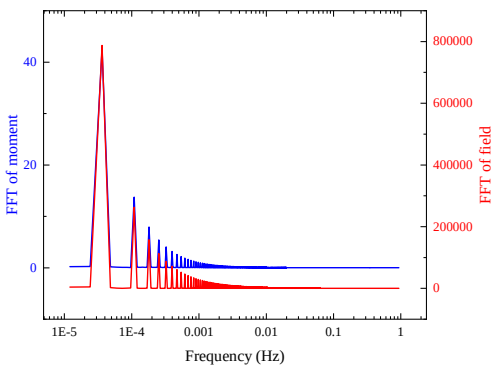

(b) 36 μHz FFT

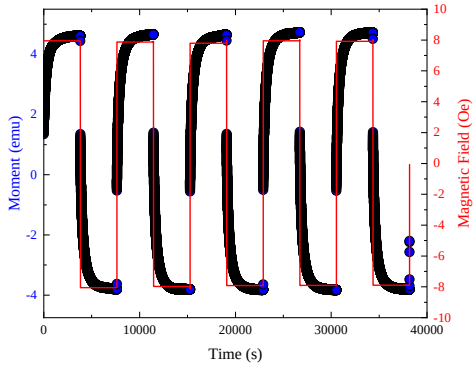

(c) 0.13 mHz $M(t)$ data

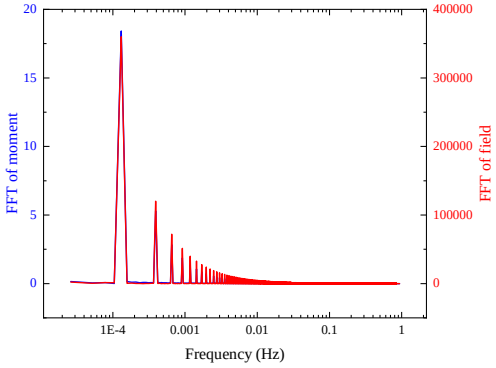

(d) 0.13 mHz FFT

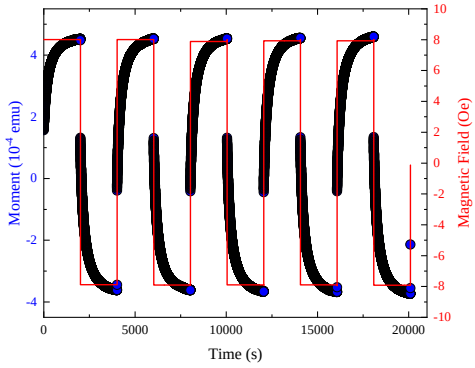

(e) 0.25 mHz $M(t)$ data

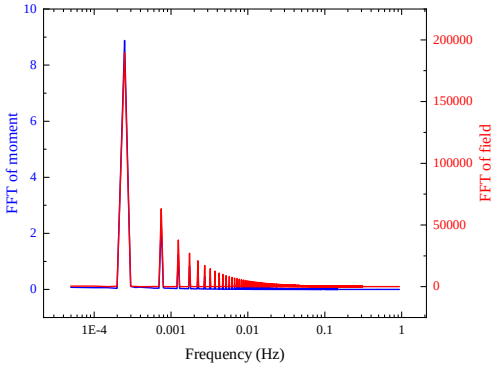

(f) 0.25 mHz FFT

Figure S4: Waveform measurements performed in zero-field at 4 K (left column) with associated Fast Fourier Transforms (FFT - right column)

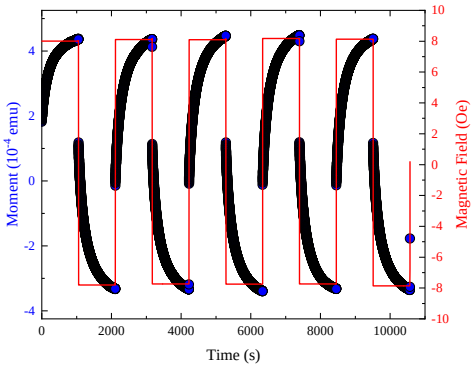

(a) 0.47 mHz $M(t)$ data

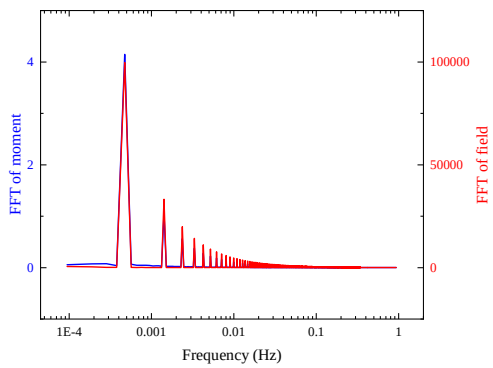

(b) 0.47 mHz FFT

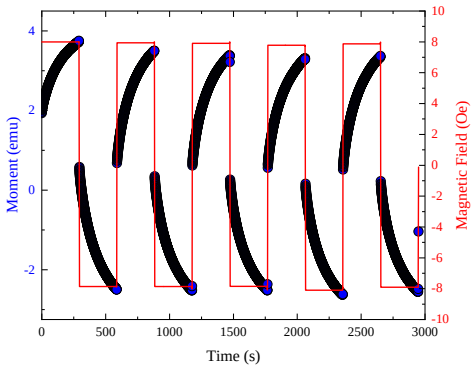

(c) 1.7 mHz $M(t)$ data

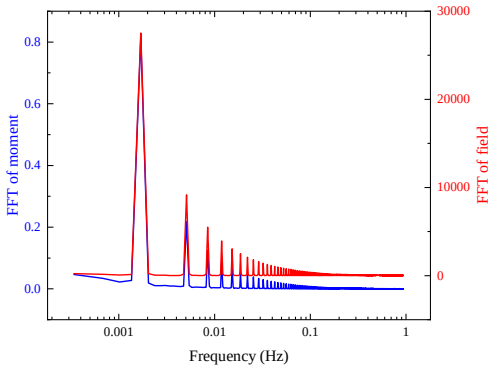

(d) 1.7 mHz FFT

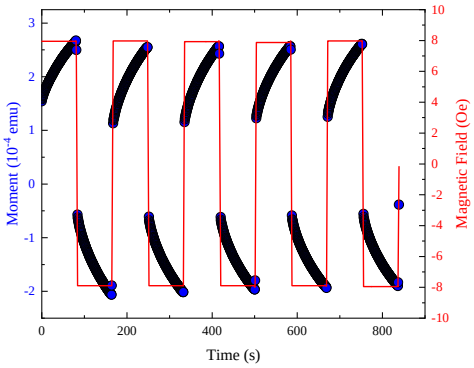

(e) 6.2 mHz $M(t)$ data

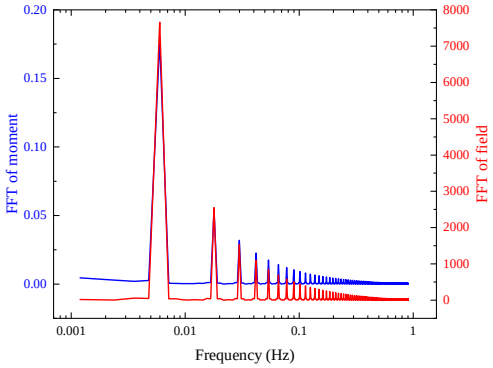

(f) 6.2 mHz FFT

Figure S5: Waveform measurements performed in zero-field at 4 K (left column) with associated Fast Fourier Transforms (FFT - right column)

S1.3 6 K Data

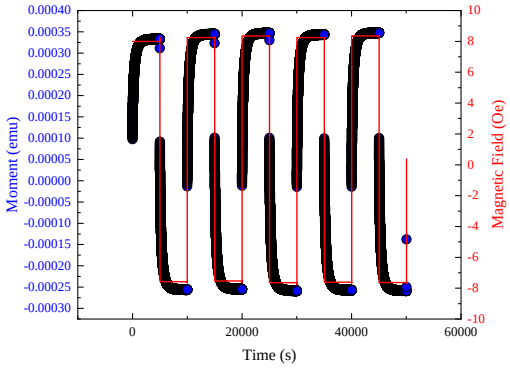

(a) 0.1 mHz $M(t)$ data

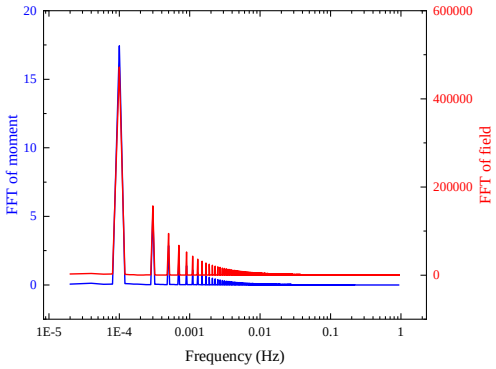

(b) 0.1 mHz FFT

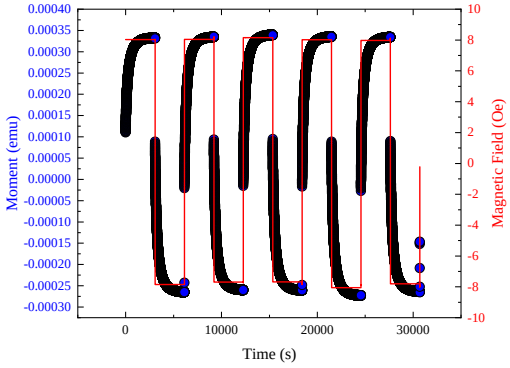

(c) 0.16 mHz $M(t)$ data

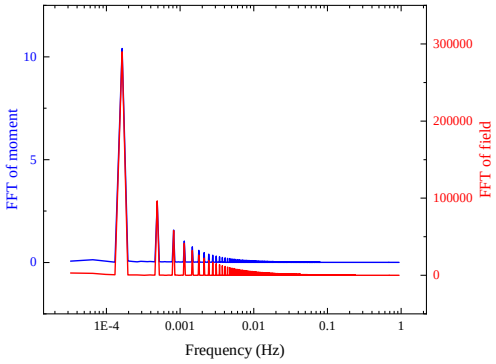

(d) 0.16 mHz FFT

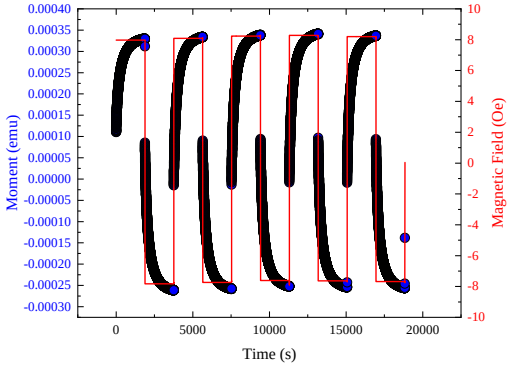

(e) 0.27 mHz $M(t)$ data

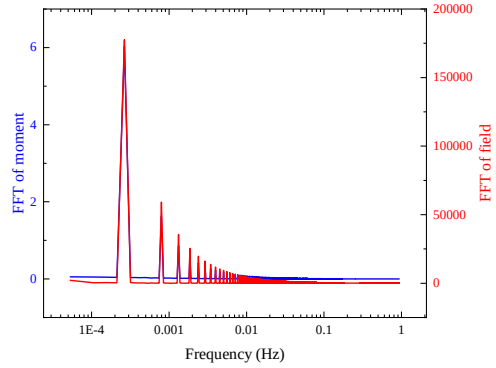

(f) 0.27 mHz FFT

Figure S6: Waveform measurements performed in zero-field at 6 K (left column) with associated Fast Fourier Transforms (FFT - right column)

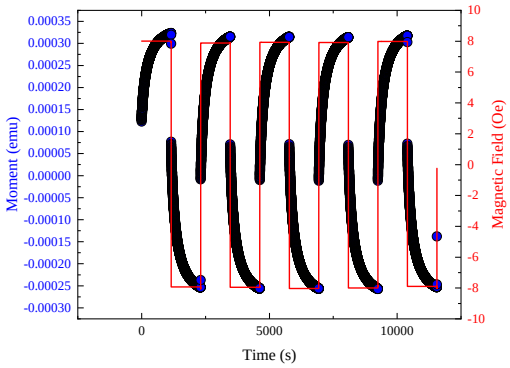

(a) 0.43 mHz $M(t)$ data

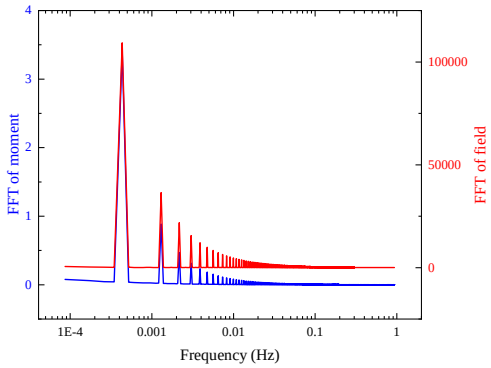

(b) 0.43 mHz FFT

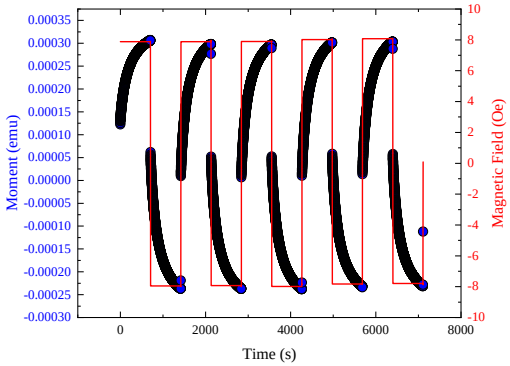

(c) 0.7 mHz $M(t)$ data

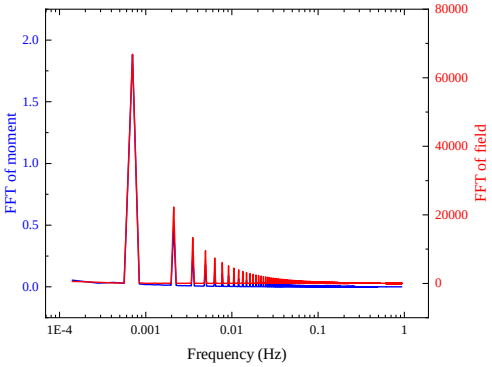

(d) 0.7 mHz FFT

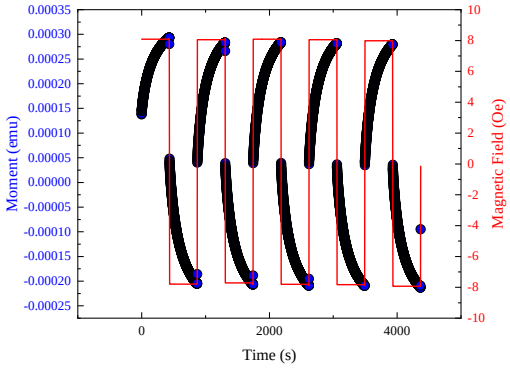

(e) 1.1 mHz $M(t)$ data

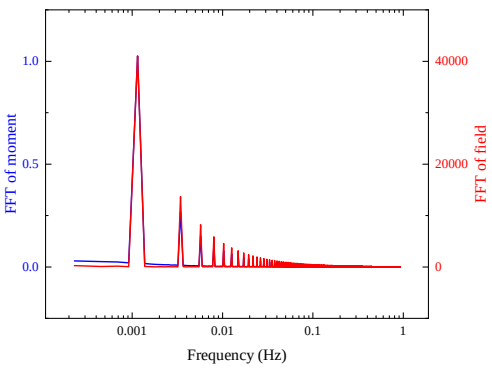

(f) 1.1 mHz FFT

Figure S7: Waveform measurements performed in zero-field at 6 K (left column) with associated Fast Fourier Transforms (FFT - right column)

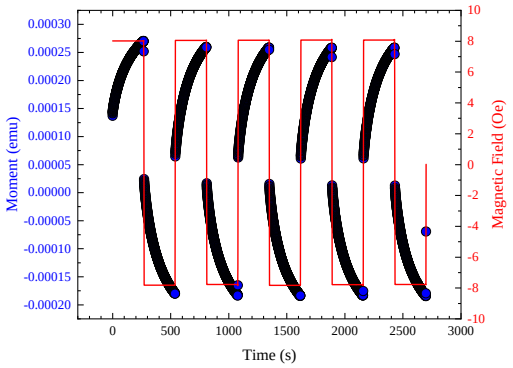

(a) 1.9 mHz $M(t)$ data

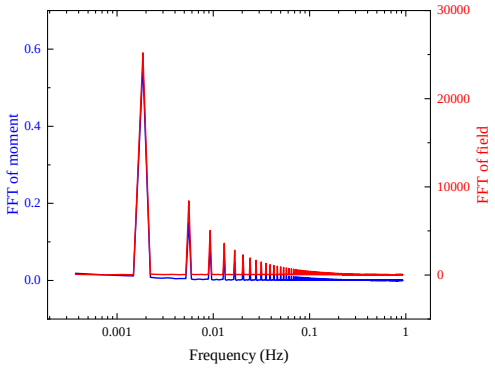

(b) 1.9 mHz FFT

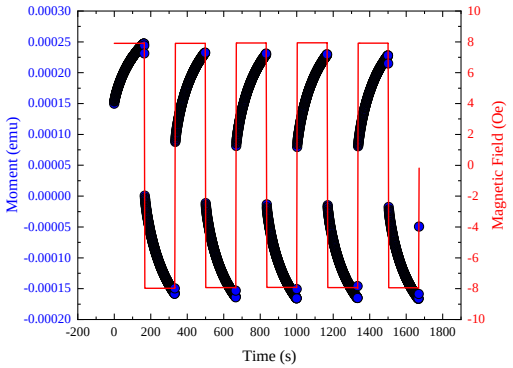

(c) 3 mHz $M(t)$ data

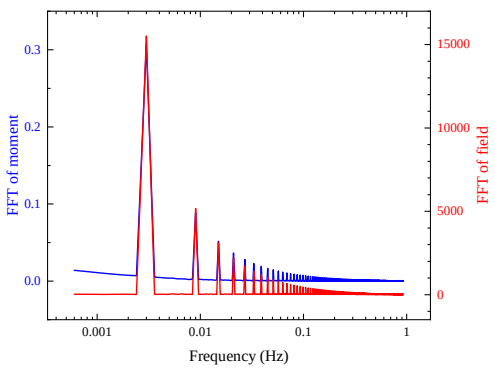

(d) 3 mHz FFT

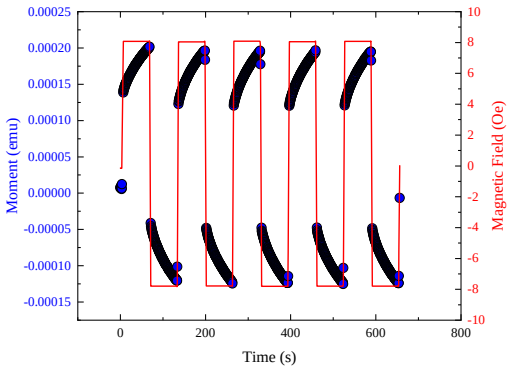

(e) 6 mHz $M(t)$ data

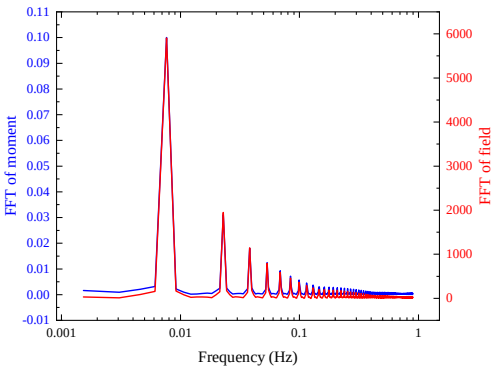

(f) 6 mHz FFT

Figure S8: Waveform measurements performed in zero-field at 6 K (left column) with associated Fast Fourier Transforms (FFT - right column)

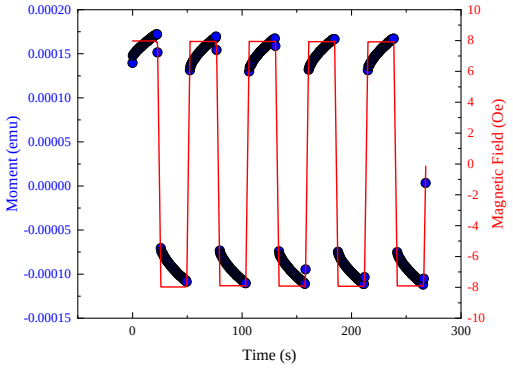

(a) 22 mHz $M(t)$ data

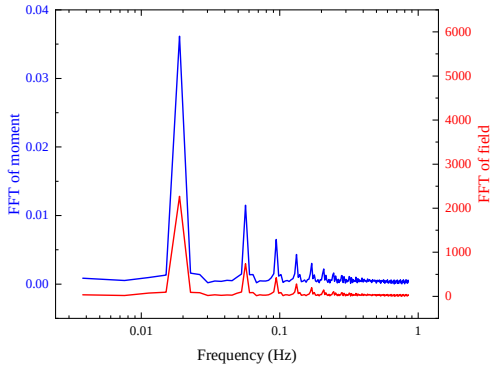

(b) 22 mHz FFT

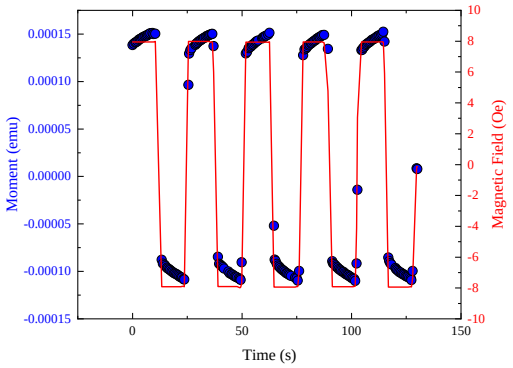

(c) 58 mHz $M(t)$ data

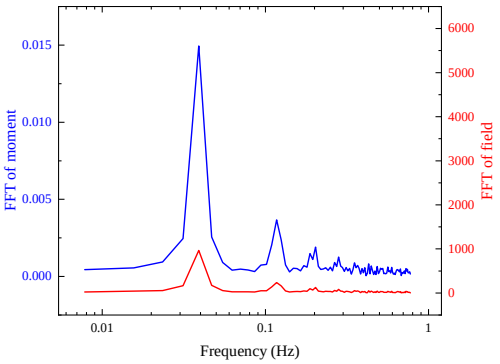

(d) 58 mHz FFT

Figure S9: Waveform measurements performed in zero-field at 6 K (left column) with associated Fast Fourier Transforms (FFT - right column)

S1.4 9 K Data

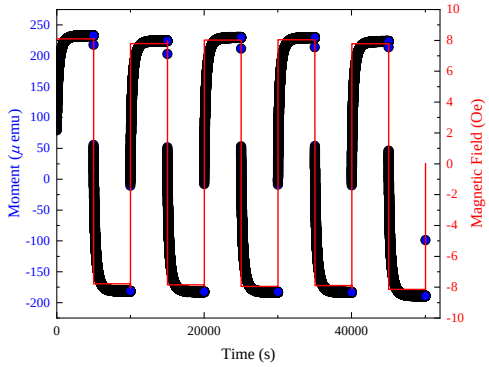

(a) 0.1 mHz $M(t)$ data

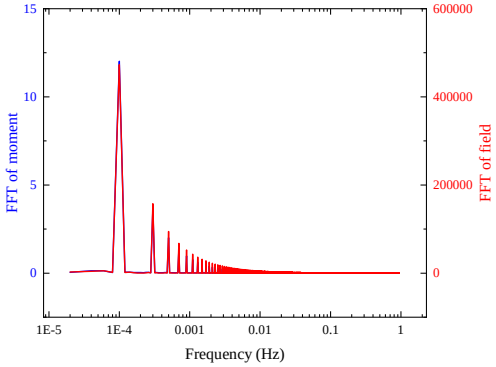

(b) 0.1 mHz FFT

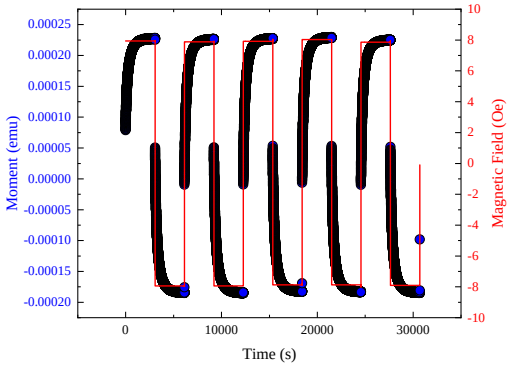

(c) 0.16 mHz $M(t)$ data

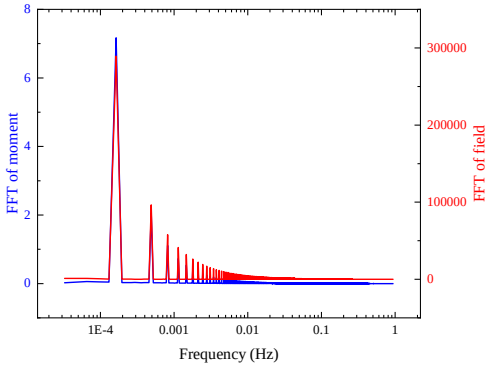

(d) 0.16 mHz FFT

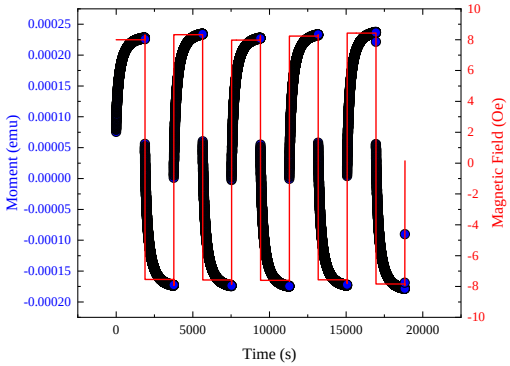

(e) 0.27 mHz $M(t)$ data

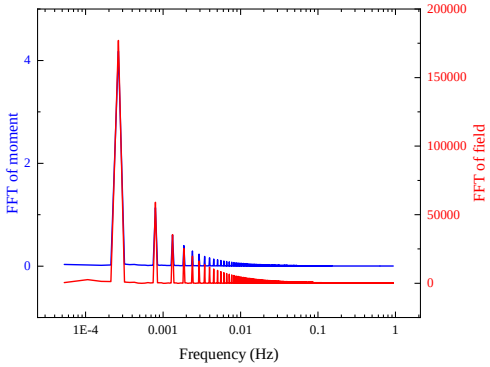

(f) 0.27 mHz FFT

Figure S10: Waveform measurements performed in zero-field at 9 K (left column) with associated Fast Fourier Transforms (FFT - right column)

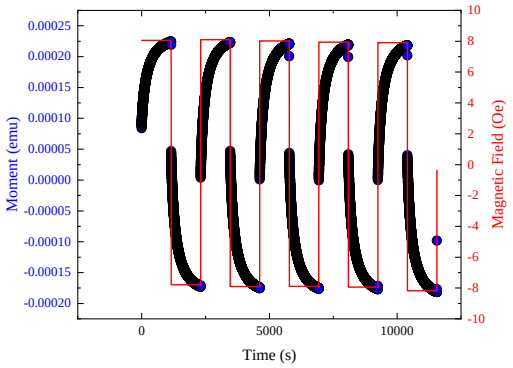

(a) 0.43 mHz $M(t)$ data

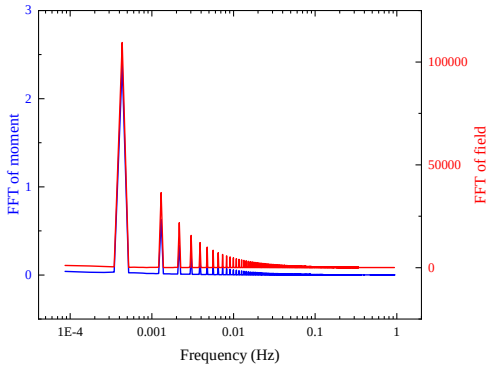

(b) 0.43 mHz FFT

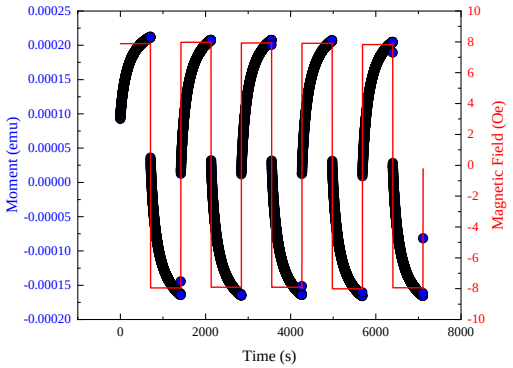

(c) 0.7 mHz $M(t)$ data

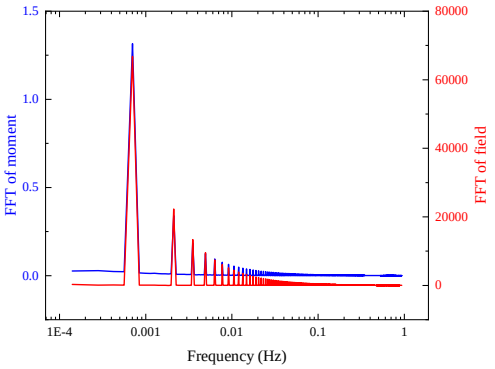

(d) 0.7 mHz FFT

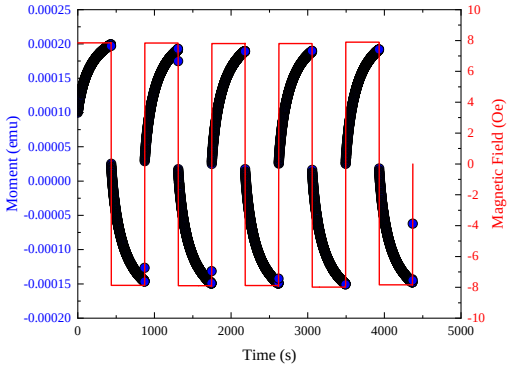

(e) 1.1 mHz $M(t)$ data

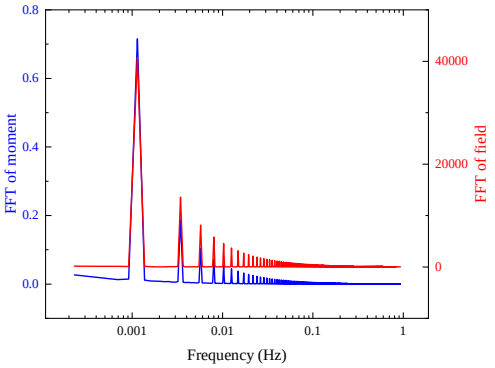

(f) 1.1 mHz FFT

Figure S11: Waveform measurements performed in zero-field at 9 K (left column) with associated Fast Fourier Transforms (FFT - right column)

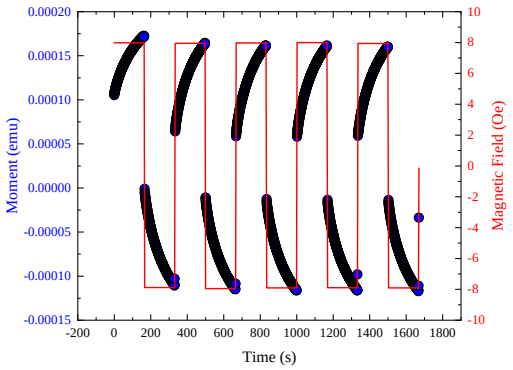

(a) 3 mHz $M(t)$ data

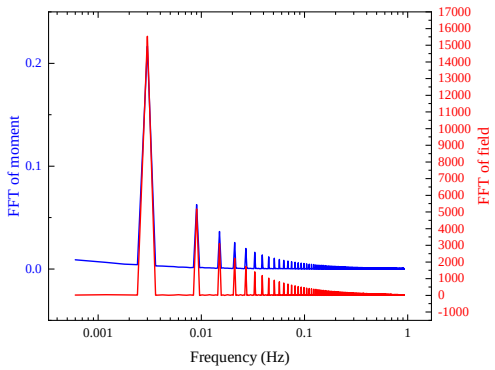

(b) 3 mHz FFT

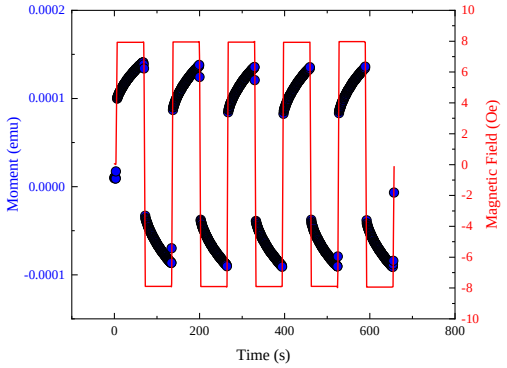

(c) 8 mHz $M(t)$ data

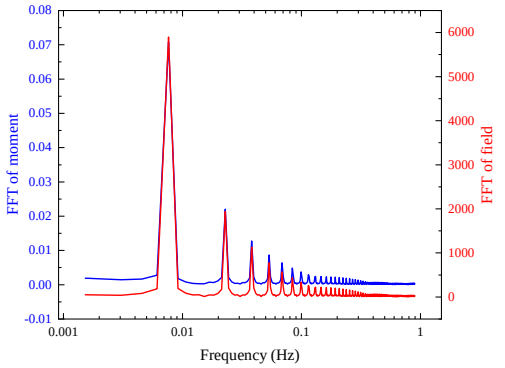

(d) 8 mHz FFT

Figure S12: Waveform measurements performed in zero-field at 9 K (left column) with associated Fast Fourier Transforms (FFT - right column)

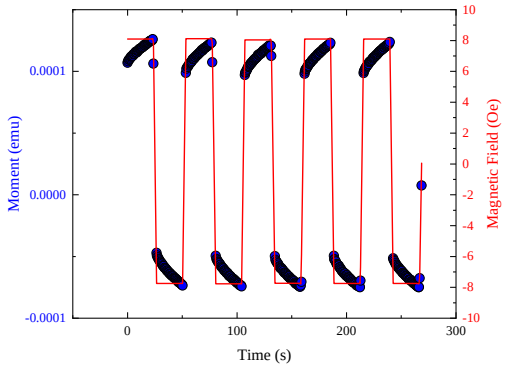

(a) 22 mHz $M(t)$ data

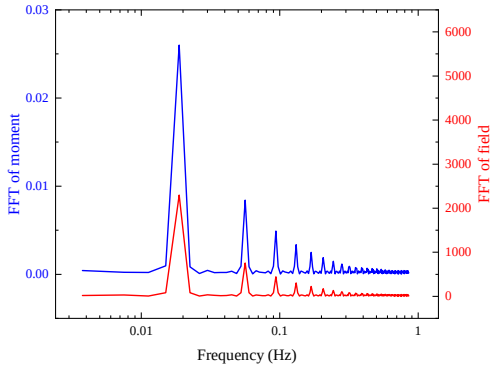

(b) 22 mHz FFT

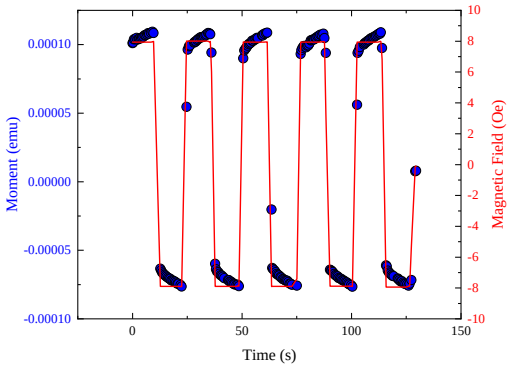

(c) 58 mHz $M(t)$ data

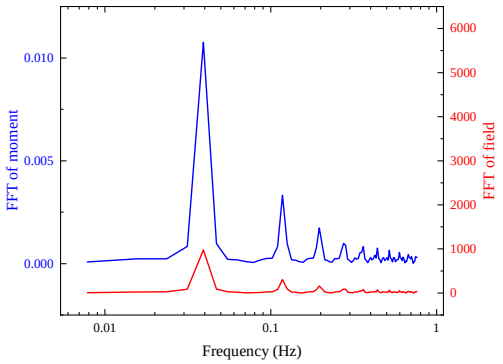

(d) 58 mHz FFT

Figure S13: Waveform measurements performed in zero-field at 9 K (left column) with associated Fast Fourier Transforms (FFT - right column)

S1.5 13 K Data

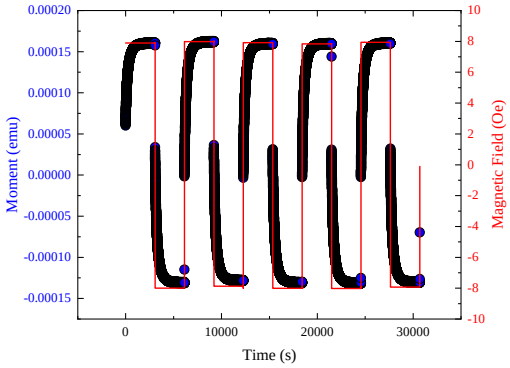

(a) 0.16 mHz $M(t)$ data

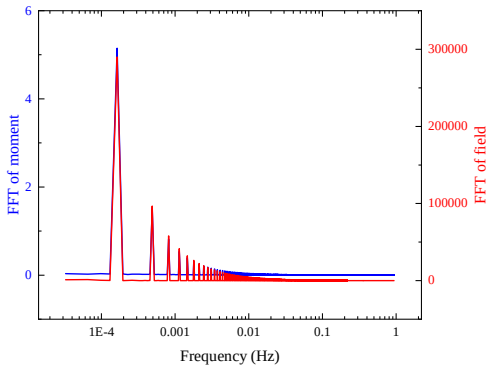

(b) 0.16 mHz FFT

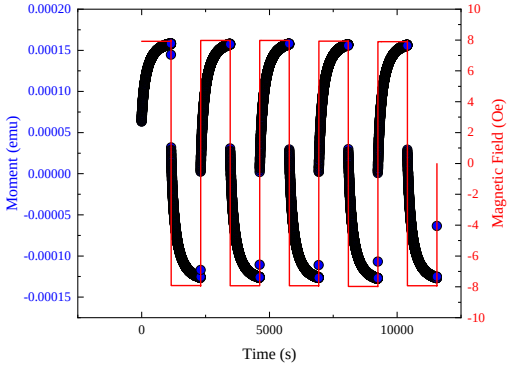

(c) 0.43 mHz $M(t)$ data

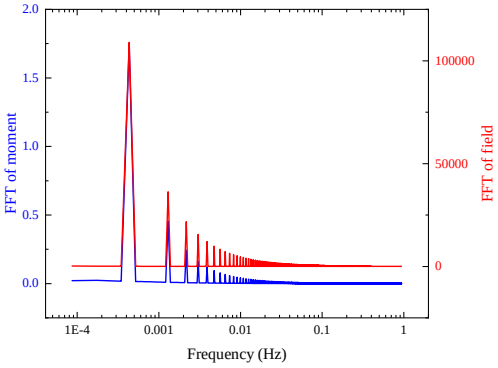

(d) 0.43 mHz FFT

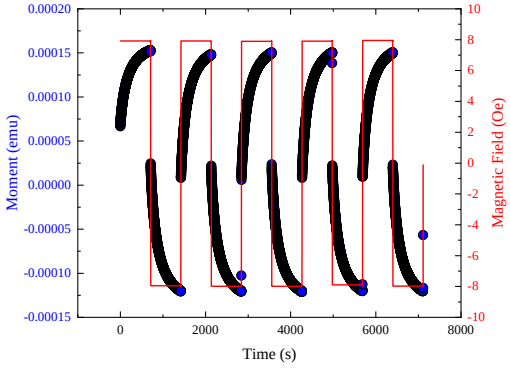

(e) 0.7 mHz $M(t)$ data

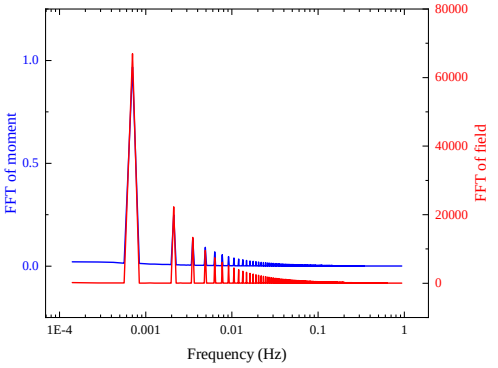

(f) 0.7 mHz FFT

Figure S14: Waveform measurements performed in zero-field at 13 K (left column) with associated Fast Fourier Transforms (FFT - right column)

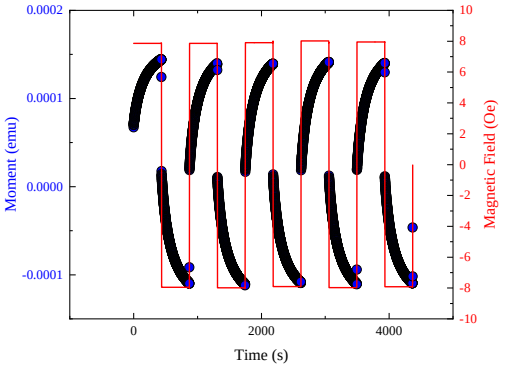

(a) 1.1 mHz $M(t)$ data

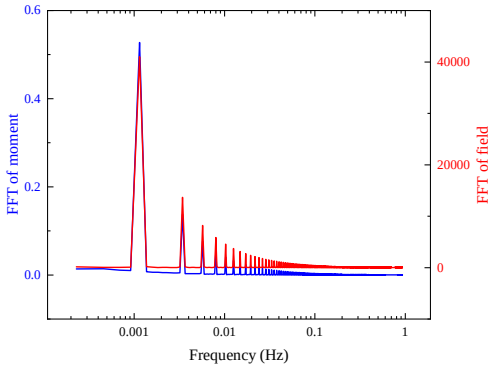

(b) 1.1 mHz FFT

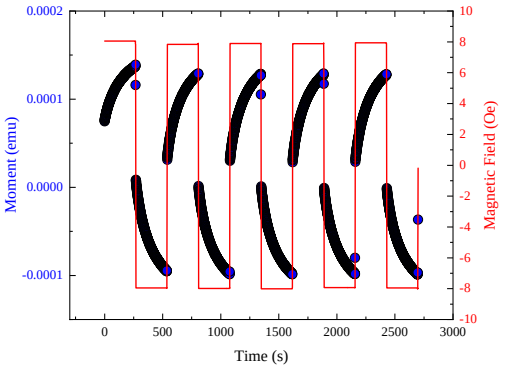

(c) 1.9 mHz $M(t)$ data

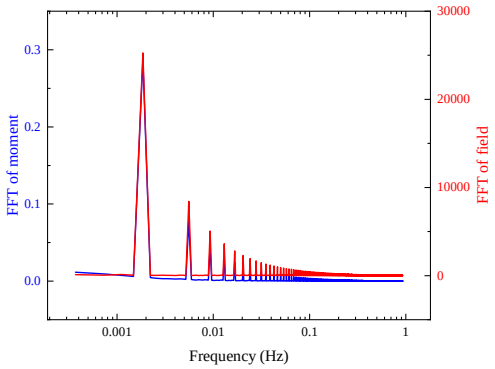

(d) 1.9 mHz FFT

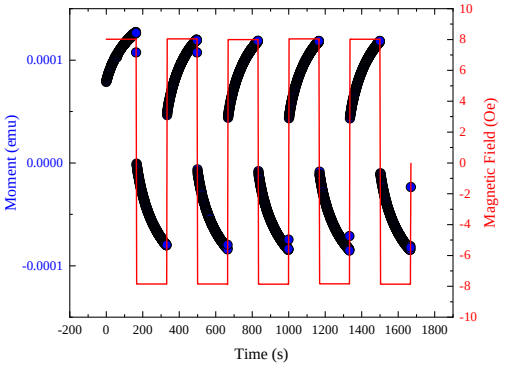

(e) 3 mHz $M(t)$ data

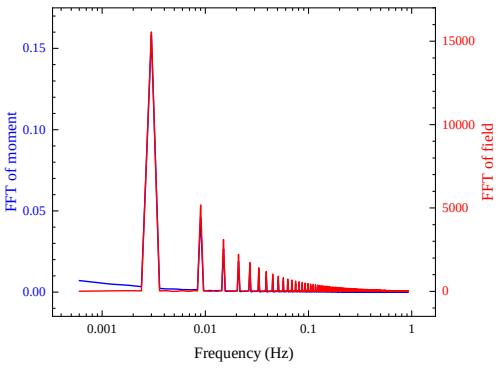

(f) 3 mHz FFT

Figure S15: Waveform measurements performed in zero-field at 13 K (left column) with associated Fast Fourier Transforms (FFT - right column)

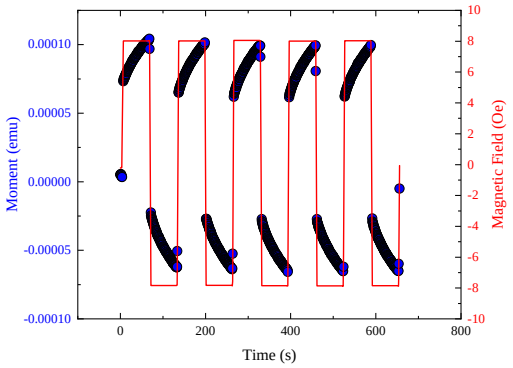

(a) 8 mHz $M(t)$ data

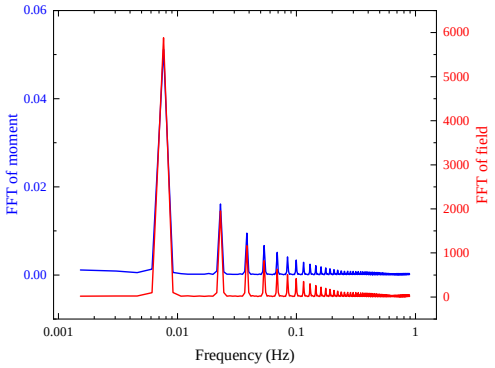

(b) 8 mHz FFT

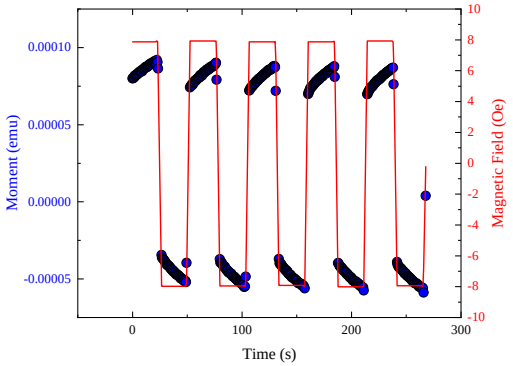

(c) 22 mHz $M(t)$ data

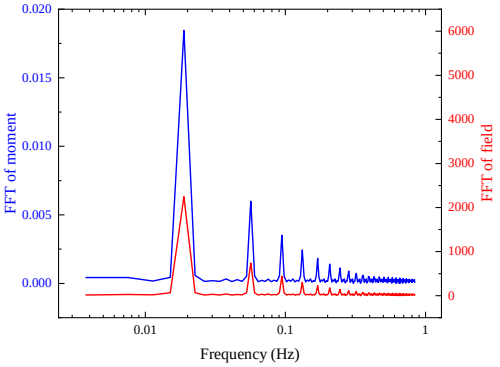

(d) 22 mHz FFT

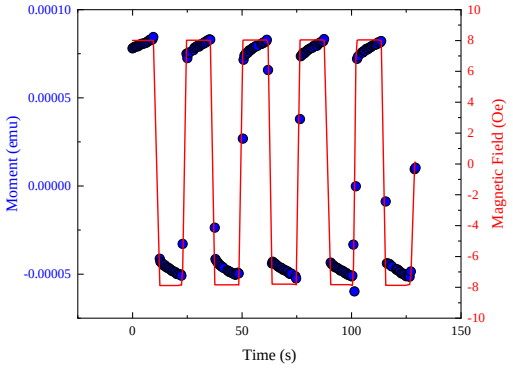

(e) 58 mHz $M(t)$ data

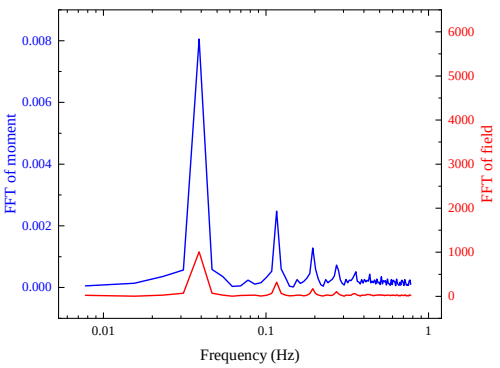

(f) 58 mHz FFT

Figure S16: Waveform measurements performed in zero-field at 13 K (left column) with associated Fast Fourier Transforms (FFT - right column)

S1.6 16 K Data

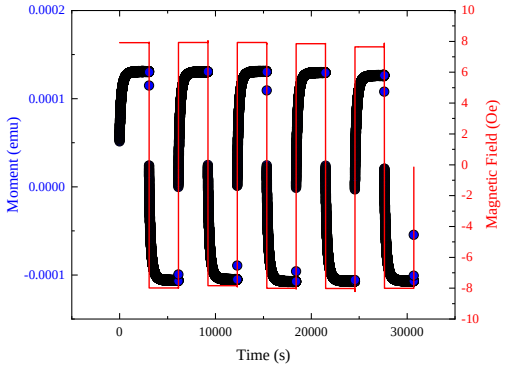

(a) 0.16 mHz $M(t)$ data

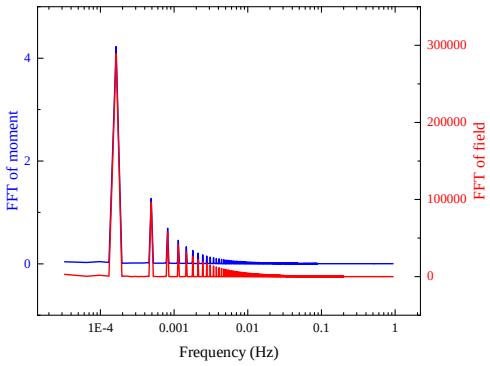

(b) 0.16 mHz FFT

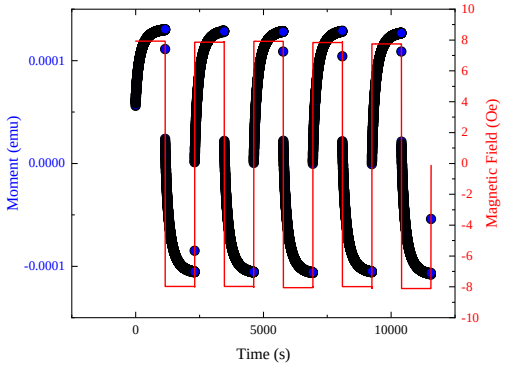

(c) 0.43 mHz $M(t)$ data

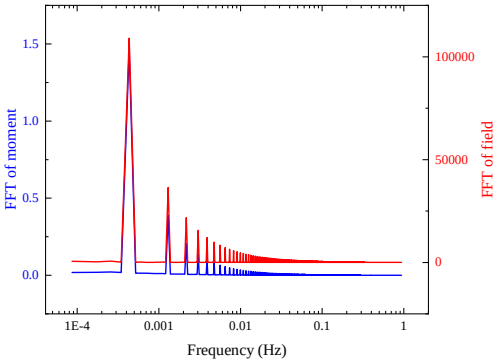

(d) 0.43 mHz FFT

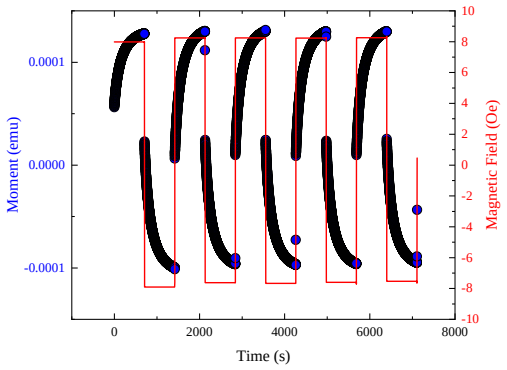

(e) 0.7 mHz $M(t)$ data

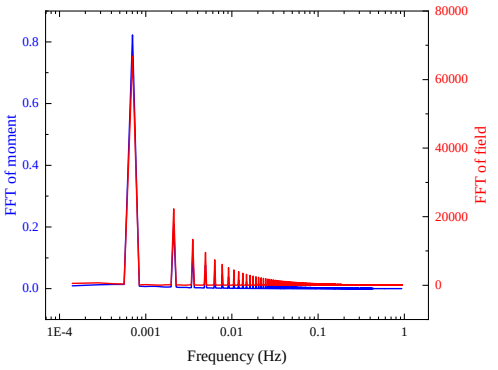

(f) 0.7 mHz FFT

Figure S17: Waveform measurements performed in zero-field at 16 K (left column) with associated Fast Fourier Transforms (FFT - right column)

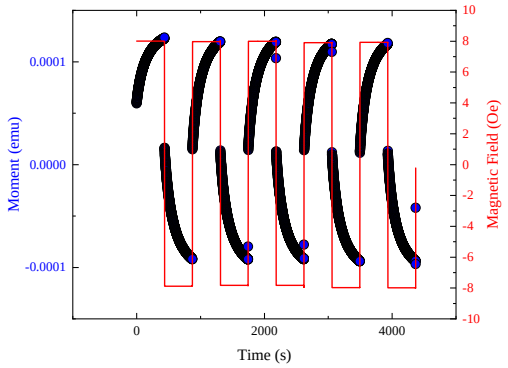

(a) 1.1 mHz $M(t)$ data

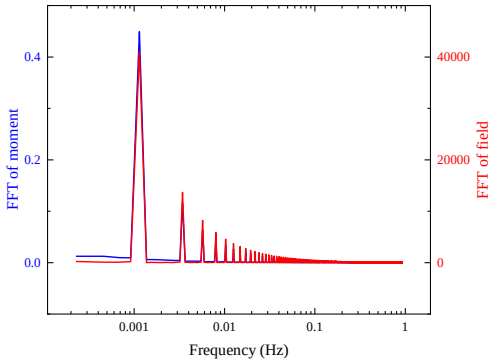

(b) 1.1 mHz FFT

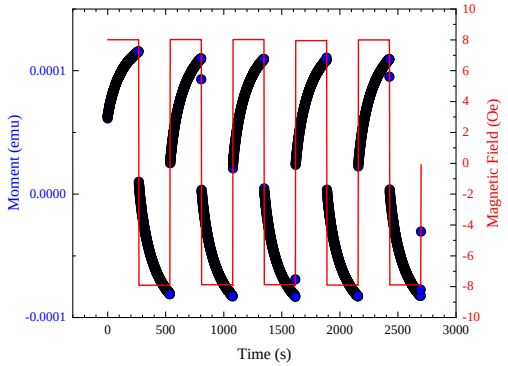

(c) 1.9 mHz $M(t)$ data

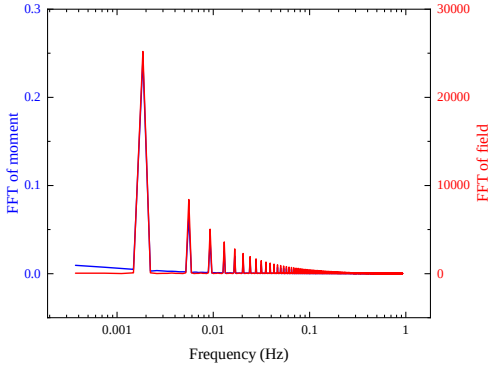

(d) 1.9 mHz FFT

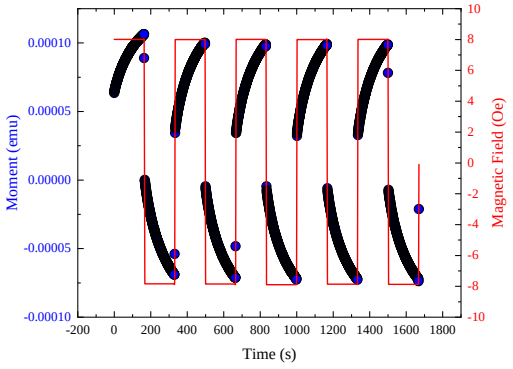

(e) 3 mHz $M(t)$ data

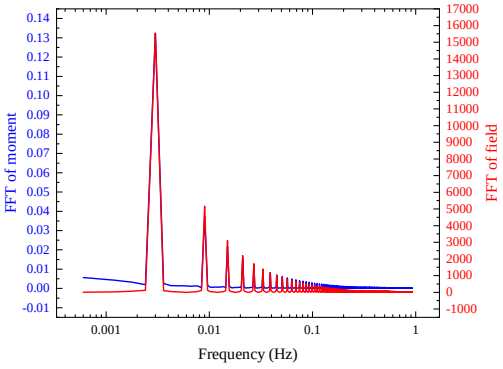

(f) 3 mHz FFT

Figure S18: Waveform measurements performed in zero-field at 16 K (left column) with associated Fast Fourier Transforms (FFT - right column)

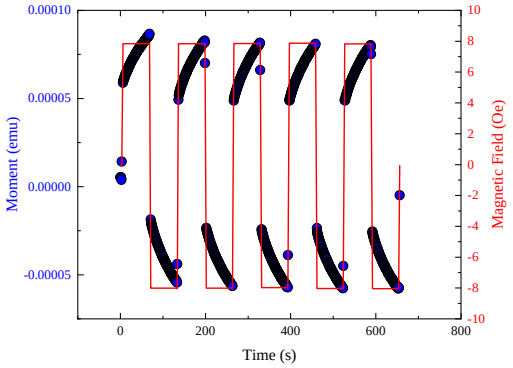

(a) 8 mHz $M(t)$ data

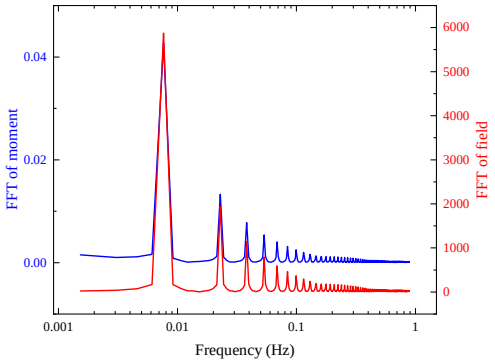

(b) 8 mHz FFT

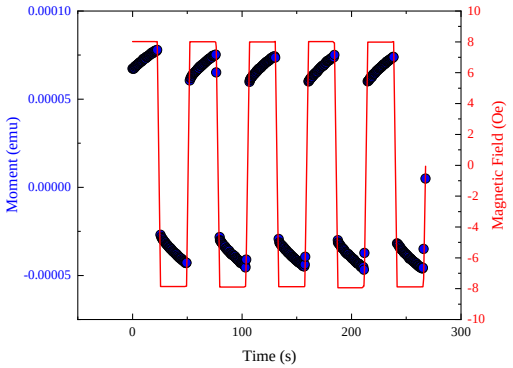

(c) 22 mHz $M(t)$ data

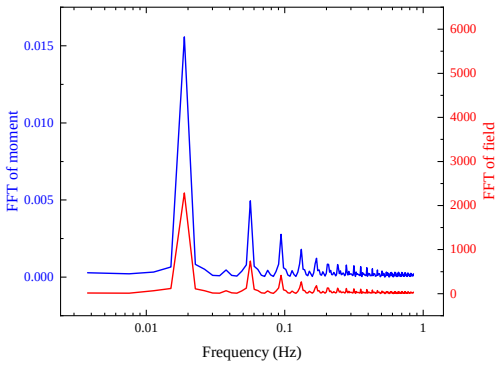

(d) 22 mHz FFT

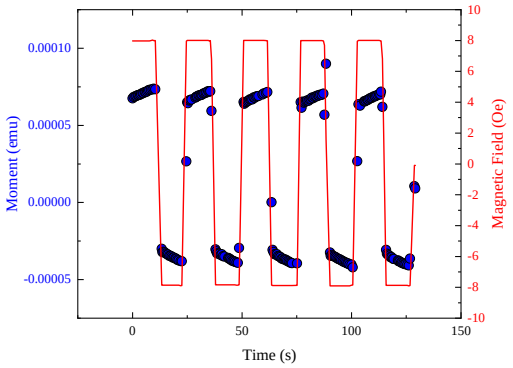

(e) 58 mHz $M(t)$ data

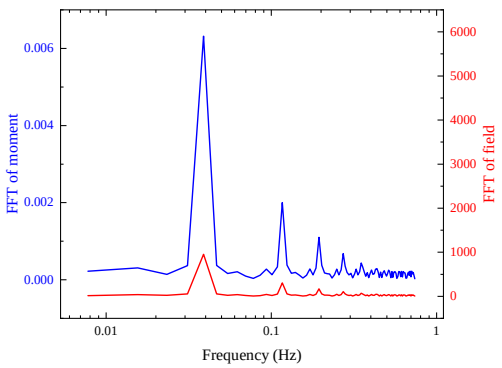

(f) 58 mHz FFT

Figure S19: Waveform measurements performed in zero-field at 16 K (left column) with associated Fast Fourier Transforms (FFT - right column)

S1.7 20 K Data

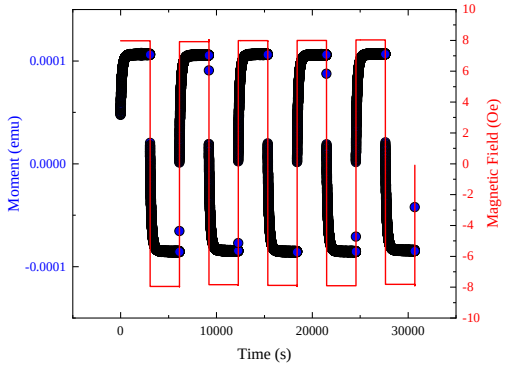

(a) 0.16 mHz $M(t)$ data

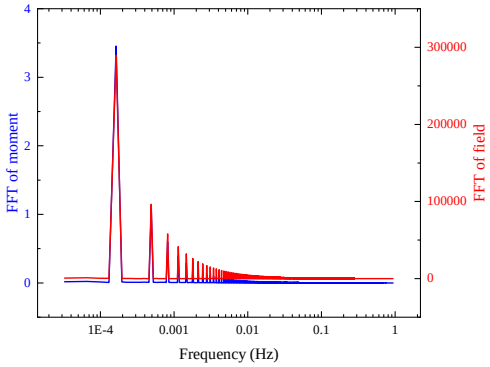

(b) 0.16 mHz FFT

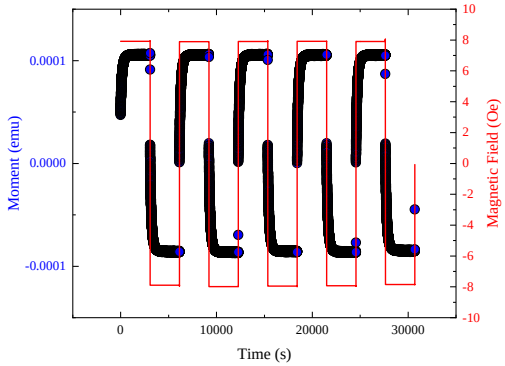

(c) 0.16 mHz $M(t)$ data

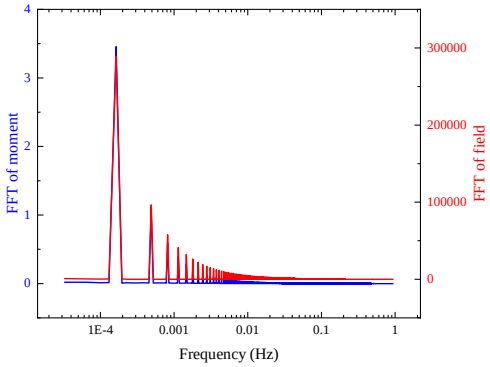

(d) 0.16 mHz FFT

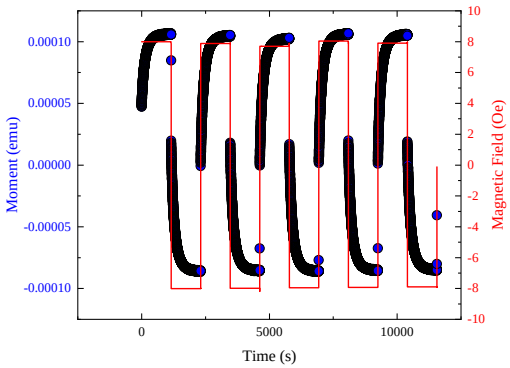

(e) 0.43 mHz $M(t)$ data

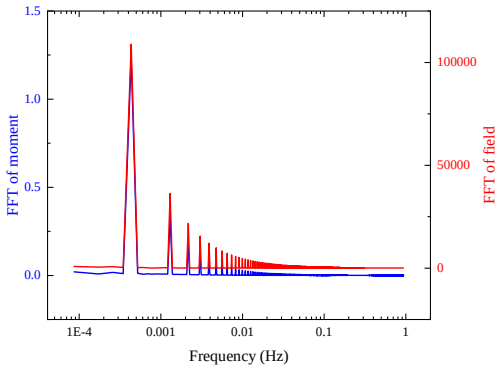

(f) 0.43 mHz FFT

Figure S20: Waveform measurements performed in zero-field at 20 K (left column) with associated Fast Fourier Transforms (FFT - right column). Two data sets were collected at this temperature, some frequencies appear twice.

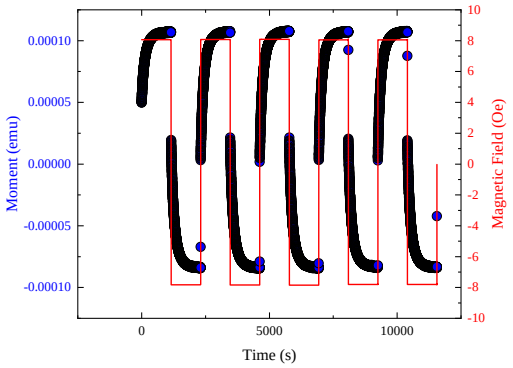

(a) 0.43 mHz $M(t)$ data

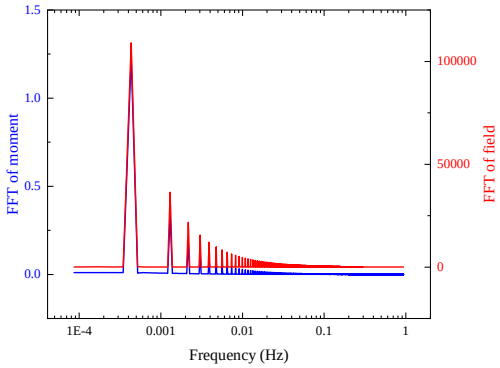

(b) 0.43 mHz FFT

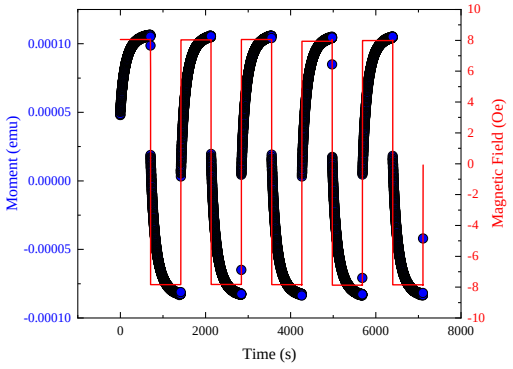

(c) 0.7 mHz $M(t)$ data

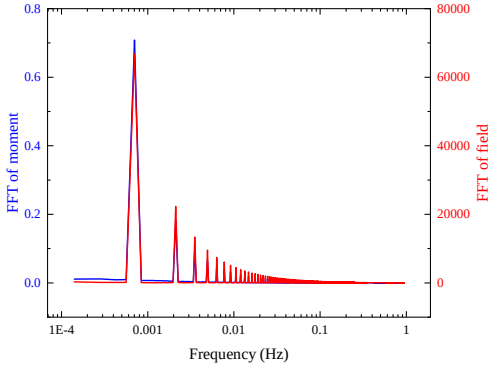

(d) 0.7 mHz FFT

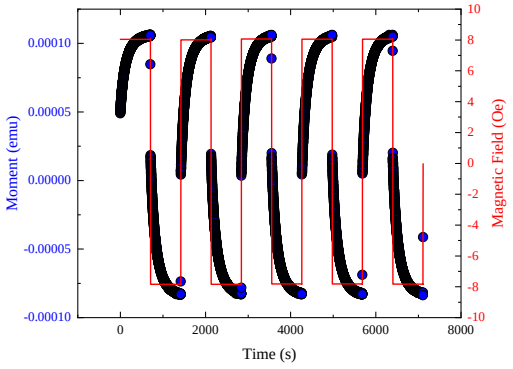

(e) 0.7 mHz $M(t)$ data

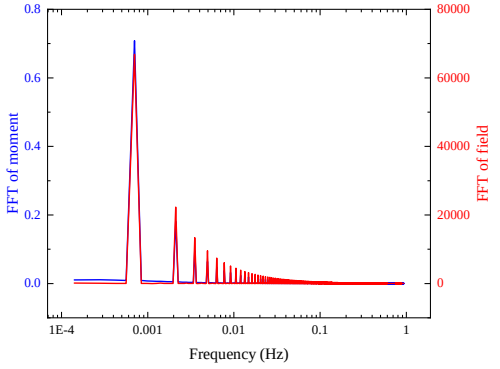

(f) 0.7 mHz FFT

Figure S21: Waveform measurements performed in zero-field at 20 K (left column) with associated Fast Fourier Transforms (FFT - right column). Two data sets were collected at this temperature, some frequencies appear twice.

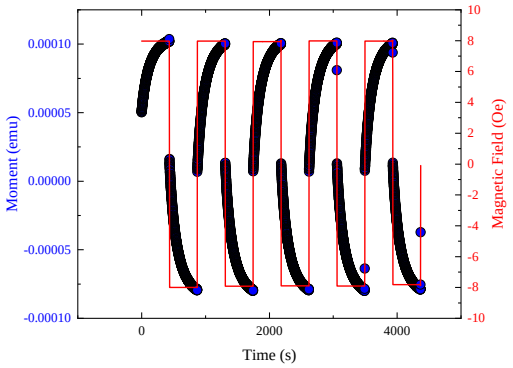

(a) 1.1 mHz $M(t)$ data

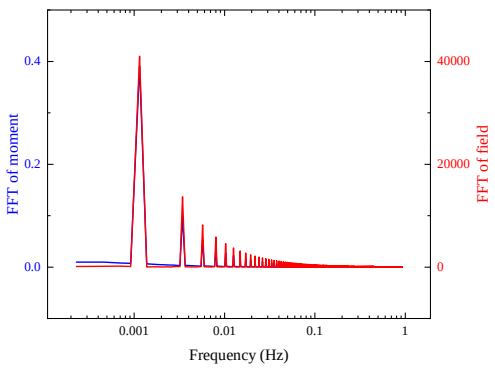

(b) 1.1 mHz FFT

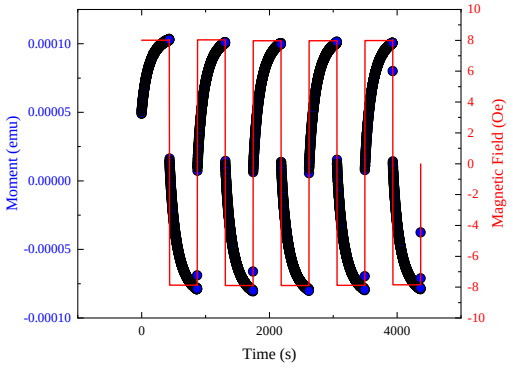

(c) 1.1 mHz $M(t)$ data

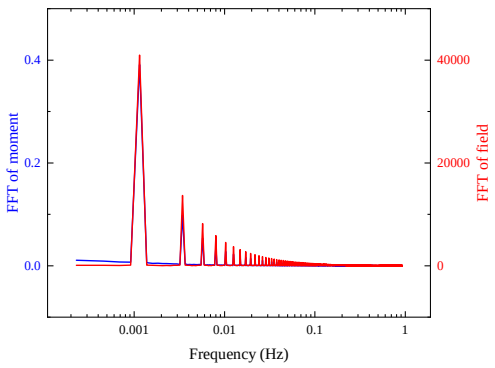

(d) 1.1 mHz FFT

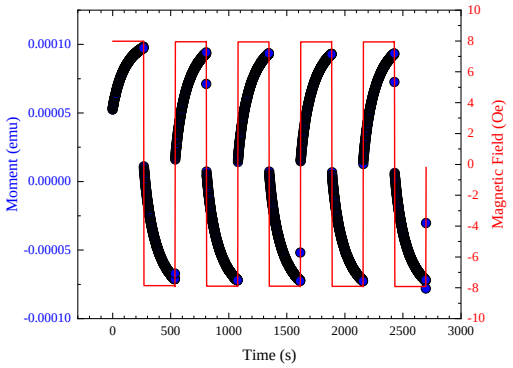

(e) 1.9 mHz $M(t)$ data

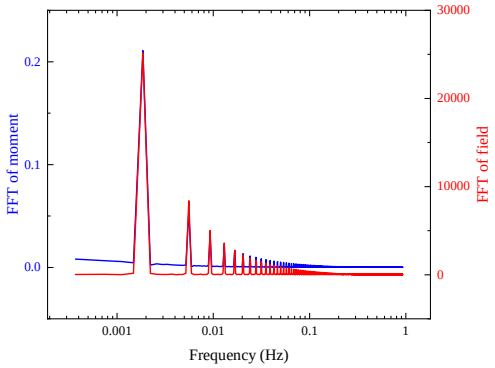

(f) 1.9 mHz FFT

Figure S22: Waveform measurements performed in zero-field at 20 K (left column) with associated Fast Fourier Transforms (FFT - right column). Two data sets were collected at this temperature, some frequencies appear twice.

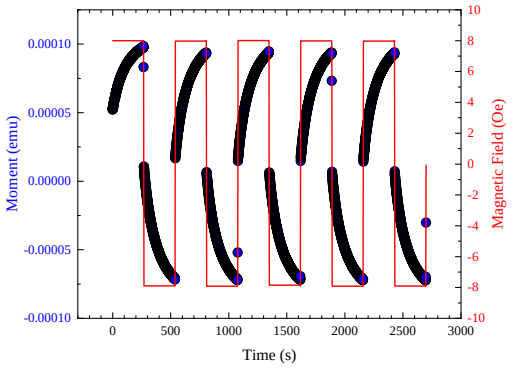

(a) 1.9 mHz $M(t)$ data

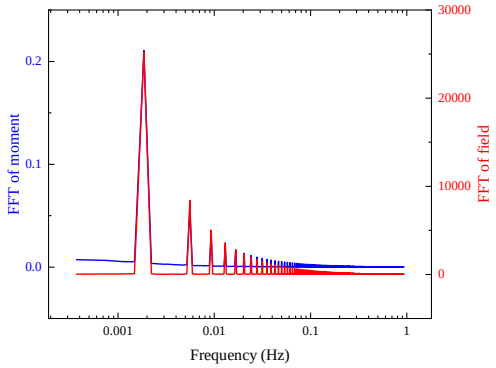

(b) 1.9 mHz FFT

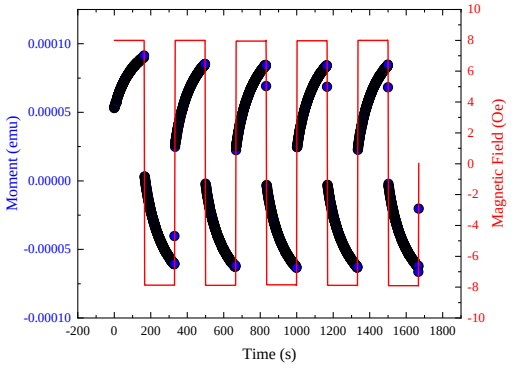

(c) 3 mHz $M(t)$ data

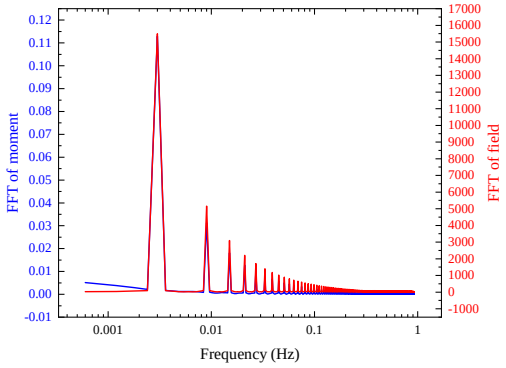

(d) 3 mHz FFT

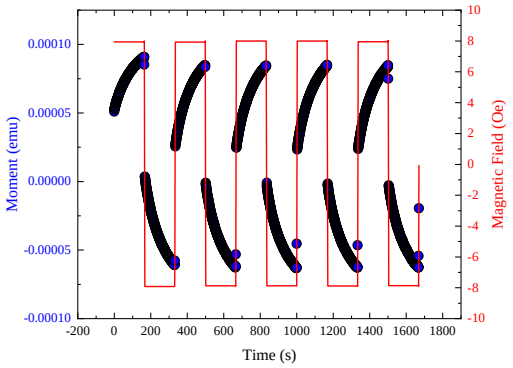

(e) 3 mHz $M(t)$ data

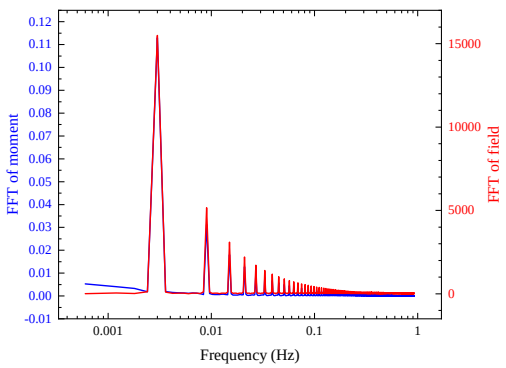

(f) 3 mHz FFT

Figure S23: Waveform measurements performed in zero-field at 20 K (left column) with associated Fast Fourier Transforms (FFT - right column). Two data sets were collected at this temperature, some frequencies appear twice.

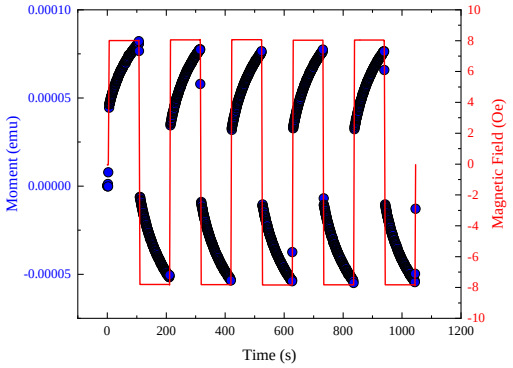

(a) 5 mHz $M(t)$ data

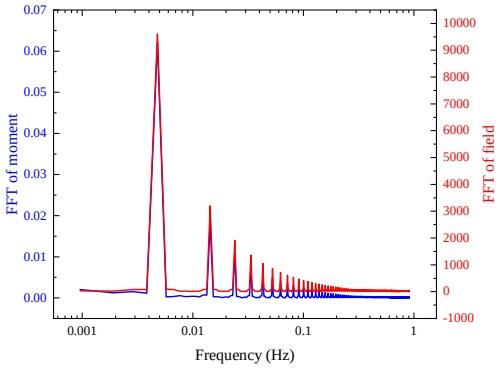

(b) 5 mHz FFT

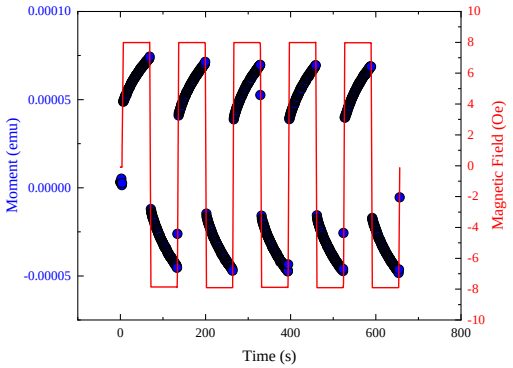

(c) 8 mHz $M(t)$ data

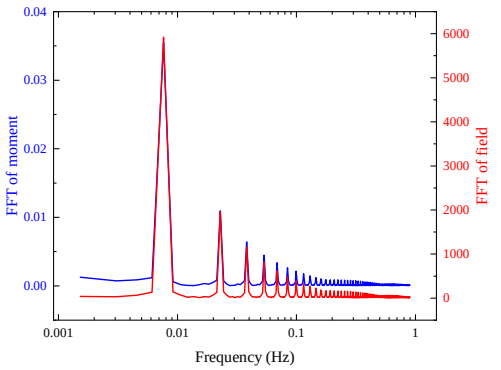

(d) 8 mHz FFT

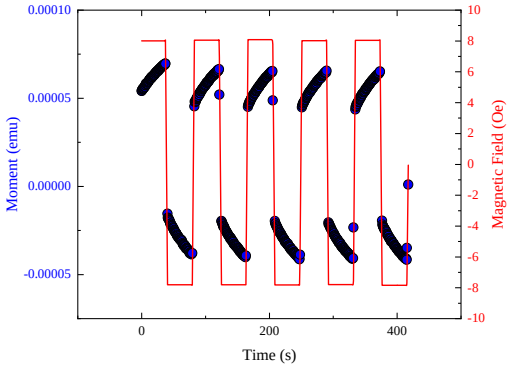

(e) 13 mHz $M(t)$ data

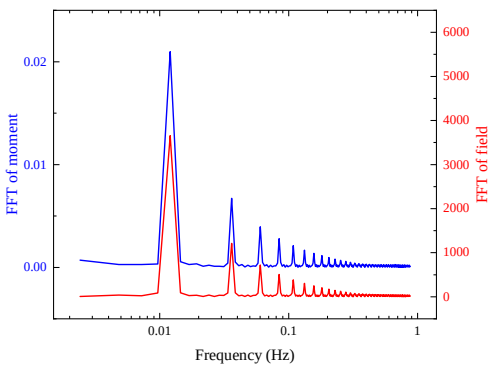

(f) 13 mHz FFT

Figure S24: Waveform measurements performed in zero-field at 20 K (left column) with associated Fast Fourier Transforms (FFT - right column). Two data sets were collected at this temperature, some frequencies appear twice.

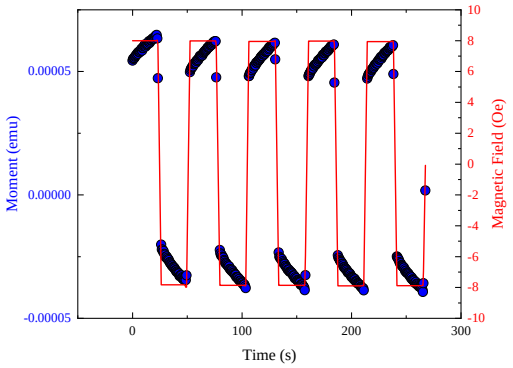

(a) 22 mHz $M(t)$ data

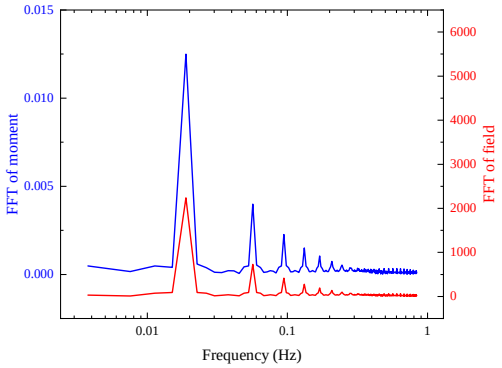

(b) 22 mHz FFT

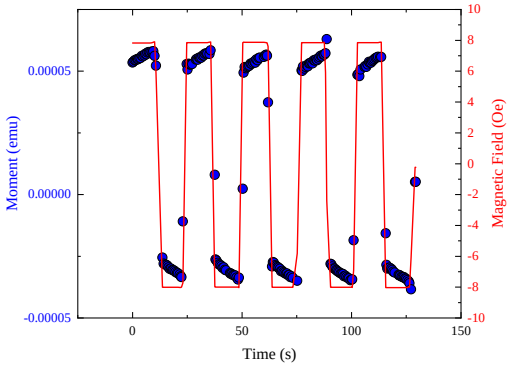

(c) 58 mHz $M(t)$ data

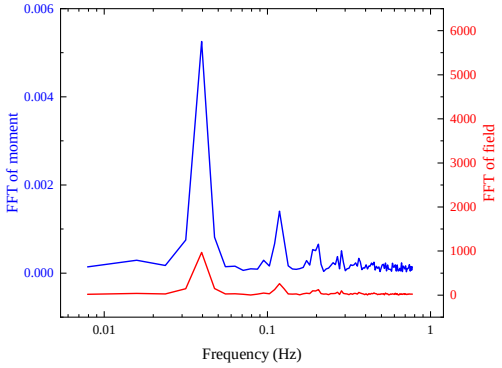

(d) 58 mHz FFT

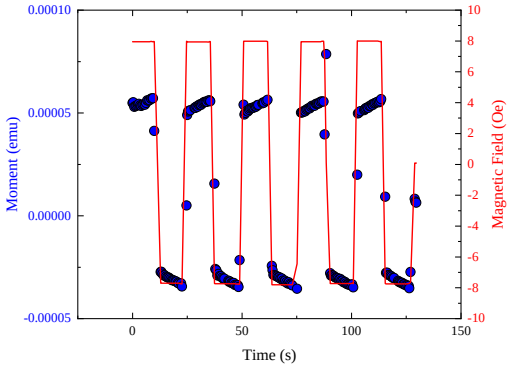

(e) 58 mHz $M(t)$ data

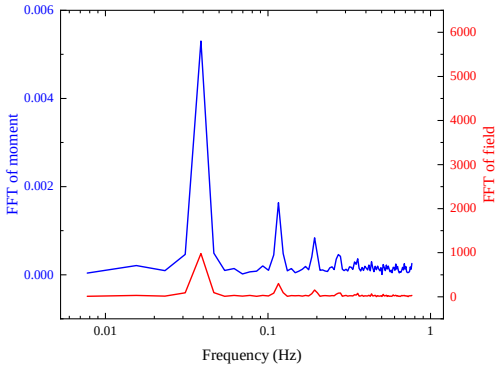

(f) 58 mHz FFT

Figure S25: Waveform measurements performed in zero-field at 20 K (left column) with associated Fast Fourier Transforms (FFT - right column). Two data sets were collected at this temperature, some frequencies appear twice.

S1.8 23 K Data

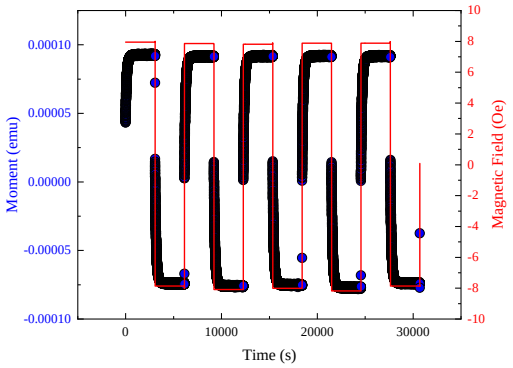

(a) 0.16 mHz $M(t)$ data

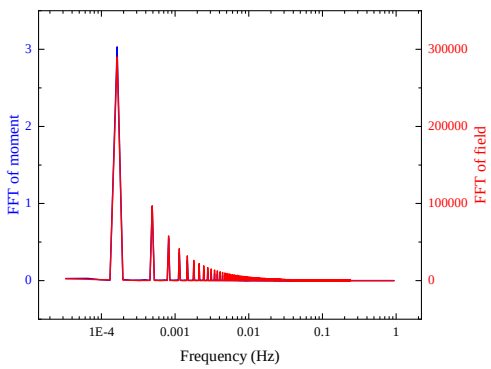

(b) 0.16 mHz FFT

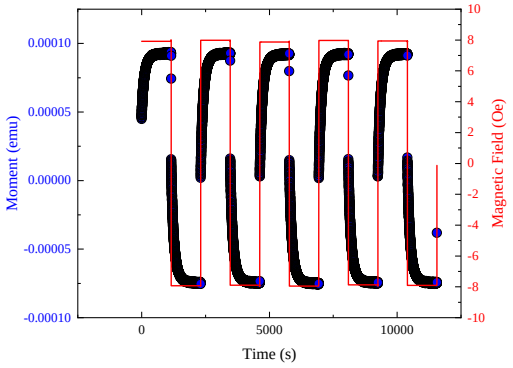

(c) 0.43 mHz $M(t)$ data

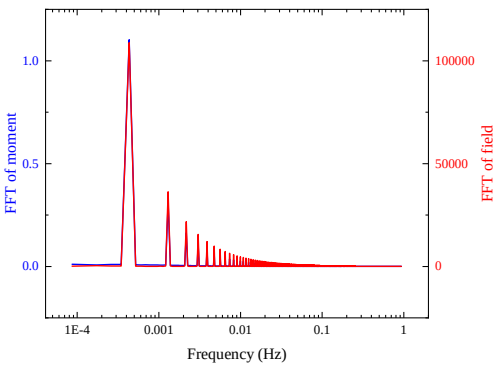

(d) 0.43 mHz FFT

Figure S26: Waveform measurements performed in zero-field at 23 K (left column) with associated Fast Fourier Transforms (FFT - right column)

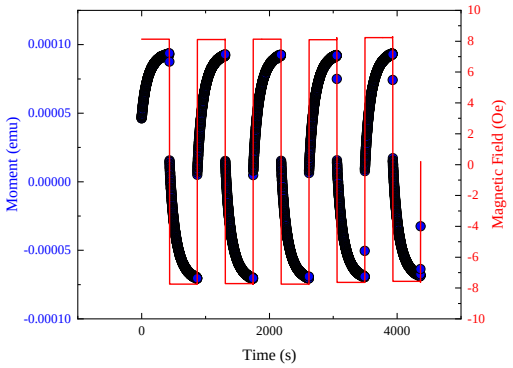

(a) 1.1 mHz $M(t)$ data

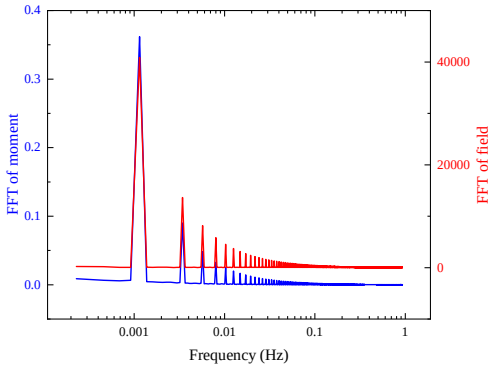

(b) 1.1 mHz FFT

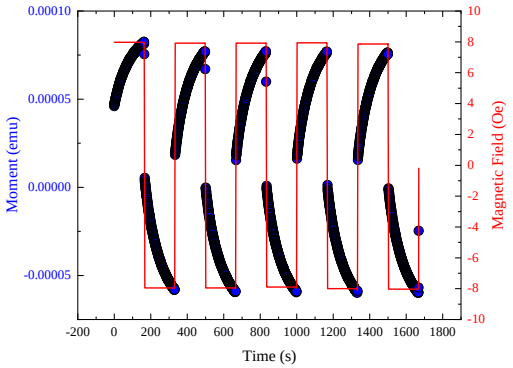

(c) 3 mHz $M(t)$ data

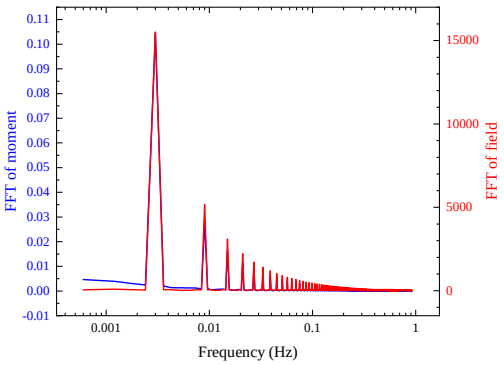

(d) 3 mHz FFT

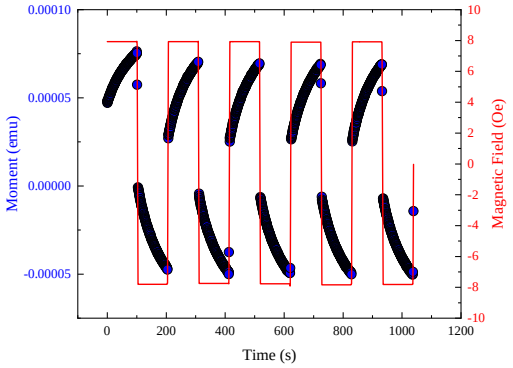

(e) 5 mHz $M(t)$ data

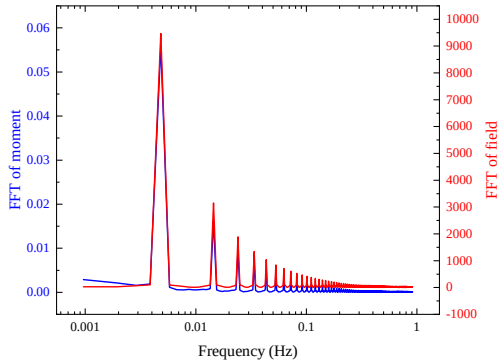

(f) 5 mHz FFT

Figure S27: Waveform measurements performed in zero-field at 23 K (left column) with associated Fast Fourier Transforms (FFT - right column)

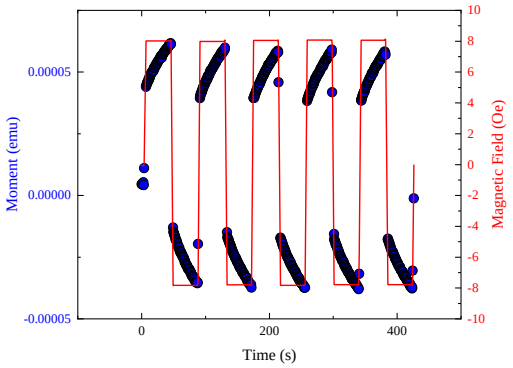

(a) 13 mHz $M(t)$ data

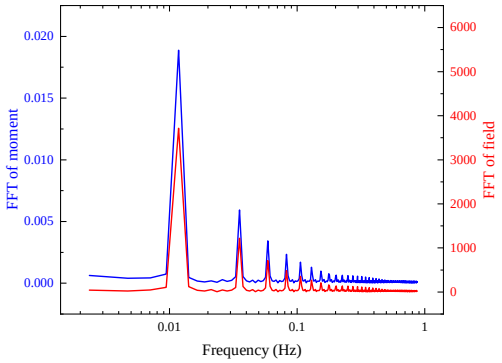

(b) 13 mHz FFT

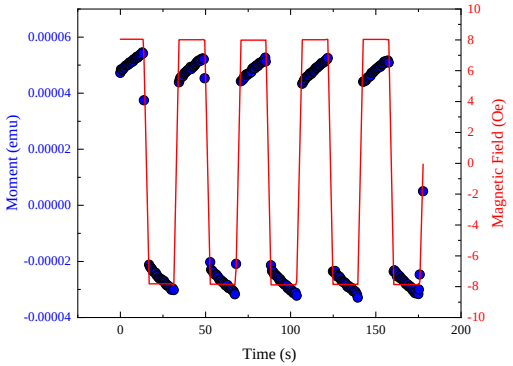

(c) 35 mHz $M(t)$ data

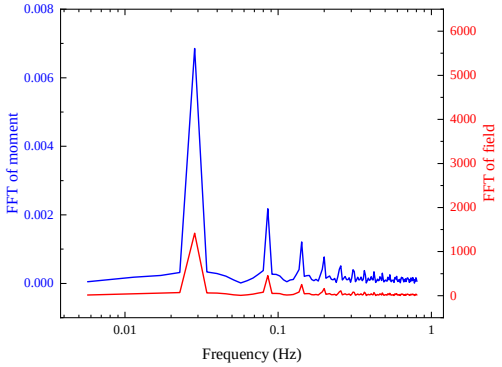

(d) 35 mHz FFT

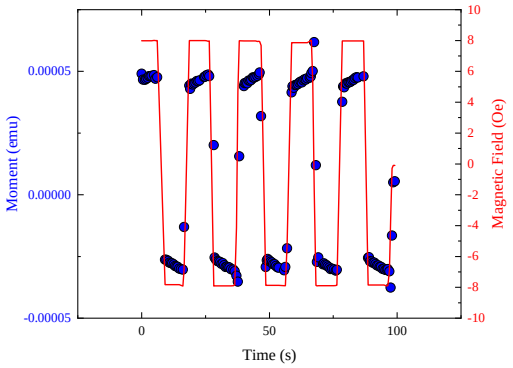

(e) 90 mHz $M(t)$ data

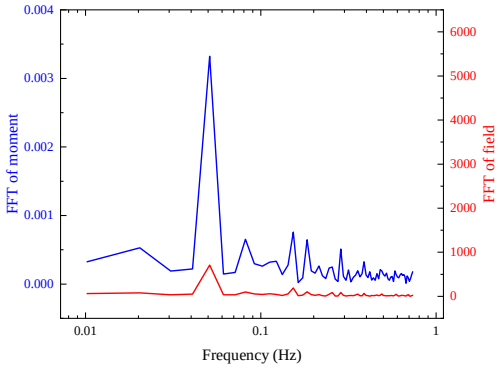

(f) 90 mHz FFT

Figure S28: Waveform measurements performed in zero-field at 23 K (left column) with associated Fast Fourier Transforms (FFT - right column)

S1.9 Fitting to Generalised Debye model

Table S1: Frequencies, susceptibilities and phase angles extracted from Waveform measurements of $[Dy(Dtp)_2][Al\{OC(CF_3)_3\}_4]$ performed at 2 K

Temperature (K)	Frequency (Hz)	χ' (cm^3mol^{-1})	χ'' (cm^3mol^{-1})	Phase (rad)
2	3.61946×10^{-5}	4.35626	0.2539	0.05822
2	6.88534×10^{-5}	4.18119	0.4076	0.09718
2	1.3097×10^{-4}	4.21854	0.77515	0.18172
2	2.48917×10^{-4}	3.79159	1.03754	0.26711
2	4.72839×10^{-4}	3.27261	1.17157	0.34378
2	0.0017	2.27579	0.75407	0.31996
2	0.00596	1.89638	0.29457	0.1541

Table S2: Frequencies, susceptibilities and phase angles extracted from Waveform measurements of $[Dy(Dtp)_2][Al\{OC(CF_3)_3\}_4]$ performed at 4 K

Temperature (K)	Frequency (Hz)	χ' (cm^3mol^{-1})	χ'' (cm^3mol^{-1})	Phase (rad)
4	3.09846×10^{-5}	2.68838	0.08306	0.03088
4	1.30964×10^{-4}	2.53497	0.36025	0.14117
4	2.48868×10^{-4}	2.29104	0.49927	0.21457
4	4.73168×10^{-4}	2.00106	0.5736	0.27916
4	0.0017	1.41082	0.46157	0.31619
4	0.00597	1.13043	0.24849	0.21638

Table S3: Frequencies, susceptibilities and phase angles extracted from Waveform measurements of $[Dy(Dtp)_2][Al\{OC(CF_3)_3\}_4]$ performed at 6 K

Temperature (K)	Frequency (Hz)	χ' (cm^3mol^{-1})	χ'' (cm^3mol^{-1})	Phase (rad)
6	9.99269×10^{-5}	1.84014	0.18998	0.10287
6	7.03517×10^{-4}	1.34866	0.40504	0.29176
6	1.6287×10^{-4}	1.77567	0.27115	0.15154
6	2.65439×10^{-4}	1.66286	0.35047	0.20772
6	4.32639×10^{-4}	1.50859	0.39582	0.25659
6	0.00115	1.19385	0.37745	0.30622
6	0.00185	1.0575	0.32518	0.29832
6	0.003	0.95696	0.25756	0.26291
6	0.00764	0.83579	0.138	0.16364
6	0.01887	0.79394	0.06645	0.08351
6	0.03908	0.77205	0.05203	0.06729

Table S4: Frequencies, susceptibilities and phase angles extracted from Waveform measurements of $[Dy(Dtp)_2][Al\{OC(CF_3)_3\}_4]$ performed at 9 K

Temperature (K)	Frequency (Hz)	χ' (cm^3mol^{-1})	χ'' (cm^3mol^{-1})	Phase (rad)
9	9.99269×10^{-5}	1.267	0.11782	0.09273
9	7.03517×10^{-4}	0.94731	0.27178	0.2794
9	1.6287×10^{-4}	1.22882	0.17154	0.1387
9	2.65439×10^{-4}	1.15865	0.22753	0.19391
9	4.32639×10^{-4}	1.05843	0.26305	0.24359
9	0.00114	0.84159	0.25634	0.29567
9	0.00185	0.74767	0.22114	0.28758
9	0.003	0.67478	0.17752	0.25726
9	0.00763	0.59336	0.09453	0.15798
9	0.01874	0.5648	0.04517	0.07981
9	0.03926	0.55079	0.03036	0.05507

Table S5: Frequencies, susceptibilities and phase angles extracted from Waveform measurements of $[Dy(Dtp)_2][Al\{OC(CF_3)_3\}_4]$ performed at 13 K

Temperature (K)	Frequency (Hz)	χ' (cm^3mol^{-1})	χ'' (cm^3mol^{-1})	Phase (rad)
13	7.03383×10^{-4}	0.69586	0.19508	0.27333
13	1.62871×10^{-4}	0.88194	0.10491	0.11839
13	4.32624×10^{-4}	0.77598	0.18088	0.22901
13	0.00114	0.61603	0.1877	0.29576
13	0.00185	0.54608	0.16403	0.2918
13	0.003	0.49174	0.13176	0.2618
13	0.00765	0.42968	0.06958	0.16054
13	0.01885	0.41027	0.03169	0.07708
13	0.03879	0.39864	0.02601	0.06517

Table S6: Frequencies, susceptibilities and phase angles extracted from Waveform measurements of $[Dy(Dtp)_2][Al\{OC(CF_3)_3\}_4]$ performed at 16 K

Temperature (K)	Frequency (Hz)	χ' (cm^3mol^{-1})	χ'' (cm^3mol^{-1})	Phase (rad)
16	7.03509×10^{-4}	0.59403	0.16147	0.2654
16	1.62883×10^{-4}	0.72781	0.07222	0.0989
16	4.32563×10^{-4}	0.65932	0.13944	0.20842
16	0.00114	0.52444	0.16117	0.29816
16	0.00185	0.4607	0.14306	0.30109
16	0.003	0.41157	0.11577	0.2742
16	0.00764	0.35865	0.06175	0.1705
16	0.01881	0.3401	0.02919	0.08562
16	0.03884	0.33071	0.0156	0.04714

Table S7: Frequencies, susceptibilities and phase angles extracted from Waveform measurements of $[Dy(Dtp)_2][Al\{OC(CF_3)_3\}_4]$ performed at 20 K. Two data sets were collected at this temperature, some frequencies appear twice.

Temperature (K)	Frequency (Hz)	χ' (cm^3mol^{-1})	χ'' (cm^3mol^{-1})	Phase (rad)
20	1.62877×10^{-4}	0.59629	0.04418	0.07395
20	1.62877×10^{-4}	0.59508	0.04413	0.07403
20	4.32618×10^{-4}	0.55824	0.0971	0.17221
20	4.32618×10^{-4}	0.55867	0.09697	0.17186
20	7.03507×10^{-4}	0.5156	0.12466	0.23722
20	7.03507×10^{-4}	0.51531	0.12422	0.23654
20	0.00114	0.4575	0.13725	0.29145
20	0.00114	0.45611	0.13684	0.29148
20	0.00185	0.39864	0.12945	0.31398
20	0.00185	0.3976	0.12894	0.31359
20	0.003	0.34899	0.10712	0.29781
20	0.003	0.34867	0.10701	0.29777
20	0.00479	0.31329	0.08212	0.25635
20	0.00764	0.29433	0.05767	0.19349
20	0.01205	0.28439	0.03935	0.13751
20	0.01886	0.27836	0.02615	0.09367
20	0.0387	0.27014	0.0165	0.06101
20	0.03952	0.27045	0.01716	0.06338

Table S8: Frequencies, susceptibilities and phase angles extracted from Waveform measurements of $[Dy(Dtp)_2][Al\{OC(CF_3)_3\}_4]$ performed at 23 K

Temperature (K)	Frequency (Hz)	χ' (cm^3mol^{-1})	χ'' (cm^3mol^{-1})	Phase (rad)
23	1.6288×10^{-4}	0.52225	0.03073	0.05878
23	4.32596×10^{-4}	0.502	0.07184	0.14214
23	0.00114	0.42678	0.11955	0.27312
23	0.00185	0.37069	0.1204	0.31406
23	0.003	0.32011	0.10375	0.31341
23	0.00482	0.285	0.08021	0.27435
23	0.01178	0.25124	0.03967	0.15662
23	0.02853	0.24143	0.01695	0.07011
23	0.05101	0.23345	0.02294	0.09795

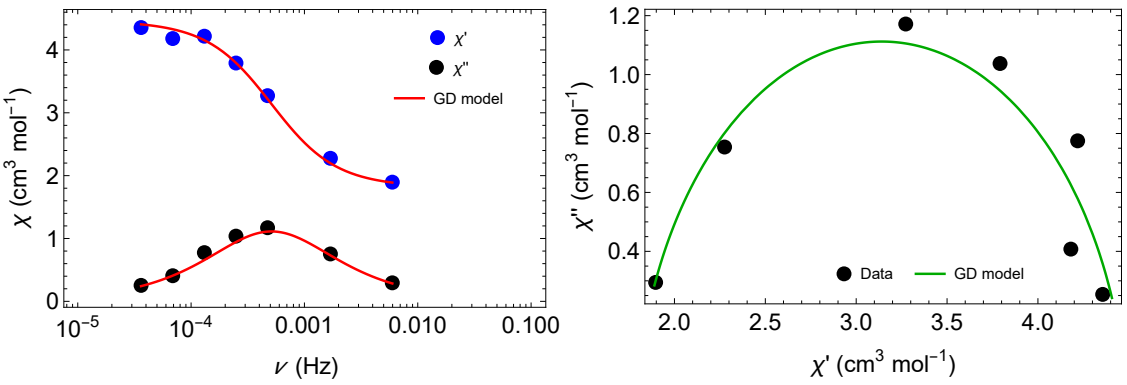

(a) 2 K susceptibility data

(b) 2 K Cole-Cole plot

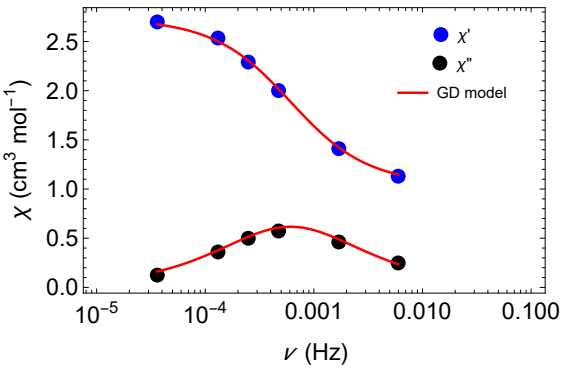

(c) 4 K susceptibility data

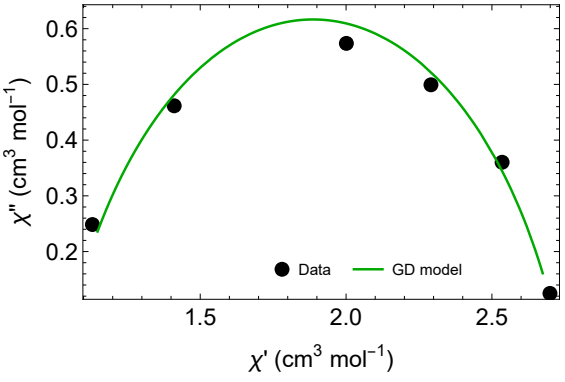

(d) 4 K Cole-Cole plot

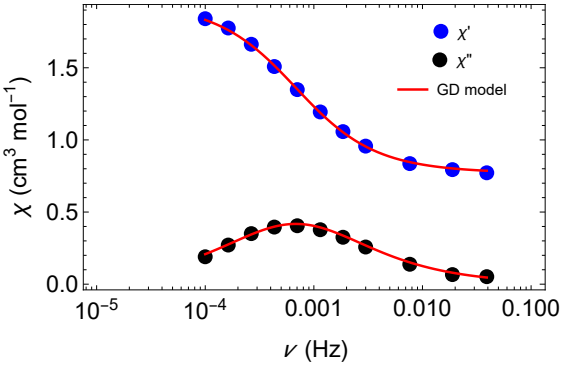

(e) 6 K susceptibility data

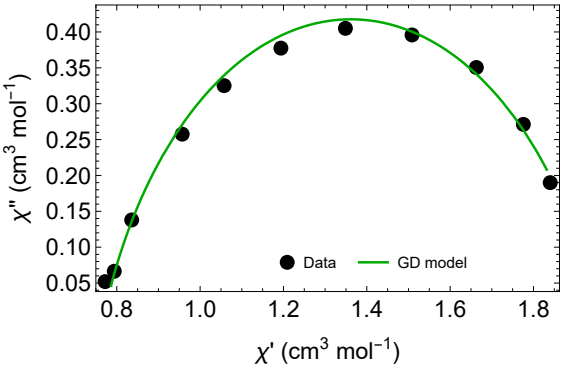

(f) 6 K Cole-Cole plot

Figure S29: In- and out-of-phase susceptibility data of $[Dy(Dtp)_2][Al\{OC(CF_3)_3\}_4]$ extracted from Waveform measurements fitted to the Generalised Debye model (Eq. 1 (left column) with associated Cole-Cole plots (right column). Results of the fit are shown in Table S9.

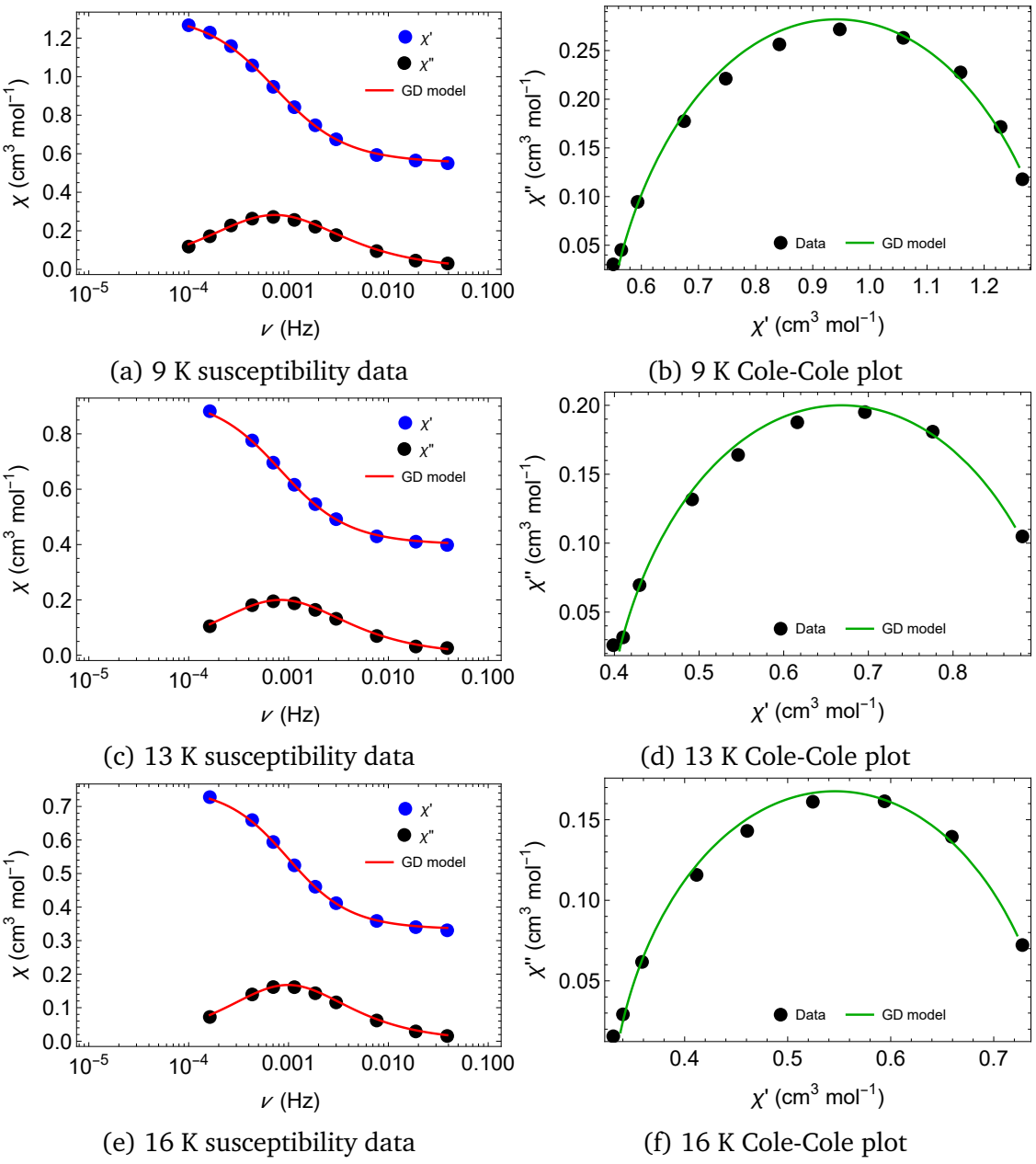

(a) 9 K susceptibility data

(b) 9 K Cole-Cole plot

(c) 13 K susceptibility data

(d) 13 K Cole-Cole plot

(e) 16 K susceptibility data

(f) 16 K Cole-Cole plot

Figure S30: In- and out-of-phase susceptibility data of $[Dy(Dtp)_2][Al\{OC(CF_3)_3\}_4]$ extracted from Waveform measurements fitted to the Generalised Debye model (Eq. 1 (left column) with associated Cole-Cole plots (right column). Results of the fit are shown in Table S9.

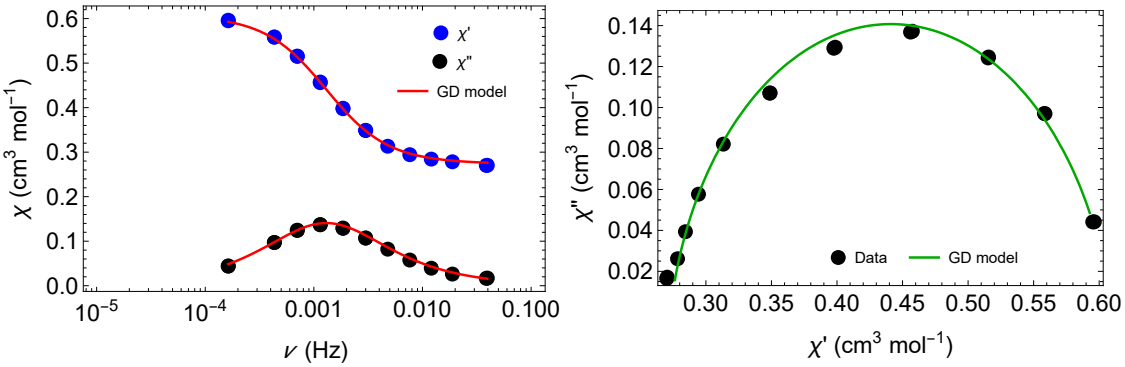

(a) 20 K susceptibility data

(b) 20 K Cole-Cole plot

(c) 23 K susceptibility data

(d) 23 K Cole-Cole plot

Figure S31: In- and out-of-phase susceptibility data of $[Dy(Dtp)_2][Al\{OC(CF_3)_3\}_4]$ extracted from Waveform measurements fitted to the Generalised Debye model (Eq. 1 (left column) with associated Cole-Cole plots (right column). Results of the fit are shown in Table S9.

Table S9: Results of fitting the waveform susceptibility data to a Generalised Debye model (Eq. 1) shown graphically in Fig. S29 - S31. Here, $\Delta\chi = \chi_T - \chi_S$

Temperature (K)	χ_S (cm^3 mol^{-1})	$\Delta\chi$ (cm^3 mol^{-1})	τ_{debye} (s)	α
2	1.80(8)	2.7(1)	311(21)	0.116(39)
4	1.03(4)	1.710(6)	259(15)	0.198(29)
6	0.767(8)	1.19(2)	233.3(5.6)	0.220(11)
9	0.549(5)	0.78(1)	217.7(5.3)	0.206(12)
13	0.398(4)	0.54(1)	190.9(5.9)	0.188(15)
16	0.332(3)	0.427(7)	161.1(4.0)	0.152(13)
20	0.273(2)	0.337(4)	122.4(1.8)	0.1133(88)
23	0.238(3)	0.293(6)	97.7(3.3)	0.101(19)

S2 DC decay analysis

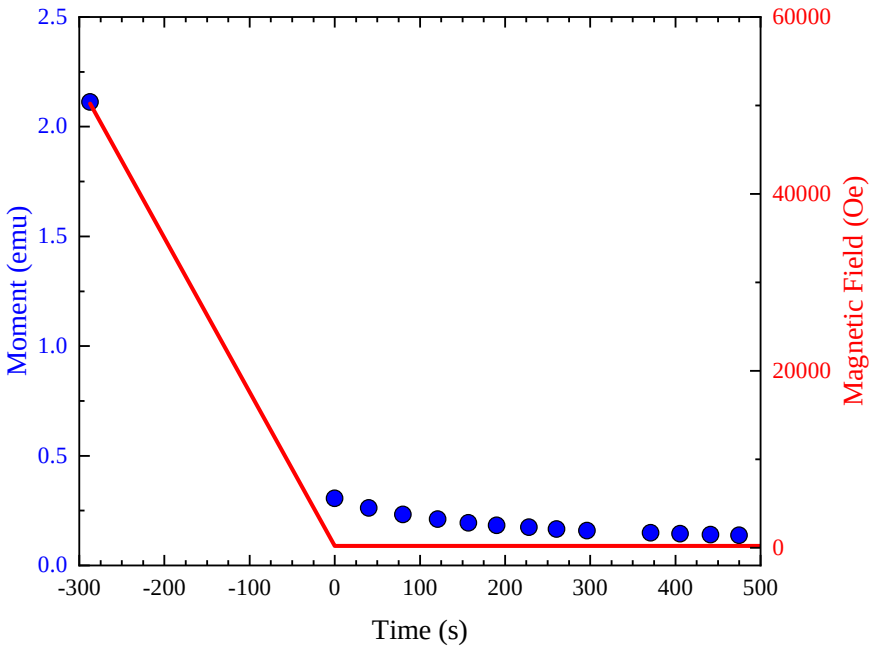

Figure S32: Current method of performing DC decay measurements in the molecular magnetism community. One or two measurements are made at saturation (in this case 5 T) before the field is dropped to target as fast as possible. A wait command for field stability is used before the first measurement point.[1,2] Data is taken from Ding *et al.*[2] and were performed at 2 K and target field of 230 Oe.

S2.1 Determining M_0

Justification for the method for determining where M_0 is reached using the time when $d^3M/dt^3 = 0$. The field is swept at a fixed rate from an initial to a final value. For an ideal fast relaxing sample ($\tau = 0$) the moment will mimic the change in field. This causes a step function in dM/dt at the points that field sweep rate changes (Fig. S33). This corresponds to a peak in d^2M/dt^2 and derivative shape in d^3M/dt^3. The exact point at which the field is settled occurs at the centre of this derivative shape when $d^3M/dt^3 = 0$. As can be observed for all our field sweeps, this occurs within 1.5 s of the first measured point (Fig. S34 and S35).

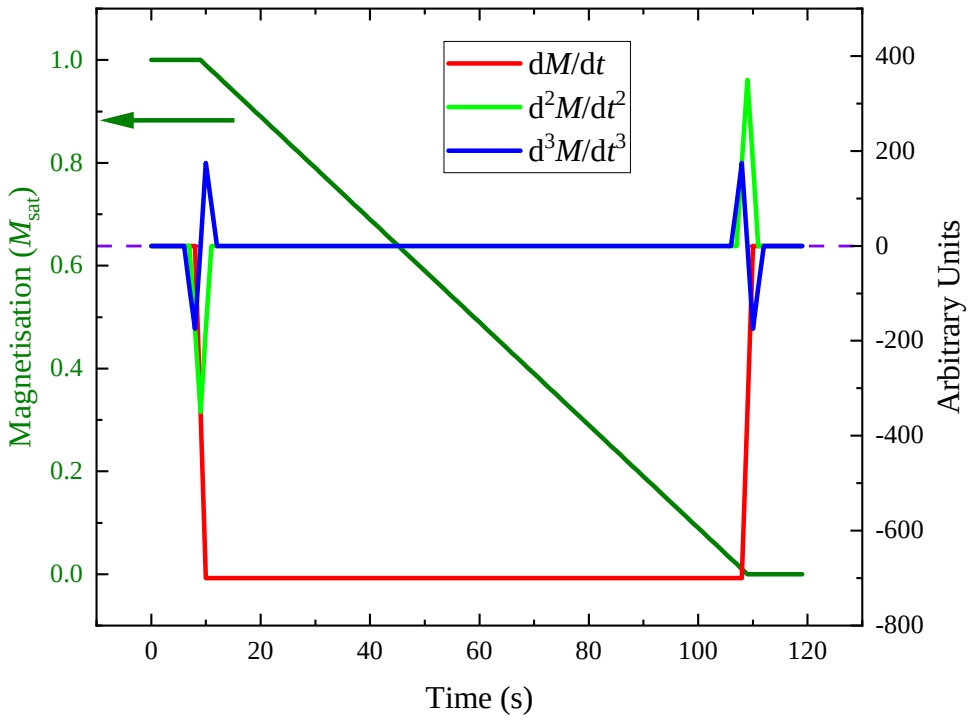

Figure S33: What would occur in an ideal, fast relaxing sample during the field change from saturation to zero.

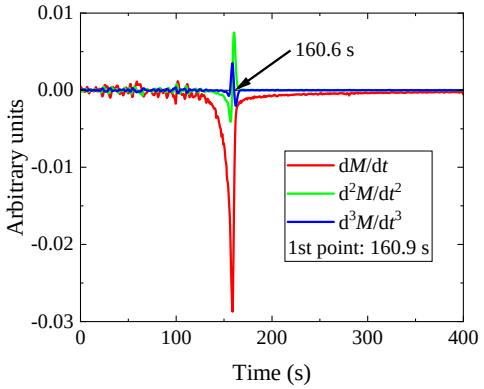

(a) 2 K data

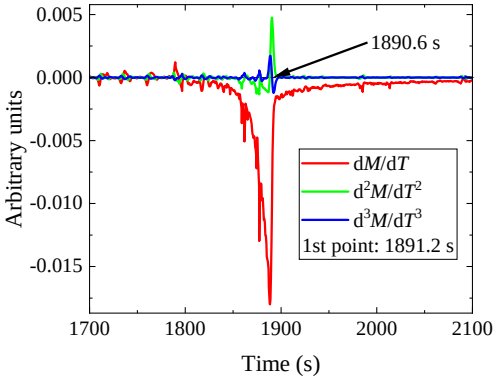

(b) 4 K data

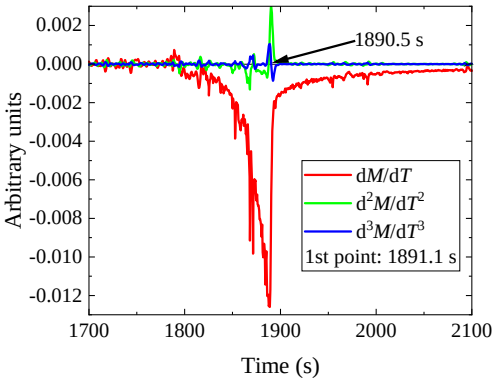

(c) 6 K data

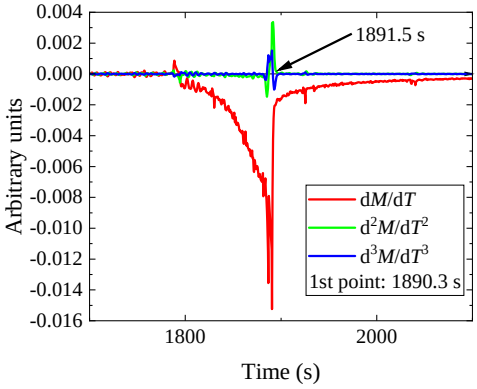

(d) 9 K data

Figure S34: Differentials of the magnetisation in the region of the applied field change in the DC decay measurements. Where the value of $dM^3/dt^2 = 0$ is where the field is stable at target.

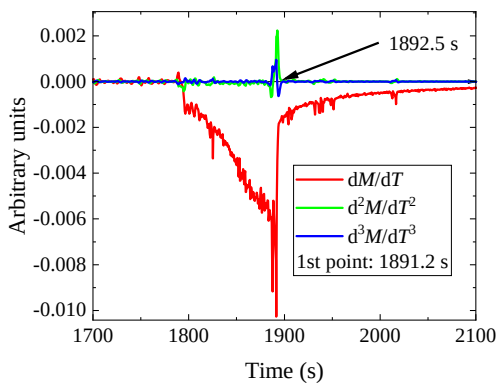

(a) 13 K data

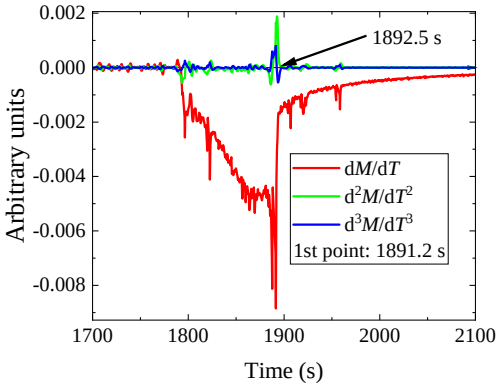

(b) 16 K data

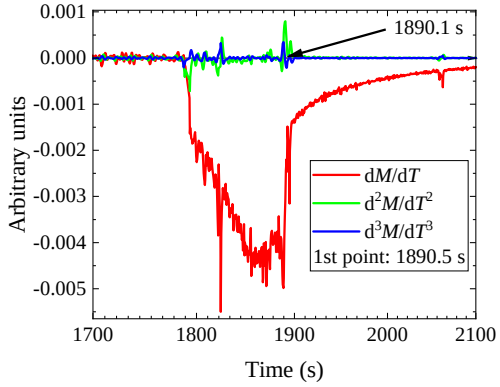

(c) 20 K data

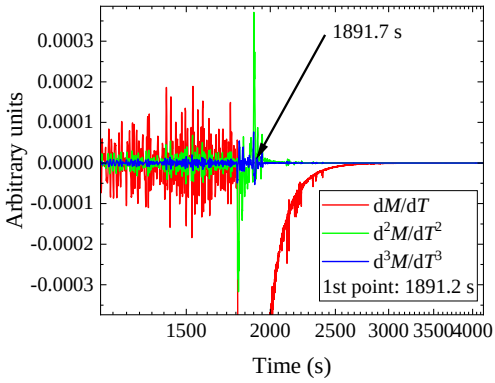

(d) 23 K data

Figure S35: Differentials of the magnetisation in the region of the applied field change in the DC decay measurements. Where the value of $\mathrm{d}M^3/\mathrm{d}t^2 = 0$ is where the field is stable at target.

S2.2 Measurement setup

Comparison of the different methods of setting up a magnetisation measurement using a Quantum Design MPMS3 SQUID magnetometer (Section 4.2).

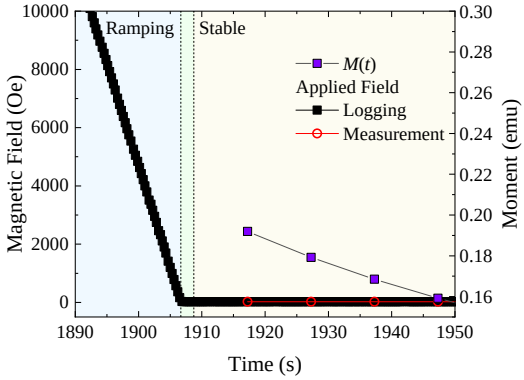

(a) DC mode with 4 s measurement time and a wait command for field stability.

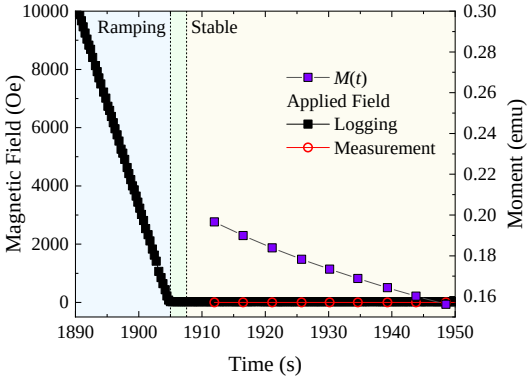

(b) DC mode with 1 s measurement time and a wait command for field stability.

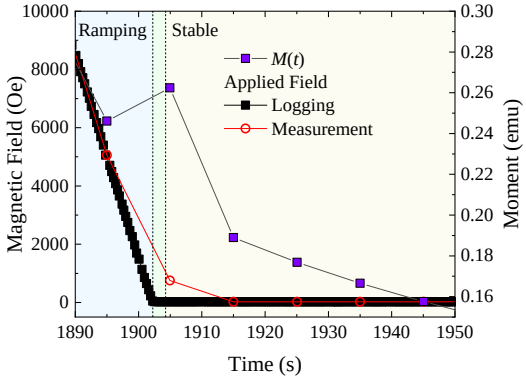

(c) DC mode with 4 s measurement time and measuring through the field change.

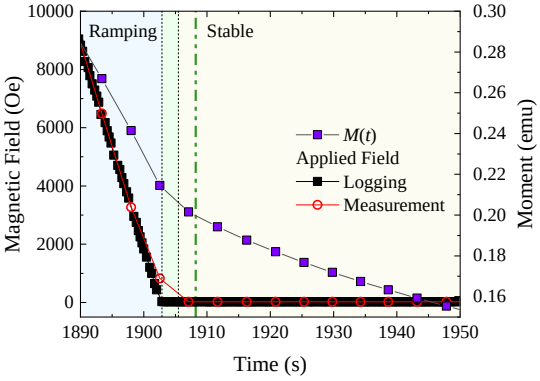

(d) DC mode with 1 s measurement time and measuring through the field change.

Figure S36: Test of the wait command versus measuring through the field change when ramping the magnetic field in a QD MPMS3 from $7 \rightarrow 0$ T for DC mode with measurement times of 4 and 1 s. The logging of the magnetic field is also shown in black squares. The light blue shaded regions indicates a ramping field status, light green the stabilisation of the magnetic field and the light yellow the stable magnetic field status. The green dash dot dot line is where the $\mathrm{d}^3M/\mathrm{d}t^3$ data crosses zero as described in Section S2.1. The results are shown in Table S10.

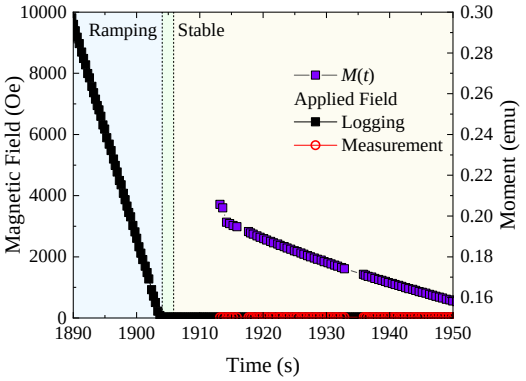

(a) VSM mode with a wait command for field stability and auto-ranging.

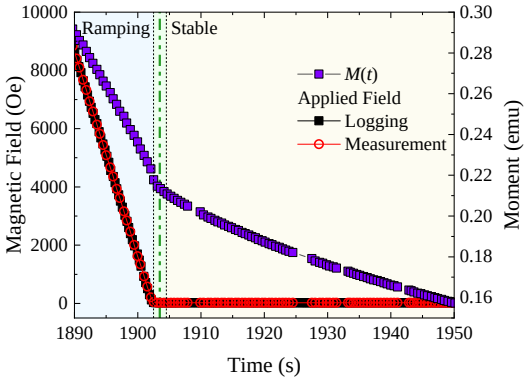

(b) VSM mode measuring through the field change and auto-ranging.

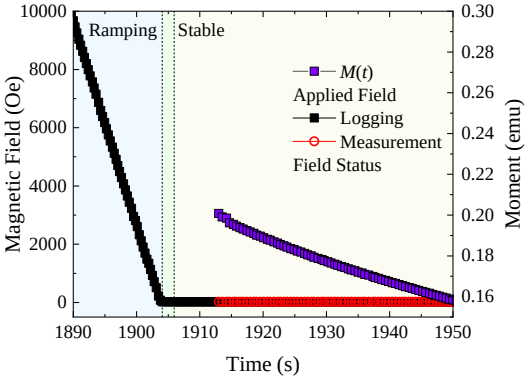

(c) VSM mode with a wait command for field stability and fixed ranges.

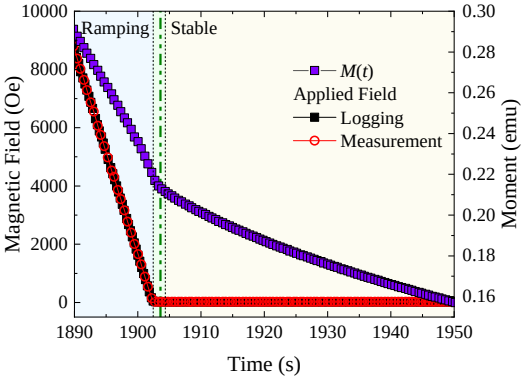

(d) VSM mode measuring through the field change and fixed ranges.

Figure S37: Test of the wait command versus measuring through the field change when ramping the magnetic field in a QD MPMS3 from 7 $\rightarrow$ 0 T for VSM mode with auto- and fixed-ranges. The logging of the magnetic field is also shown in black squares. The light blue shaded regions indicates a ramping field status, light green the stabilisation of the magnetic field and the light yellow the stable magnetic field status. The green dash dot dot line is where the d^3M/dt^3 data crosses zero as described in Section S2.1. The results are shown in Table S10.

Table S10: Comparison of the different methods of a dc decay measurement setup using a QD MPMS3 shown in Fig. S36 and S37.

Method	Measurement time (s)	Continuous or wait	Time to ramp start (s)	field sweep time (s)	Time to stabilise field (s)	1st point after target field (s)	1st point after stable field (s)	M_0 (emu)
DC Mode, 30 mm	4	Wait	2.54	100.84	1.55	10.06	8.51	0.19190
		Continuous	2.38	100.81	1.73	12.45	10.72	0.18899
	1	Wait	2.52	101.05	2.25	6.65	4.40	0.19658
		Continuous	2.44	100.97	2.30	3.91	1.61	0.20157
VSM mode, 1 mm	0.5 Autorange	Wait	2.26	101.23	1.54	8.85	7.31	0.20573
		Continuous	2.23	100.96	1.72	0.31	-1.41	0.21460
	0.5 Fixed range	Wait	2.05	101.06	1.60	8.66	7.06	0.20079
		Continuous	1.91	101.23	1.58	0.54	-1.04	0.21422

S2.3 How much data should be fit?

Comparison of how fitting different amount of the DC decay trace affects the fitted parameters to determine how much data should be fitted (Section 4.2)

Table S11: τ^* and β parameters obtained from fitting DC decay data to Eq. 11 with M_0 fixed to the first measured point and $t_{\text{offset}} = 0$. M_{eq}, τ^* and β were freely fitted. Data were fitted for various percentages of the decay (99% refers to fitting up to $0.01M_0$). The values shown in this table are for decays measured between 2 and 9 K.

Temperature (K)	2			4			6			9		
% Fitted	τ^* (s)	β	M_{eq} (emu)	τ^* (s)	β	M_{eq} (emu)	τ^* (s)	β	M_{eq} (emu)	τ^* (s)	β	M_{eq} (emu)
100	796.5	0.487	0.00252	532.4	0.577	3.0840×10^{-4}	414.6	0.621	-8.0013×10^{-4}	305.0	0.669	-6.411×10^{-4}
99	796.5	0.487	0.00252	532.4	0.577	3.0840×10^{-4}	414.6	0.621	-8.0013×10^{-4}	305.0	0.669	-6.411×10^{-4}
95	733.3	0.520	0.00913	508.4	0.5934	0.00416	404.1	0.630	0.00138	301.4	0.673	3.615×10^{-4}
90	646.1	0.556	0.01893	470.8	0.614	0.01067	378.7	0.647	0.00701	287.2	0.687	0.00453
80	503.6	0.616	0.03886	386.4	0.657	0.02809	316.7	0.686	0.02318	251.5	0.717	0.01655
70	410.9	0.657	0.05597	308.2	0.701	0.04869	258.7	0.726	0.04204	218.0	0.743	0.03
60	337.3	0.690	0.07327	245.7	0.741	0.06962	211.5	0.762	0.06106	190.4	0.766	0.04309
50	303.3	0.705	0.0828	197.9	0.776	0.08966	172.8	0.794	0.08017	167.2	0.783	0.05585
40	339.3	0.696	0.0713	161.1	0.805	0.1086	140.8	0.823	0.0993	149.9	0.796	0.06677
30	404.4	0.685	0.05093	130.5	0.830	0.1279	123.5	0.839	0.1114	153.0	0.795	0.06437
20	496.0	0.678	0.02183	101.0	0.853	0.1506	91.73	0.865	0.1383	264.5	0.772	-0.0135
10	85.96	0.727	0.1975	2729	0.801	-1.295	62.37	0.888	0.1699	353000	0.741	-47.21

Table S12: τ^* and β parameters obtained from fitting DC decay data to Eq. 11 with M_0 fixed to the first measured point and $t_{\text{offset}} = 0$. M_{eq}, τ^* and β were freely fitted. Data were fitted for various percentages of the decay (99% refers to fitting up to $0.01M_0$). The values shown in this table are for decays measured between 13 and 23 K.

Temperature (K)	13			16			20			23		
% Fitted	τ^* (s)	β	M_{eq} (emu)	τ^* (s)	β	M_{eq} (emu)	τ^* (s)	β	M_{eq} (emu)	τ^* (s)	β	M_{eq} (emu)
100	220.6	0.743	5.399×10^{-4}	174.8	0.792	0.00101	129.6	0.847	0.00112	104.4	0.880	0.00102
99	220.6	0.743	5.399×10^{-4}	174.8	0.792	0.00101	129.6	0.847	0.00112	104.4	0.880	0.00102
95	217.2	0.751	0.00174	171.6	0.802	0.00232	127.3	0.858	0.00218	102.8	0.890	0.00186
90	209.9	0.762	0.00448	167.2	0.812	0.00424	125.2	0.865	0.00329	101.4	0.896	0.00261
80	192.9	0.784	0.01169	158.1	0.829	0.0087	121.2	0.875	0.00557	98.82	0.905	0.00423
70	175.8	0.804	0.01999	148.4	0.843	0.01404	116.6	0.884	0.00846	95.68	0.913	0.00639
60	159.6	0.820	0.02891	137.8	0.856	0.02056	111.4	0.892	0.01201	91.82	0.921	0.00928
50	144.7	0.834	0.03828	127.0	0.867	0.02792	106.1	0.899	0.01605	87.54	0.928	0.01278
40	130.7	0.845	0.04813	117.6	0.876	0.03503	99.09	0.907	0.02183	82.12	0.935	0.01762
30	111.2	0.860	0.06375	109.5	0.882	0.04182	90.23	0.915	0.02993	70.21	0.950	0.02932
20	136.3	0.848	0.04185	111.8	0.882	0.0393	74.32	0.928	0.04593	47.74	0.981	0.05462
10	2739	0.814	-1.5011	2702	0.849	-1.7338	2706	0.895	-2.1910	2726	0.935	-2.7175

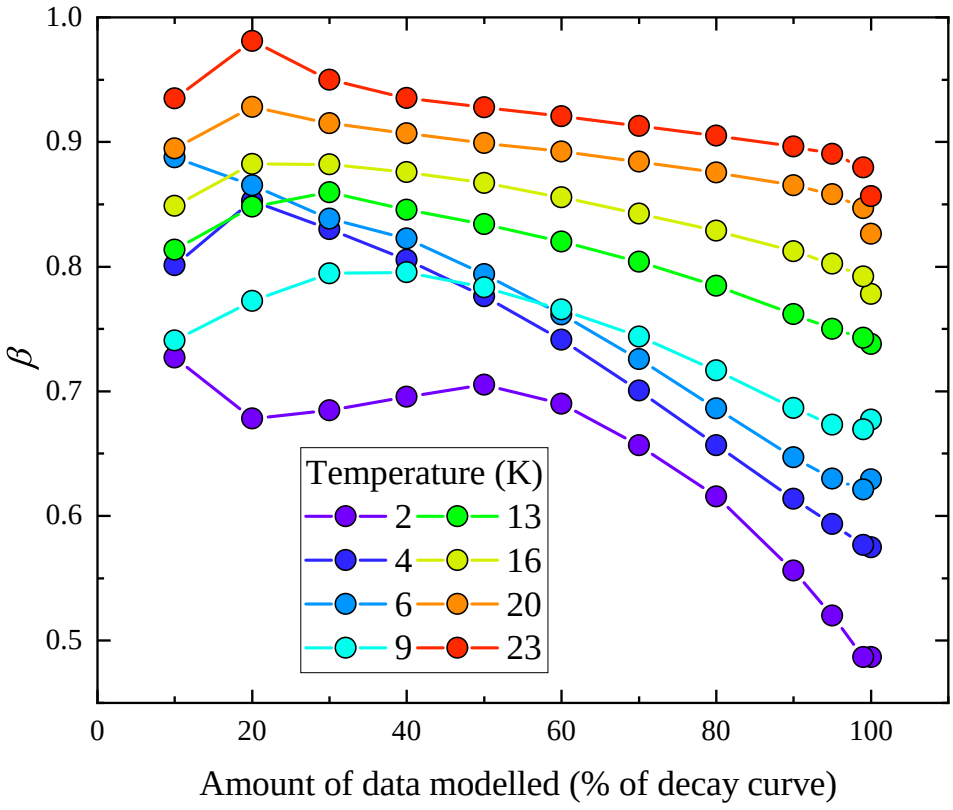

Figure S38: Dependence of how much data is fitted (% of the decay curve) on the β parameter extracted from modelling DC decay data of $[Dy(Dtp)_2][Al\{OC(CF_3)_3\}_4]$ to Eq. 11 with M_0 fixed to the first data point and $t_{offset} = 0$. All other parameters are freely fitted.

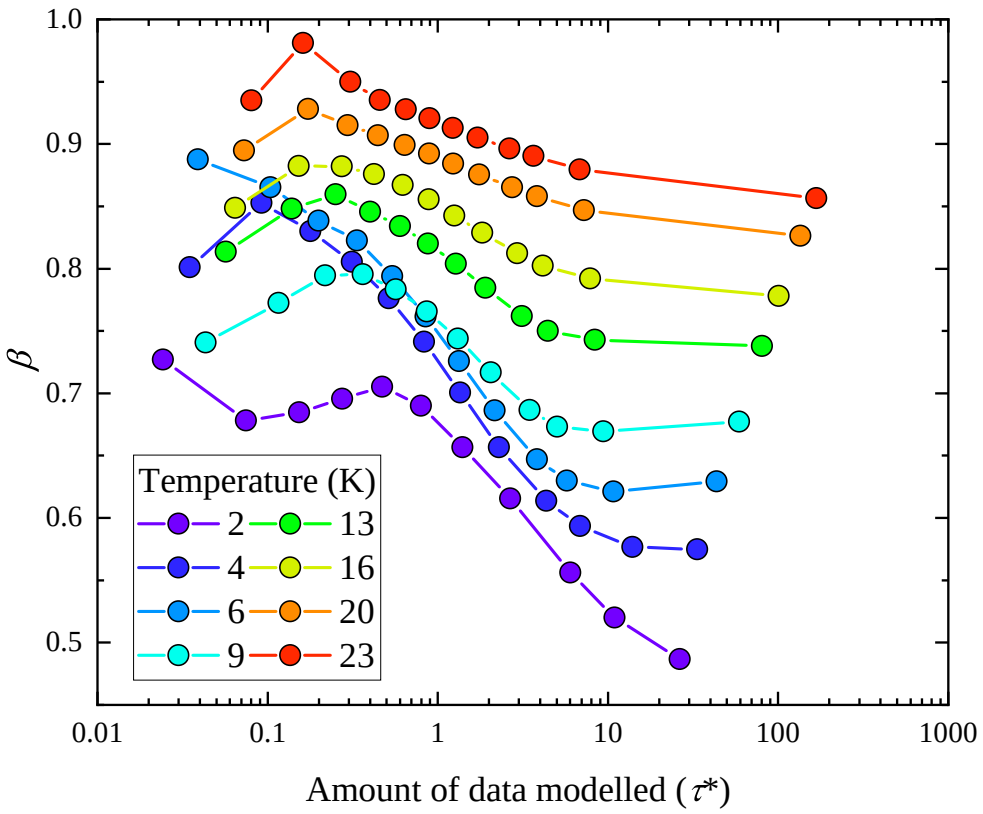

Figure S39: Dependence of how much data is fitted (% of the decay curve) on the β parameter extracted from modelling DC decay data of $[Dy(Dtp)_2][Al\{OC(CF_3)_3\}_4]$ to Eq. 11 with M_0 fixed to the first data point and $t_{offset} = 0$. All other parameters are freely fitted.

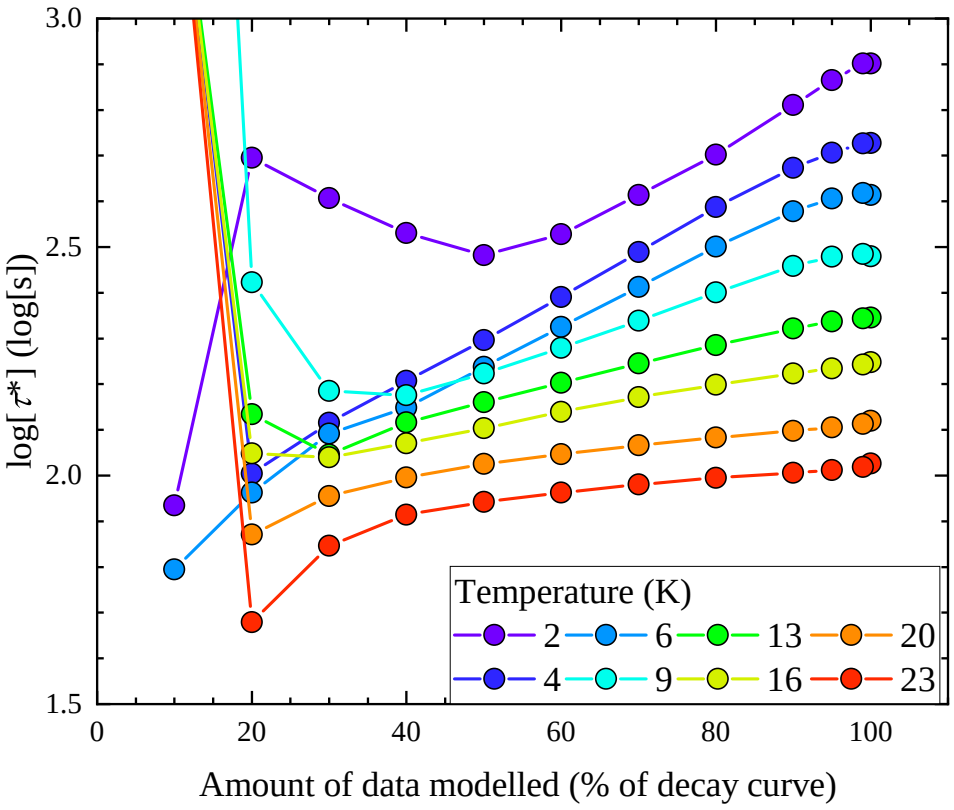

Figure S40: Dependence of how much data is fitted (% of the decay curve) on the τ^* parameter extracted from modelling DC decay data of $[Dy(Dtp)_2][Al\{OC(CF_3)_3\}_4]$to Eq. 11 with M_0 fixed to the first data point and $t_{offset} = 0$. All other parameters are freely fitted.

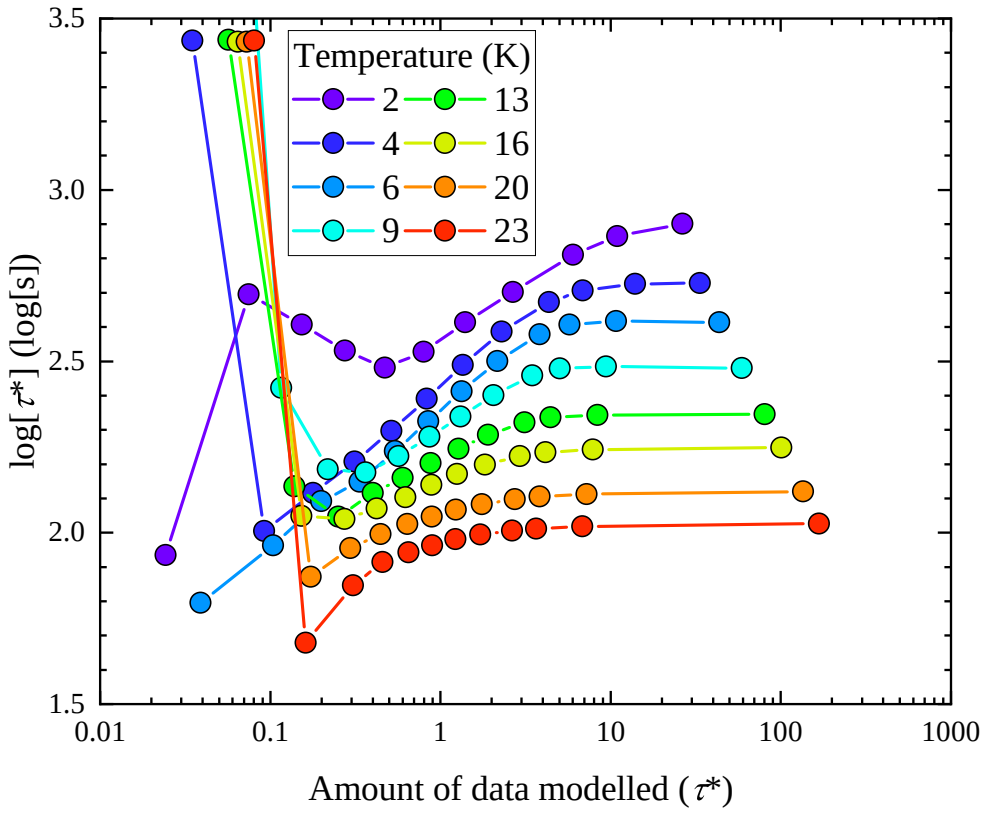

Figure S41: Dependence of how much data is fitted (% of the decay curve) on the τ^* parameter extracted from modelling DC decay data of $[Dy(Dtp)_2][Al\{OC(CF_3)_3\}_4]$ to Eq. 11 with M_0 fixed to the first data point and $t_{offset} = 0$. All other parameters are freely fitted.

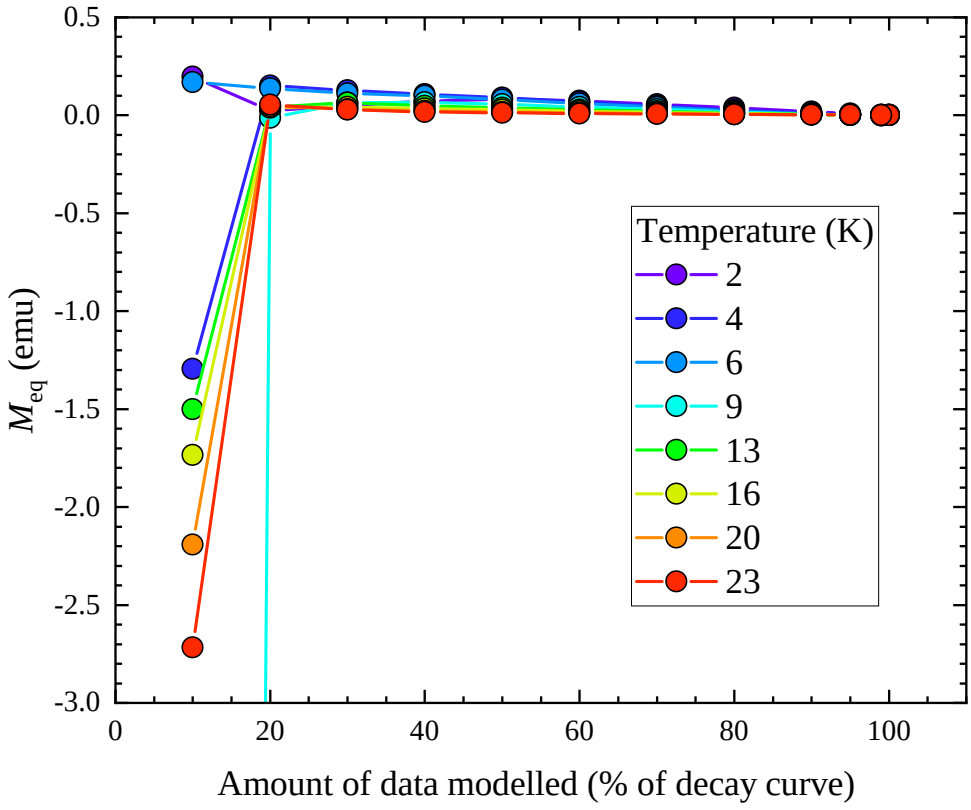

Figure S42: Dependence of how much data is fitted (% of the decay curve) on the M_{eq} parameter extracted from modelling DC decay data of $[Dy(Dtp)_2][Al\{OC(CF_3)_3\}_4]$ to Eq. 11 with M_0 fixed to the first data point and $t_{offset} = 0$. All other parameters are freely fitted.

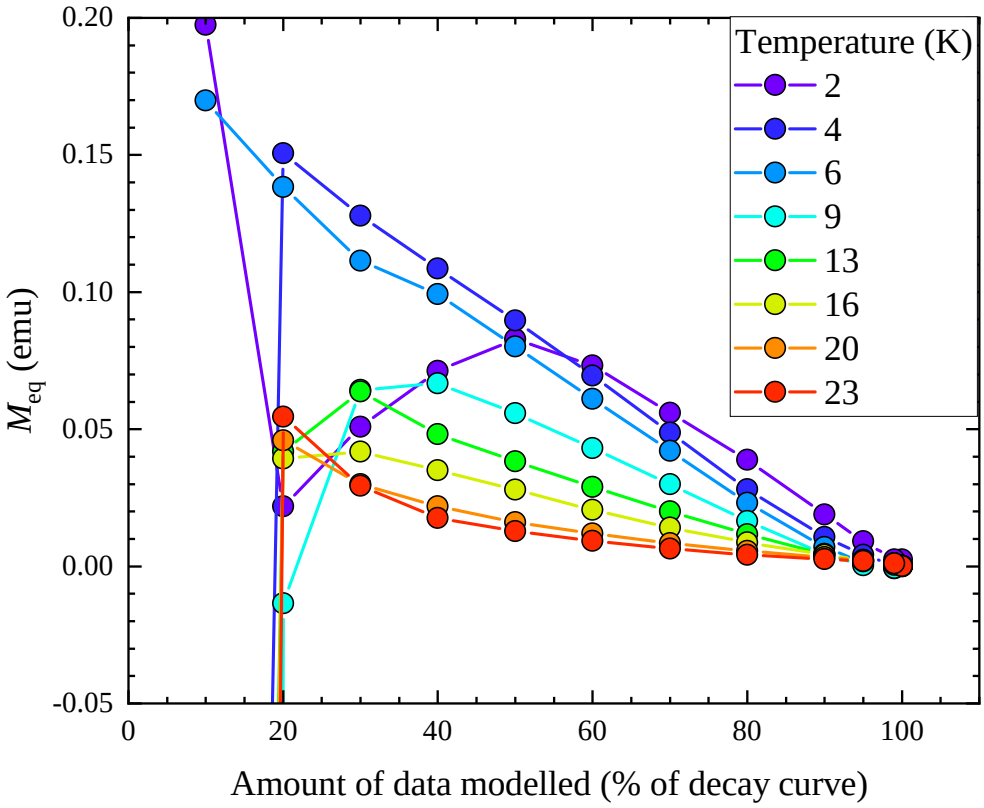

Figure S43: Zoomed in plot of Fig. S44

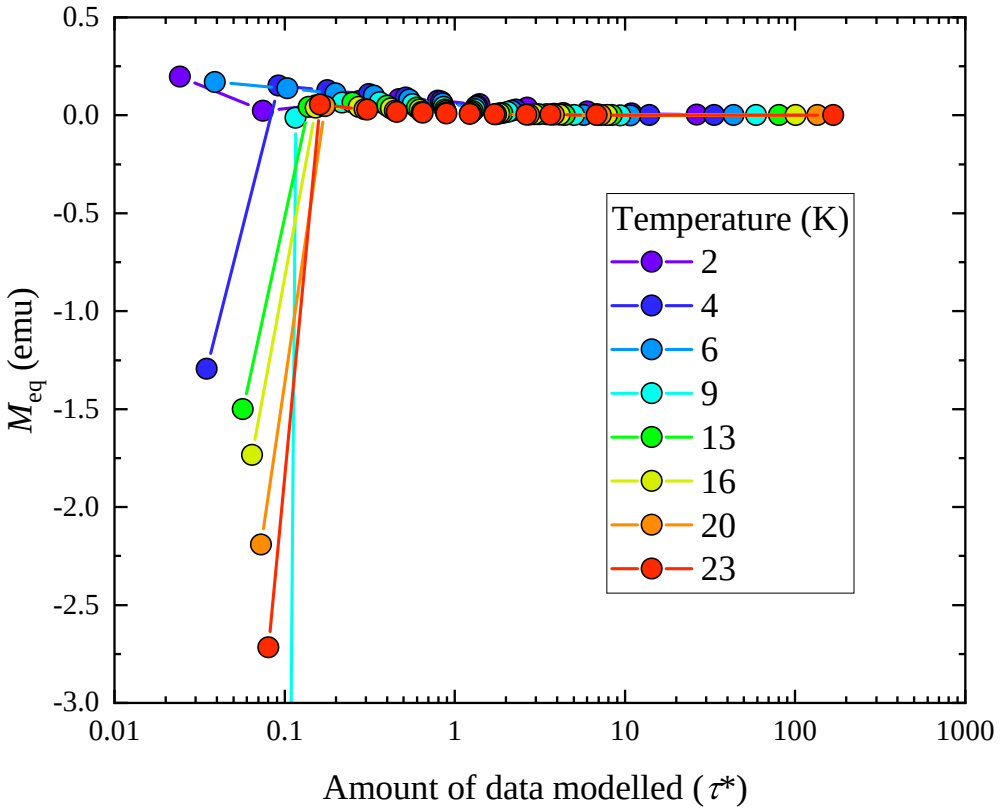

Figure S44: Dependence of how much data is fitted (% of the decay curve) on the M_{eq} parameter extracted from modelling DC decay data of $[Dy(Dtp)_2][Al\{OC(CF_3)_3\}_4]$ to Eq. 11 with M_0 fixed to the first data point and $t_{offset} = 0$. All other parameters are freely fitted.

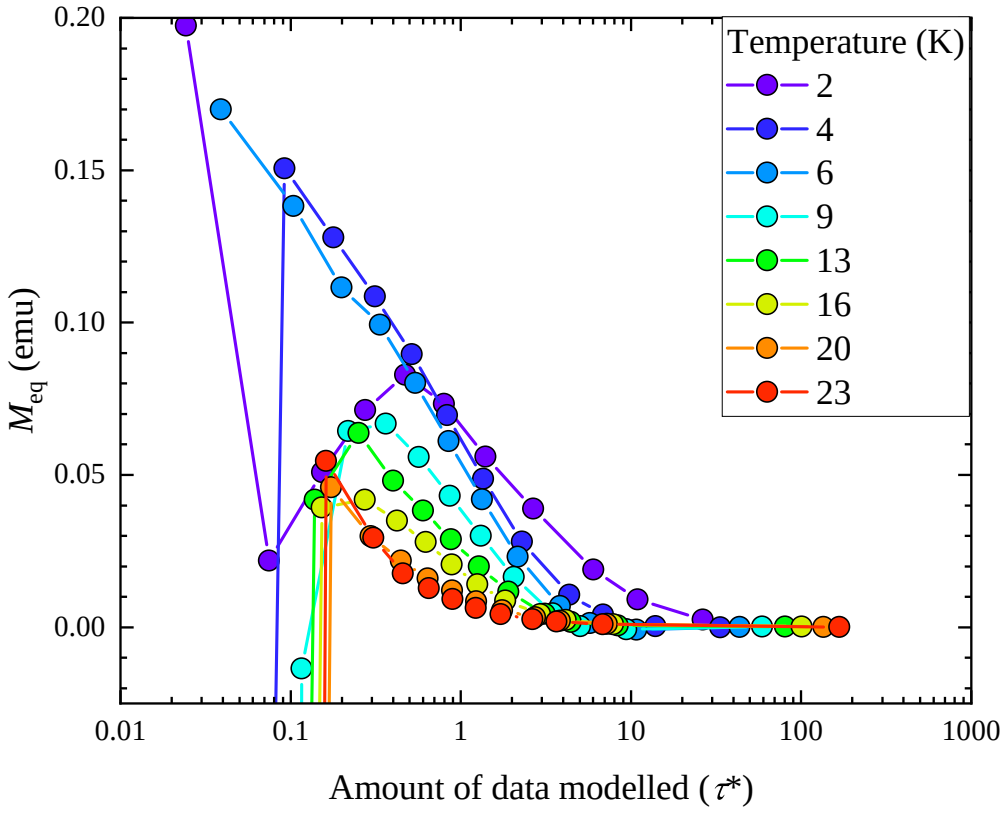

Figure S45: Zoomed in plot of Fig. S44

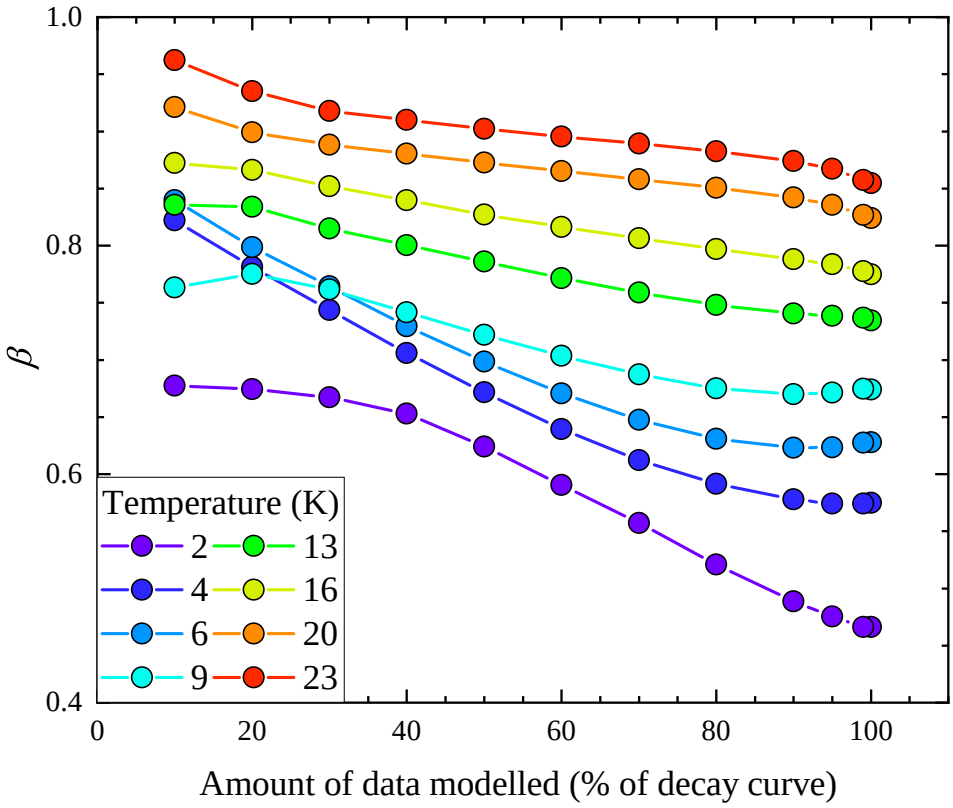

Figure S46: Dependence of how much data is fitted (% of the decay curve) on the β parameter extracted from modelling DC decay data of $[Dy(Dtp)_2][Al\{OC(CF_3)_3\}_4]$ to Eq. 11 with M_0 fixed to the first data point, M_{eq} fixed to target (in this case $M_{eq} = 0$) and $t_{offset} = 0$. τ^* and β are freely fitted.

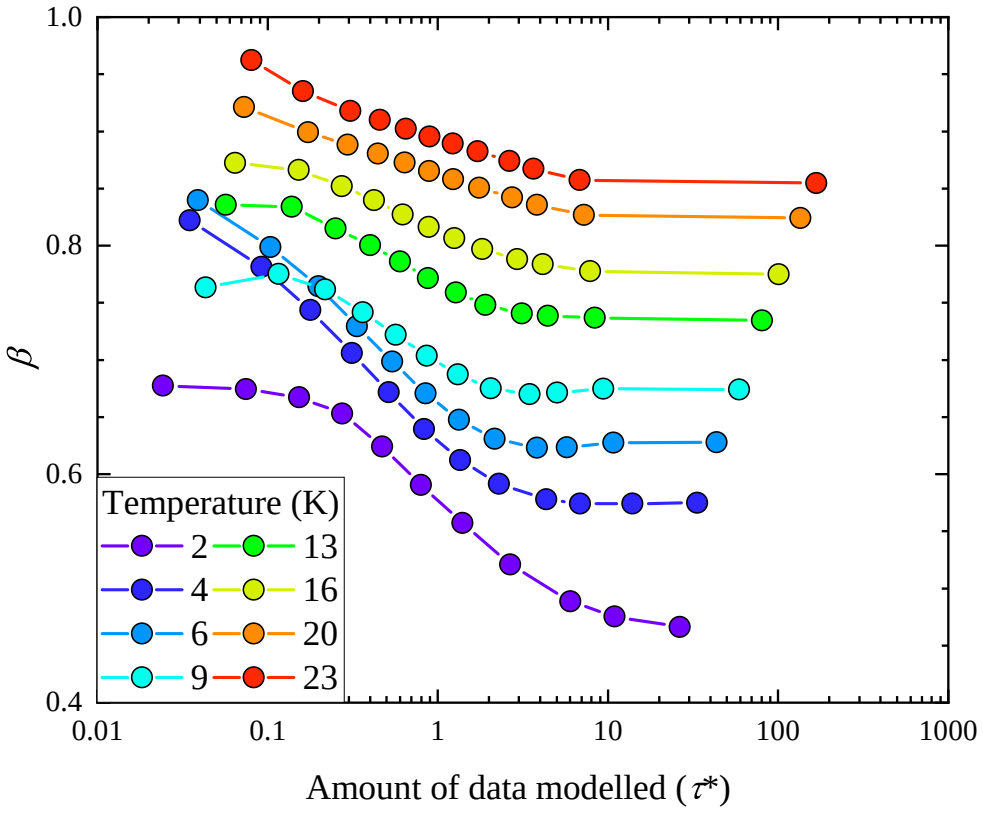

Figure S47: Dependence of how much data is fitted (% of the decay curve) on the β parameter extracted from modelling DC decay data of $[Dy(Dtp)_2][Al\{OC(CF_3)_3\}_4]$ to Eq. 11 with M_0 fixed to the first data point, M_{eq} fixed to target (in this case $M_{eq} = 0$) and $t_{offset} = 0$. τ^* and β are freely fitted.

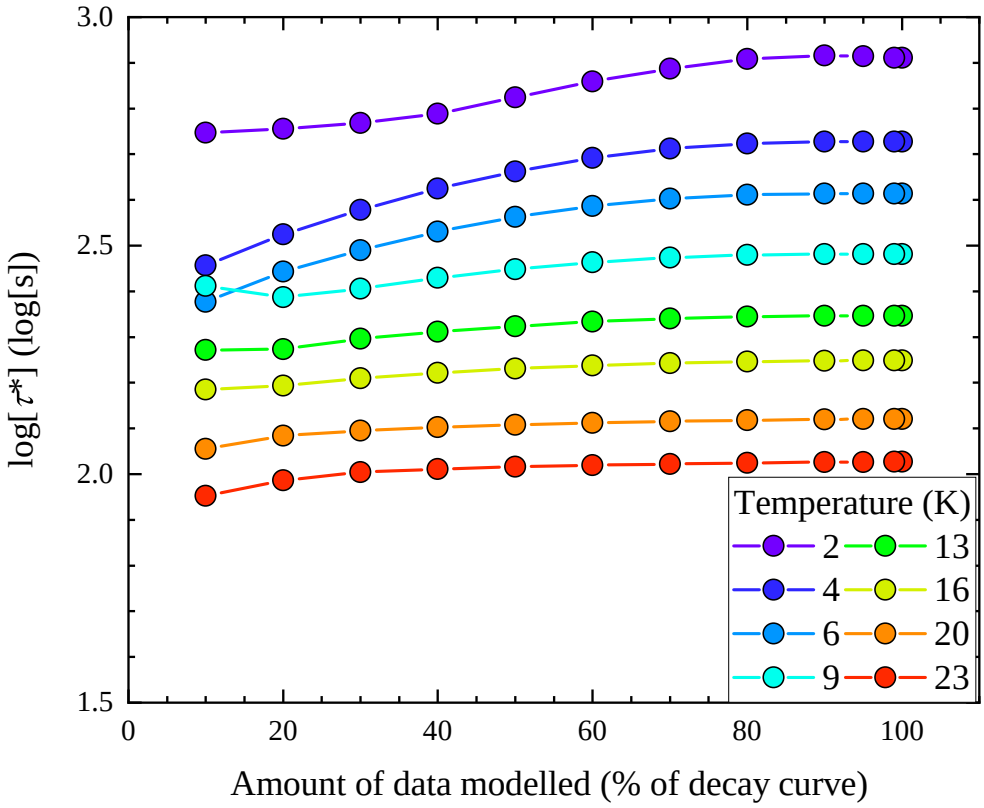

Figure S48: Dependence of how much data is fitted (% of the decay curve) on the τ^* parameter extracted from modelling DC decay data of $[Dy(Dtp)_2][Al\{OC(CF_3)_3\}_4]$ to Eq. 11 with M_0 fixed to the first data point, M_{eq} fixed to target (in this case $M_{eq} = 0$) and $t_{offset} = 0$. τ^* and β are freely fitted.

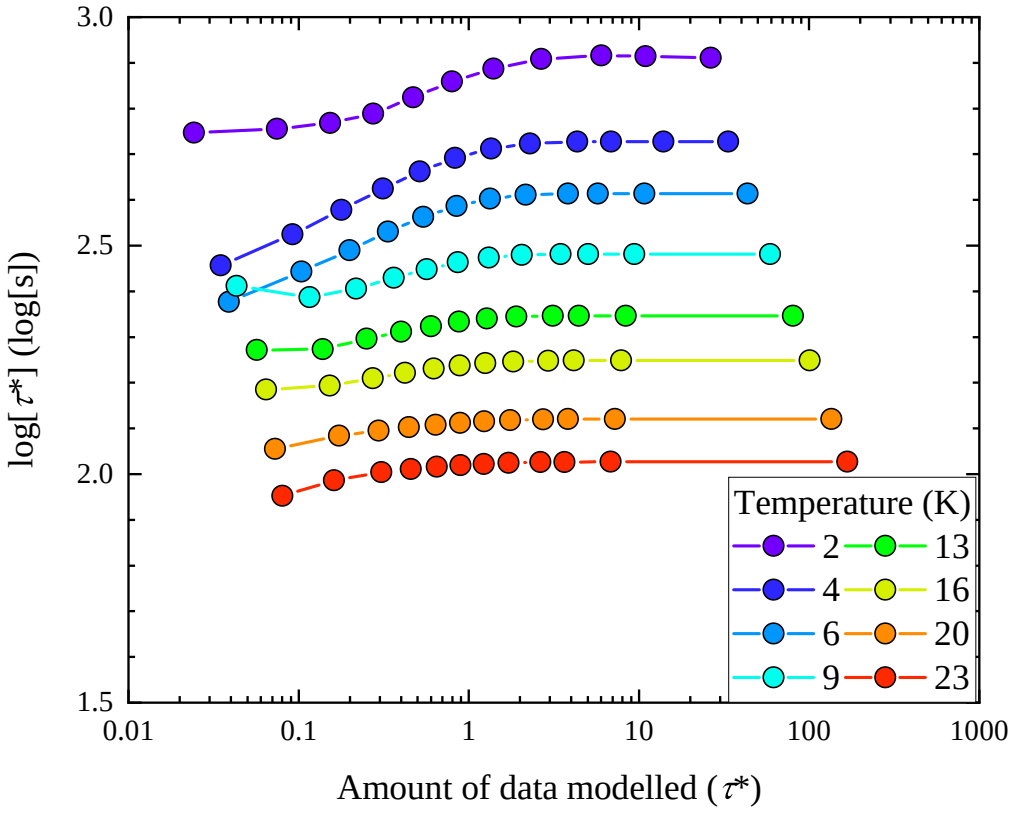

Figure S49: Dependence of how much data is fitted (% of the decay curve) on the τ^* parameter extracted from modelling DC decay data of $[Dy(Dtp)_2][Al\{OC(CF_3)_3\}_4]$ to Eq. 11 with M_0 fixed to the first data point, M_{eq} fixed to target (in this case $M_{eq} = 0$) and $t_{offset} = 0$. τ^* and β are freely fitted.

Table S13: τ^* and β parameters obtained from fitting DC decay data to Eq. 11 with M_0 fixed to the first measured point, $t_{\text{offset}} = 0$ and M_{eq} set to target (in this case $M_{\text{eq}} = 0$). τ^* and β were freely fitted. Data were fitted for various percentages of the decay (99% refers to fitting up to $0.01M_0$). The values shown in this table are for decays measured between 2 and 9 K.

Temperature (K)	2		4		6		9	
% Fitted	τ^* (s)	β	τ^* (s)	β	τ^* (s)	β	τ^* (s)	β
100	814.3	0.466	534.4	0.575	411.0	0.628	302.7	0.674
99	814.3	0.466	534.2	0.574	411.0	0.627	302.8	0.675
95	821.4	0.475	534.1	0.574	410.6	0.624	302.7	0.671
90	824.5	0.489	533.9	0.578	410.6	0.623	302.8	0.670
80	809.9	0.521	529.2	0.592	408.5	0.631	301.8	0.675
70	771.5	0.557	515.9	0.612	400.7	0.647	297.8	0.687
60	723.4	0.591	492.2	0.640	386.1	0.671	290.7	0.704
50	667.2	0.624	459.6	0.671	365.4	0.698	280.9	0.722
40	615.0	0.653	421.6	0.706	339.6	0.729	268.8	0.741
30	586.2	0.667	378.3	0.744	308.8	0.764	254.7	0.762
20	569.4	0.674	334.5	0.781	277.4	0.799	243.9	0.775
10	558.6	0.677	286.5	0.822	238.2	0.840	258.0	0.763

Table S14: τ^* and β parameters obtained from fitting DC decay data to Eq. 11 with M_0 fixed to the first measured point, $t_{\text{offset}} = 0$ and M_{eq} set to target (in this case $M_{\text{eq}} = 0$). τ^* and β were freely fitted. Data were fitted for various percentages of the decay (99% refers to fitting up to $0.01M_0$). The values shown in this table are for decays measured between 13 and 23 K.

Temperature (K)	13		16		20		23	
% Fitted	τ^* (s)	β	τ^* (s)	β	τ^* (s)	β	τ^* (s)	β
100	222.0	0.734	177.3	0.775	132.0	0.824	106.4	0.855
99	222.1	0.737	177.3	0.778	132.1	0.827	106.4	0.857
95	222.1	0.748	177.3	0.784	132.0	0.836	106.3	0.867
90	222.0	0.741	177.1	0.788	131.8	0.842	106.2	0.874
80	221.1	0.748	176.3	0.797	131.2	0.851	105.8	0.883
70	219.0	0.759	174.9	0.807	130.4	0.858	105.3	0.889
60	215.5	0.771	173.0	0.816	129.5	0.865	104.6	0.896
50	210.6	0.786	170.3	0.827	128.2	0.873	103.7	0.902
40	204.8	0.800	166.5	0.840	126.6	0.880	102.5	0.910
30	197.7	0.815	162.2	0.852	124.5	0.888	101.0	0.918
20	187.6	0.834	156.1	0.866	121.3	0.899	96.9	0.935
10	186.9	0.836	153.0	0.872	113.5	0.921	89.7	0.962

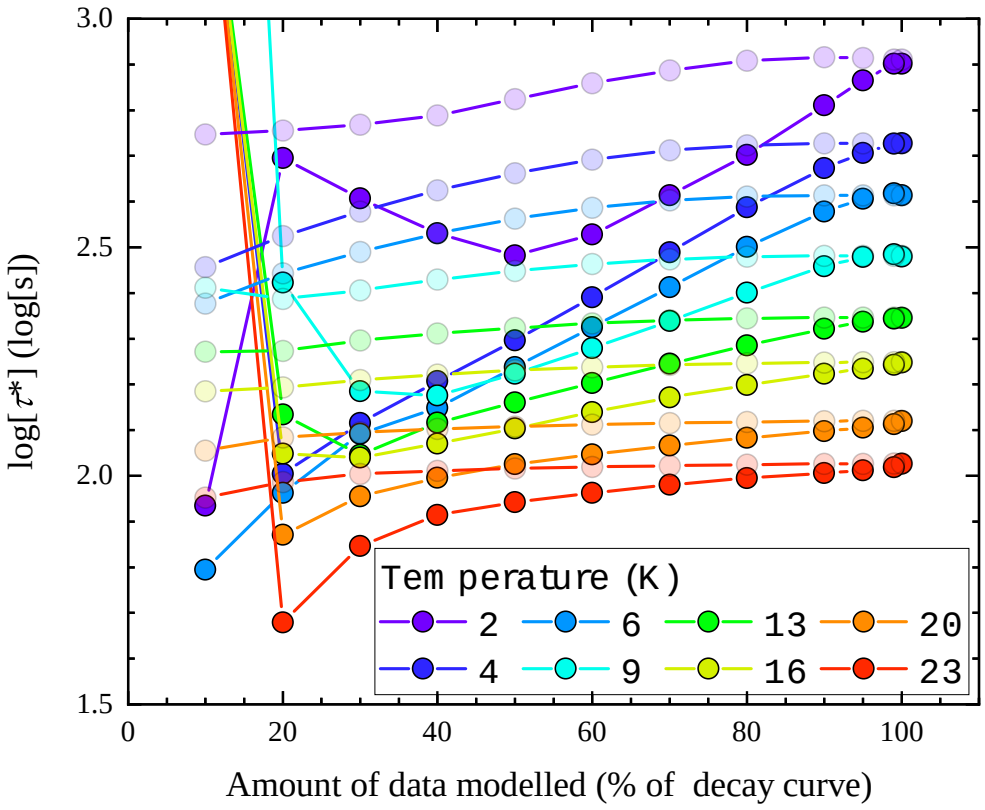

Figure S50: Comparison of Fig. S49 with $M_{eq} = 0$ (transparent) and Fig. S41 with M_{eq} free (opaque).

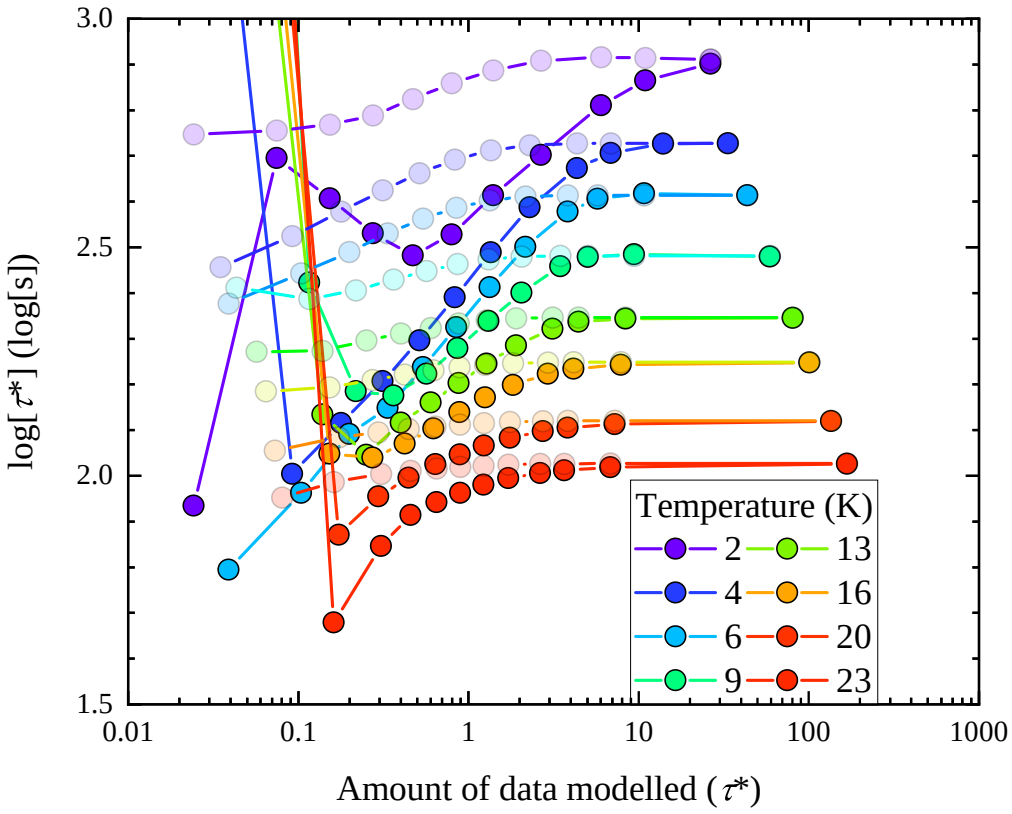

Figure S51: Comparison of Fig. S49 with $M_{eq} = 0$ (transparent) and Fig. S41 with M_{eq} free (opaque).

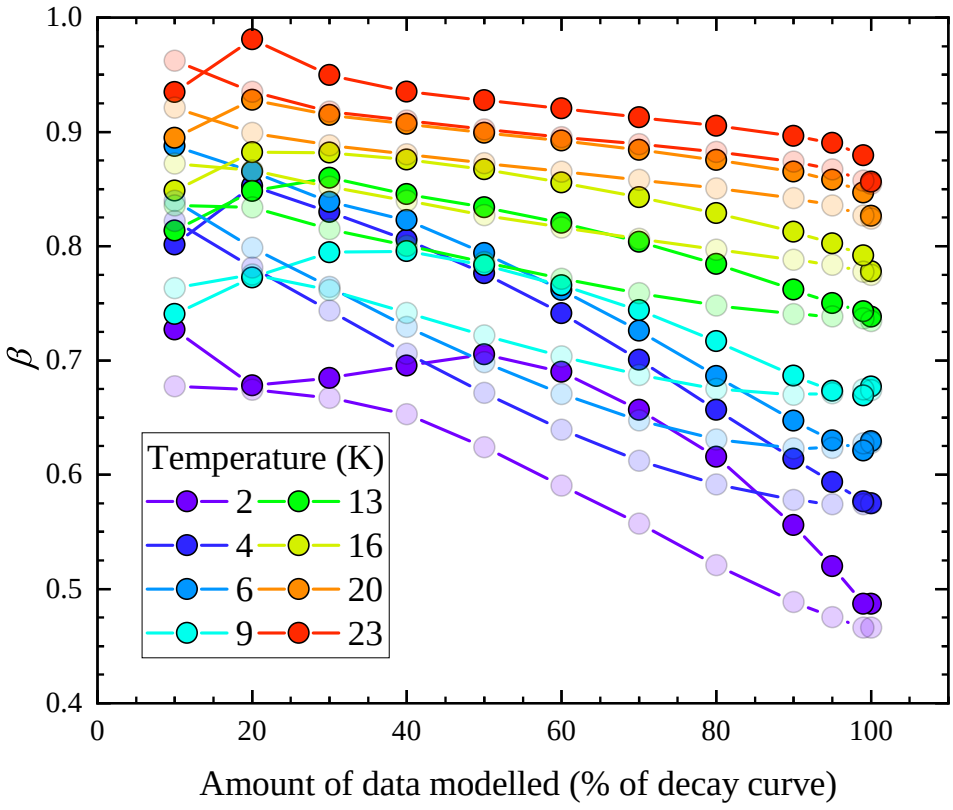

Figure S52: Comparison of Fig. S47 with $M_{eq} = 0$ (transparent) and Fig. S39 with M_{eq} free (opaque).

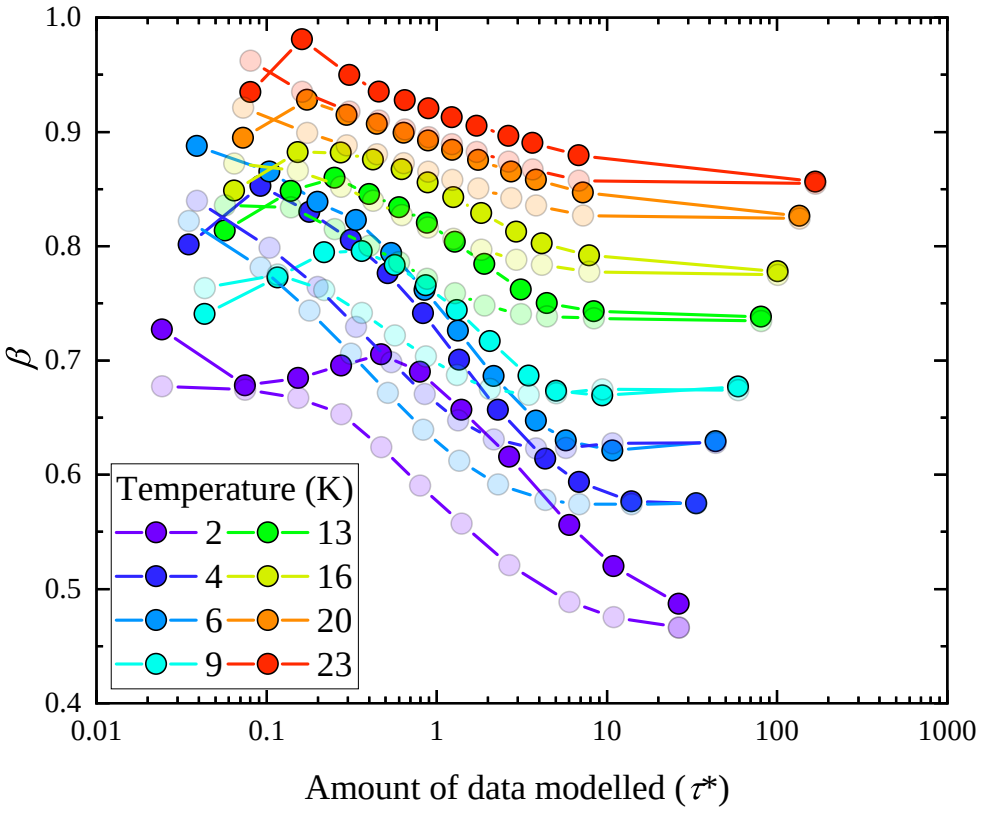

Figure S53: Comparison of Fig. S47 with $M_{eq} = 0$ (transparent) and Fig. S39 with M_{eq} free (opaque).

S2.4 DC decays full range fitting

DC decay magnetisation measurements of polycrystalline samples of $[Dy(Dtp)_2][Al\{OC(CF_3)_3\}_4]$ secured in eicosane as a function of temperature were made in a Quantum Design MPMS3 SQUID magnetometer. The resultant decay traces were analysed using Eq. 11 with different constraints on the fitted parameters as shown in Table S15 and described in Section 4.3.1. The τ^* and β parameters extracted from these fits were used to calculate τ_{mode}, $\langle\tau\rangle$ and $e^{\langle\ln[\tau]\rangle}$. These four measures of τ were then compared to the τ_{debye} extracted from Waveform measurements of $[Dy(Dtp)_2][Al\{OC(CF_3)_3\}_4]$ for all ways of fitting Eq. 11 to determine the best method and metric for characterising SMMs using DC decay measurements.

Fitting the full range of DC decay data taken shows unexpected behaviour at long timescales. These bumps cannot be fitted using an additional mono- or stretched exponential function Fig. S54-S77. We attribute this deviation to small magnetic impurities. Noticeably, the fitting algorithm ignores the deviation from the main stretched exponential function used to model the data. This is due to the very low moment where these impurities dominate ($< 1\%$ of M_0).

Table S15: Labelling scheme for different methods of fitting Eq. 11. As the superconducting magnet has been calibrated to give $H = 0$ then the target $M_{\text{eq}} = 0$.

	M_0	β	t_{offset}	M_{eq}	τ^*
Freely fit	F	F	F	F	F
Fixed to 0	-	-	0	-	-
Fixed to first point	X	-	-	-	-
Fixed to last point	-	-	-	L	-
Fixed to target	-	-	-	0	-

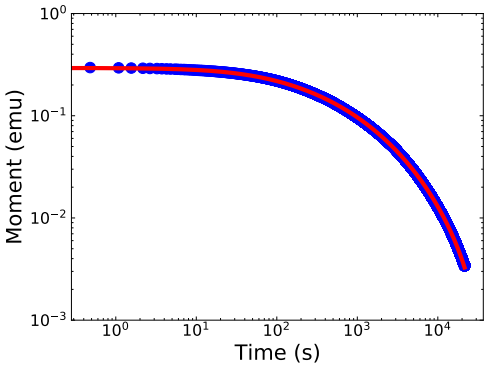

Parameter	Fit result	2 K
M_0 (emu)	0.491	F
β	0.342	F
t_{offset} (s)	36.19	F
M_{eq} (emu)	-1.97×10^{-3}	F
τ^* (s)	256.62	F

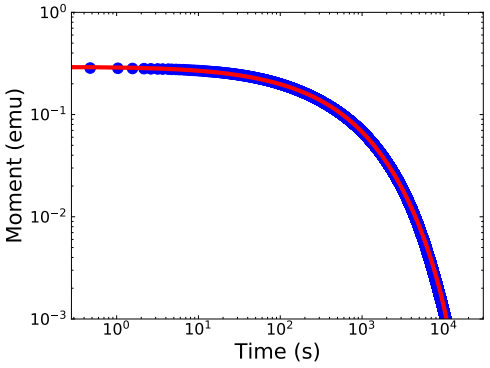

Parameter	Fit result	4 K
M_0 (emu)	0.309	F
β	0.538	F
t_{offset} (s)	2.09	F
M_{eq} (emu)	-3.40×10^{-4}	F
τ^* (s)	462.83	F

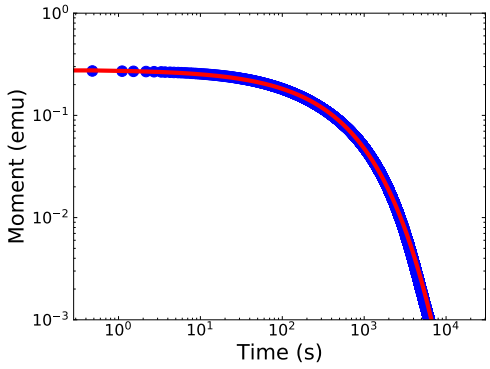

Parameter	Fit result	6 K
M_0 (emu)	0.280	F
β	0.615	F
t_{offset} (s)	3.09×10^{-2}	F
M_{eq} (emu)	5.28×10^{-5}	F
τ^* (s)	392.90	F

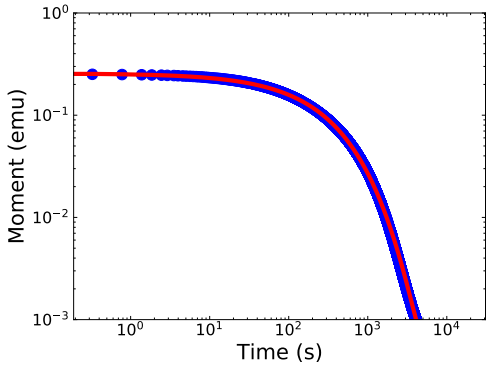

Parameter	Fit result	9 K
M_0 (emu)	0.256	F
β	0.669	F
t_{offset} (s)	1.47×10^{-2}	F
M_{eq} (emu)	2.18×10^{-4}	F
τ^* (s)	295.95	F

Figure S54: Full DC decay curves fitted to Eq. 11 with all parameters fitted freely.

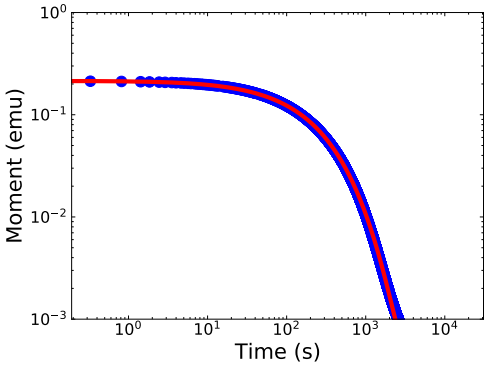

Parameter	Fit result	13 K
M_0 (emu)	0.226	F
β	0.711	F
t_{offset} (s)	3.54	F
M_{eq} (emu)	2.05×10^{-4}	F
τ^* (s)	206.70	F

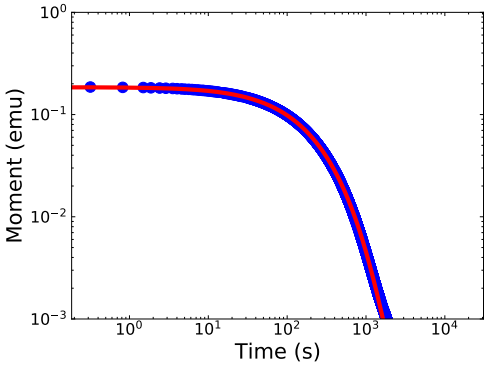

Parameter	Fit result	16 K
M_0 (emu)	0.233	F
β	0.708	F
t_{offset} (s)	18.45	F
M_{eq} (emu)	1.45×10^{-4}	F
τ^* (s)	145.20	F

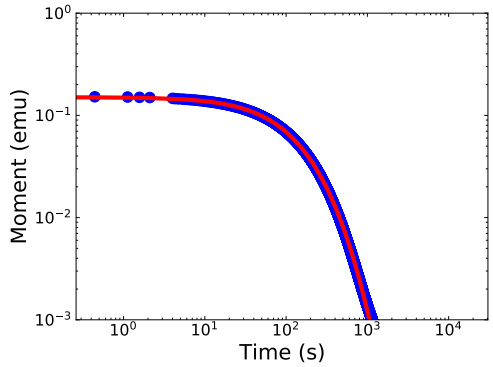

Parameter	Fit result	20 K
M_0 (emu)	0.567	F
β	0.615	F
t_{offset} (s)	88.65	F
M_{eq} (emu)	7.81×10^{-5}	F
τ^* (s)	56.08	F

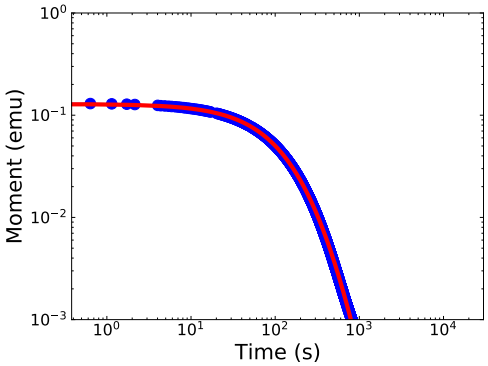

Parameter	Fit result	23 K
M_0 (emu)	1737.4	F
β	0.272	F
t_{offset} (s)	306.75	F
M_{eq} (emu)	4.61×10^{-4}	F
τ^* (s)	3.48×10^{-5}	F

Figure S55: Full DC decay curves fitted to Eq. 11 with all parameters fitted freely.

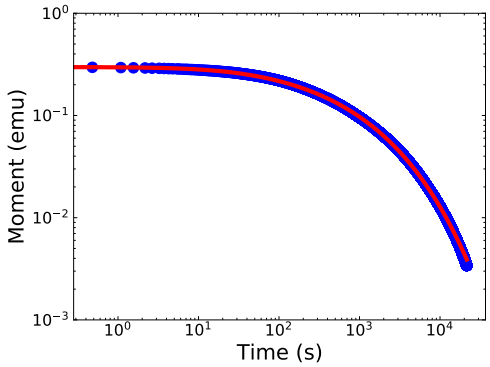

Parameter	Fit result	2 K
M_0 (emu)	0.404	F
β	0.387	F
t_{offset} (s)	18.93	F
M_{eq} (emu)	0	0
τ^* (s)	405.63	F

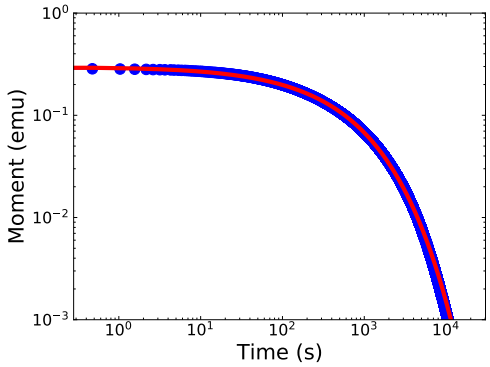

Parameter	Fit result	4 K
M_0 (emu)	0.304	F
β	0.549	F
t_{offset} (s)	0.89	F
M_{eq} (emu)	0	0
τ^* (s)	476.83	F

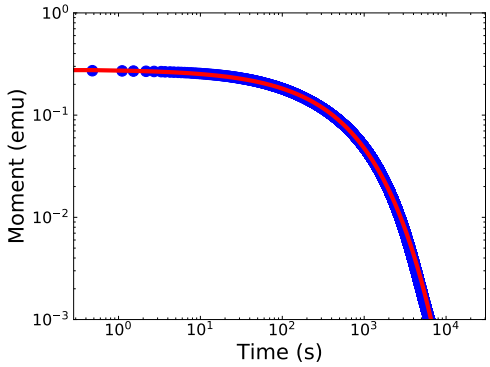

Parameter	Fit result	6 K
M_0 (emu)	0.280	F
β	0.614	F
t_{offset} (s)	0.04	F
M_{eq} (emu)	0	0
τ^* (s)	392.18	F

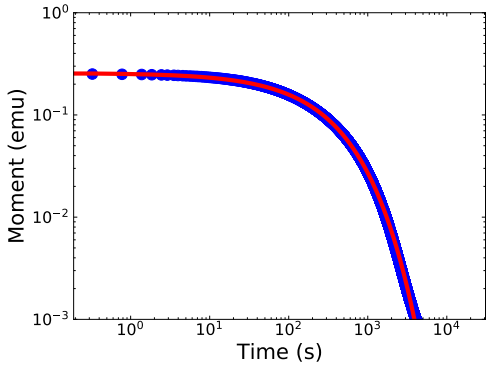

Parameter	Fit result	9 K
M_0 (emu)	0.258	F
β	0.664	F
t_{offset} (s)	0.12	F
M_{eq} (emu)	0	0
τ^* (s)	294.07	F

Figure S56: Full DC decay curves fitted to Eq. 11 with $M_{\text{eq}} = 0$ set to target and all other parameters fitted freely.

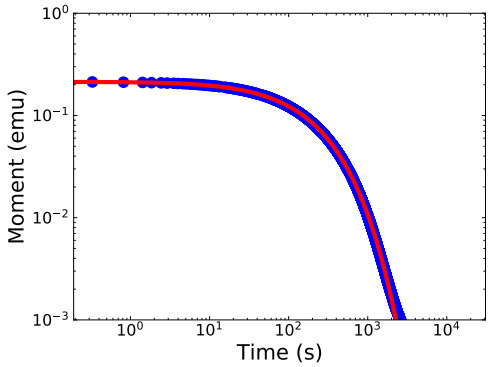

Parameter	Fit result	13 K
M_0 (emu)	0.234	F
β	0.697	F
t_{offset} (s)	6.58	F
M_{eq} (emu)	0	0
τ^* (s)	200.13	F

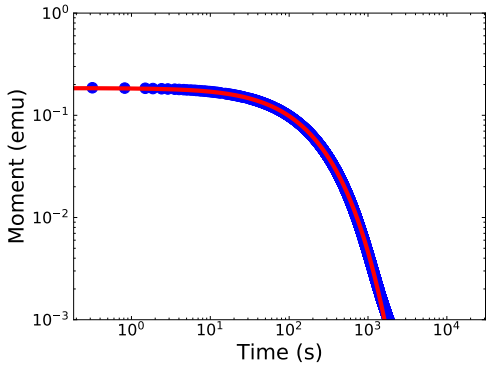

Parameter	Fit result	16 K
M_0 (emu)	0.260	F
β	0.683	F
t_{offset} (s)	27.68	F
M_{eq} (emu)	0	0
τ^* (s)	133.14	F

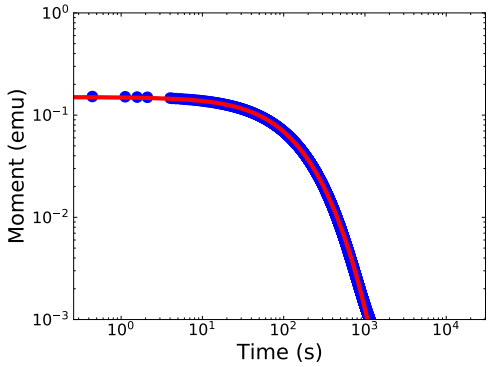

Parameter	Fit result	20 K
M_0 (emu)	1.922	F
β	0.512	F
t_{offset} (s)	146.46	F
M_{eq} (emu)	0	0
τ^* (s)	23.54	F

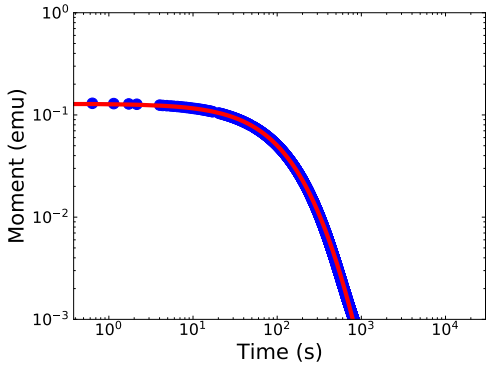

Parameter	Fit result	23 K
M_0 (emu)	1.169×10^5	F
β	0.242	F
t_{offset} (s)	316.86	F
M_{eq} (emu)	0	0
τ^* (s)	6.350×10^{-3}	F

Figure S57: Full DC decay curves fitted to Eq. 11 with $M_{\text{eq}} = 0$ set to target and all other parameters fitted freely.

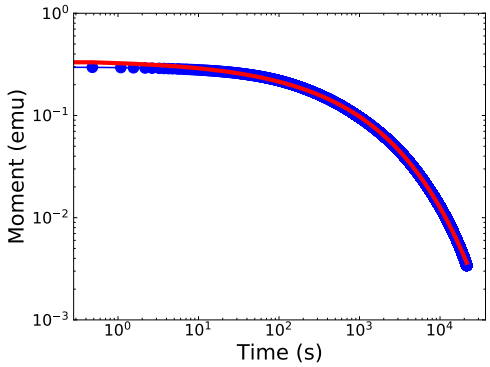

Parameter	Fit result	2 K
M_0 (emu)	0.350	F
β	0.415	F
t_{offset} (s)	0	0
M_{eq} (emu)	0	0
τ^* (s)	553.73	F

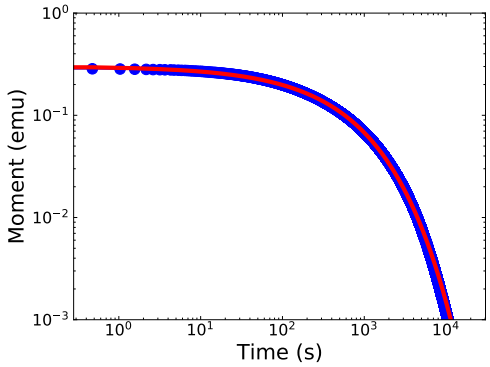

Parameter	Fit result	4 K
M_0 (emu)	0.301	F
β	0.551	F
t_{offset} (s)	0	0
M_{eq} (emu)	0	0
τ^* (s)	482.48	F

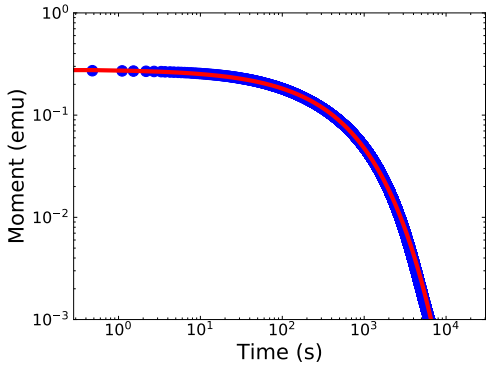

Parameter	Fit result	6 K
M_0 (emu)	0.280	F
β	0.614	F
t_{offset} (s)	0	0
M_{eq} (emu)	0	0
τ^* (s)	392.45	F

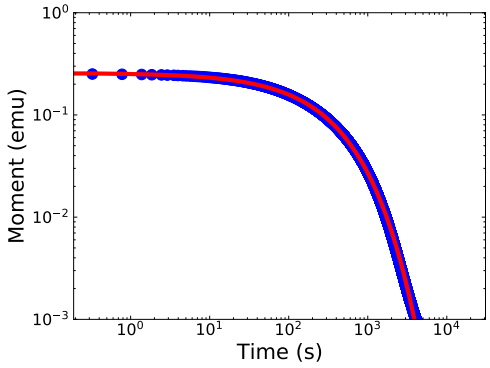

Parameter	Fit result	9 K
M_0 (emu)	0.257	F
β	0.664	F
t_{offset} (s)	0	0
M_{eq} (emu)	0	0
τ^* (s)	294.54	F

Figure S58: Full DC decay curves fitted to Eq. 11 with $M_{\text{eq}} = 0$ set to target, $t_{\text{offset}} = 0$ and all other parameters fitted freely.

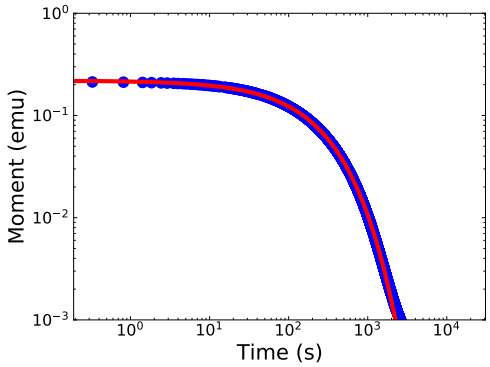

Parameter	Fit result	13 K
M_0 (emu)	0.219	F
β	0.716	F
t_{offset} (s)	0	0
M_{eq} (emu)	0	0
τ^* (s)	212.98	F

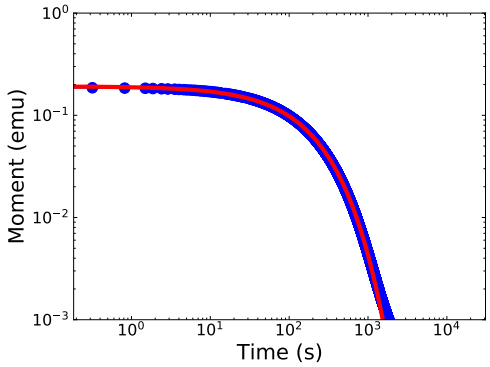

Parameter	Fit result	16 K
M_0 (emu)	0.192	F
β	0.752	F
t_{offset} (s)	0	0
M_{eq} (emu)	0	0
τ^* (s)	169.37	F

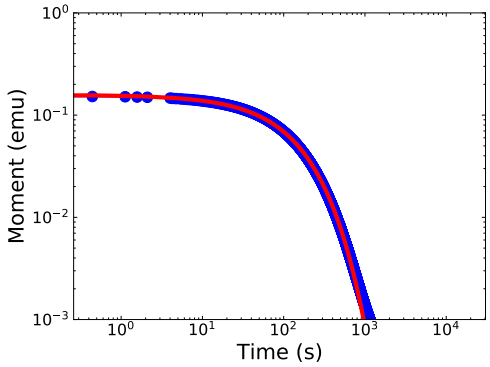

Parameter	Fit result	20 K
M_0 (emu)	0.158	F
β	0.798	F
t_{offset} (s)	0	0
M_{eq} (emu)	0	0
τ^* (s)	126.32	F

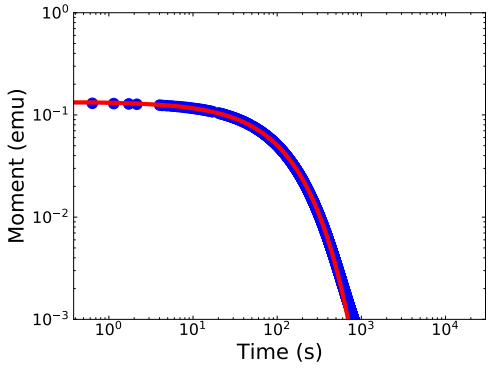

Parameter	Fit result	23 K
M_0 (emu)	0.135	F
β	0.829	F
t_{offset} (s)	0	0
M_{eq} (emu)	0	0
τ^* (s)	102.20	F

Figure S59: Full DC decay curves fitted to Eq. 11 with $M_{\text{eq}} = 0$ set to target, $t_{\text{offset}} = 0$ and all other parameters fitted freely.

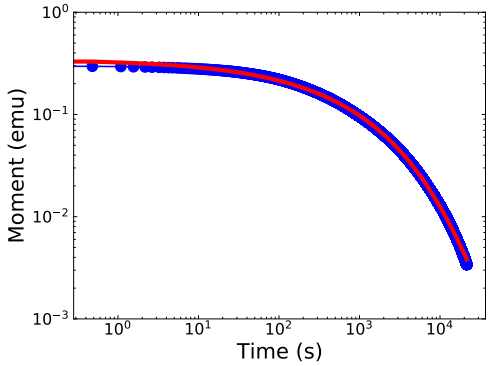

Parameter	Fit result	2 K
M_0 (emu)	0.347	F
β	0.421	F
t_{offset} (s)	0	0
M_{eq} (emu)	4.304×10^{-4}	F
τ^* (s)	565.29	F

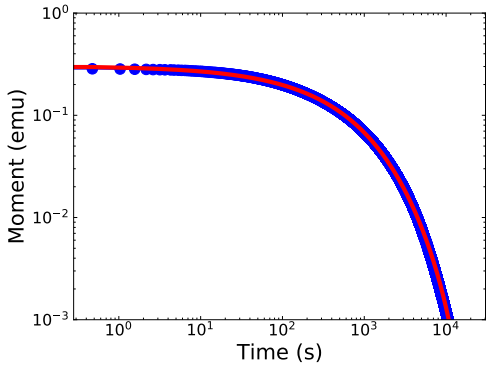

Parameter	Fit result	4 K
M_0 (emu)	0.304	F
β	0.544	F
t_{offset} (s)	0	0
M_{eq} (emu)	-2.918×10^{-4}	F
τ^* (s)	476.50	F

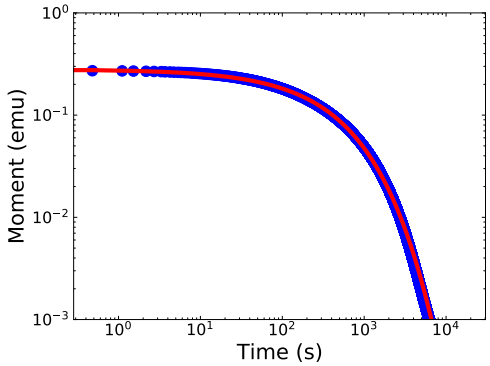

Parameter	Fit result	6 K
M_0 (emu)	0.280	F
β	0.615	F
t_{offset} (s)	0	0
M_{eq} (emu)	5.328×10^{-5}	F
τ^* (s)	393.11	F

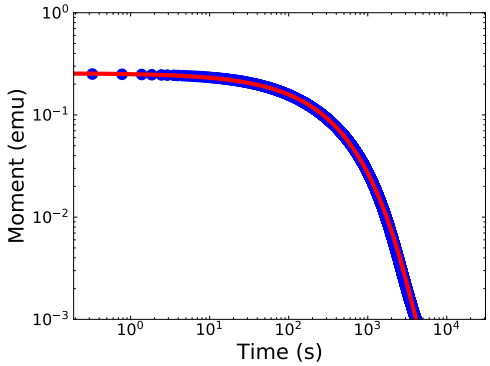

Parameter	Fit result	9 K
M_0 (emu)	0.256	F
β	0.670	F
t_{offset} (s)	0	0
M_{eq} (emu)	2.178×10^{-4}	F
τ^* (s)	296.02	F

Figure S60: Full DC decay curves fitted to Eq. 11 with $t_{\text{offset}} = 0$ and all other parameters fitted freely.

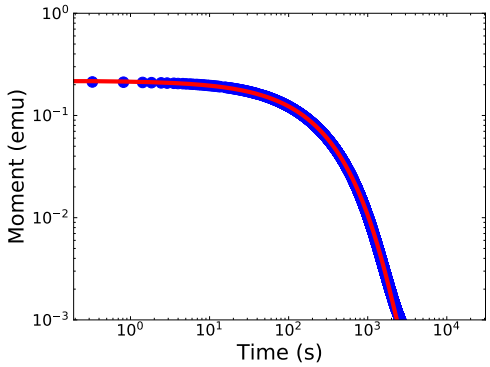

Parameter	Fit result	13 K
M_0 (emu)	0.219	F
β	0.722	F
t_{offset} (s)	0	0
M_{eq} (emu)	2.114×10^{-4}	F
τ^* (s)	213.81	F

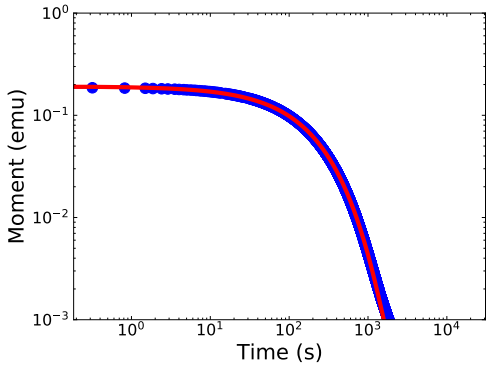

Parameter	Fit result	16 K
M_0 (emu)	0.192	F
β	0.757	F
t_{offset} (s)	0	0
M_{eq} (emu)	1.581×10^{-4}	F
τ^* (s)	169.80	F

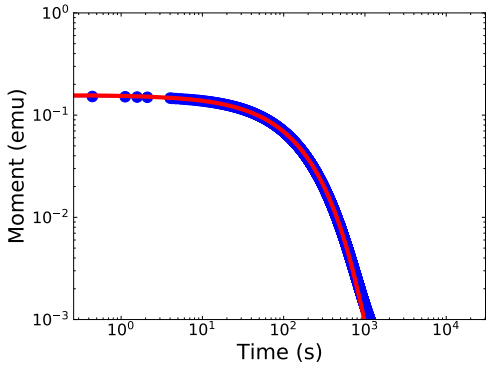

Parameter	Fit result	20 K
M_0 (emu)	0.157	F
β	0.802	F
t_{offset} (s)	0	0
M_{eq} (emu)	9.551×10^{-5}	F
τ^* (s)	126.50	F

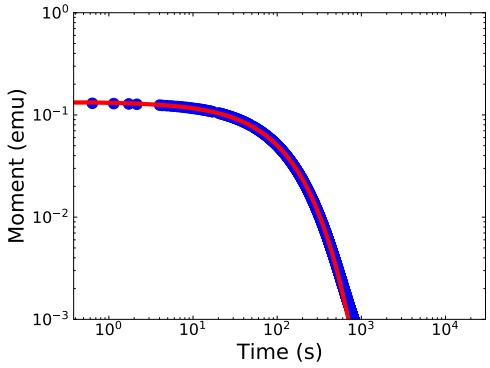

Parameter	Fit result	23 K
M_0 (emu)	0.134	F
β	0.832	F
t_{offset} (s)	0	0
M_{eq} (emu)	6.426×10^{-5}	F
τ^* (s)	102.29	F

Figure S61: Full DC decay curves fitted to Eq. 11 with $t_{\text{offset}} = 0$ and all other parameters fitted freely.

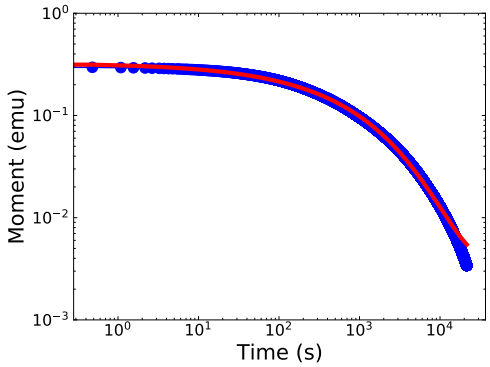

Parameter	Fit result	2 K
M_0 (emu)	0.326	F
β	0.462	F
t_{offset} (s)	0	0
M_{eq} (emu)	3.411×10^{-3}	L
τ^* (s)	645.21	F

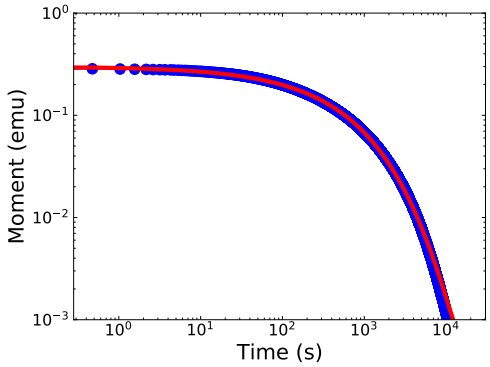

Parameter	Fit result	4 K
M_0 (emu)	0.300	F
β	0.556	F
t_{offset} (s)	0	0
M_{eq} (emu)	2.546×10^{-4}	L
τ^* (s)	487.45	F

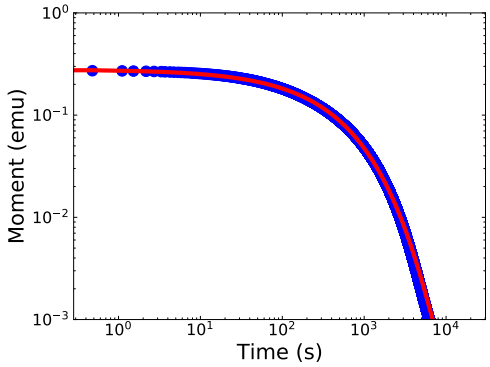

Parameter	Fit result	6 K
M_0 (emu)	0.279	F
β	0.619	F
t_{offset} (s)	0	0
M_{eq} (emu)	1.971×10^{-4}	L
τ^* (s)	394.82	F

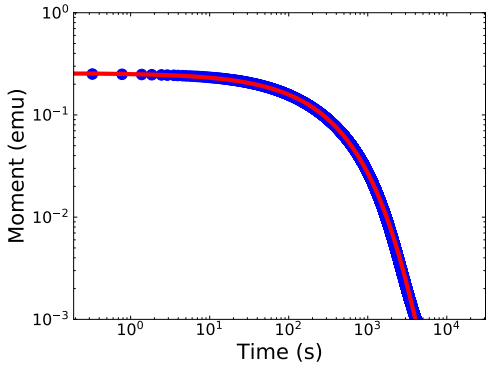

Parameter	Fit result	9 K
M_0 (emu)	0.257	F
β	0.668	F
t_{offset} (s)	0	0
M_{eq} (emu)	1.452×10^{-4}	L
τ^* (s)	295.54	F

Figure S62: Full DC decay curves fitted to Eq. 11 with $t_{\text{offset}} = 0$, M_{eq} set to the last measured values and all other parameters fitted freely.

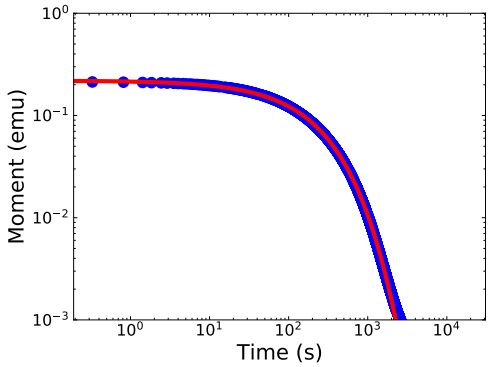

Parameter	Fit result	13 K
M_0 (emu)	0.219	F
β	0.718	F
t_{offset} (s)	0	0
M_{eq} (emu)	6.649×10^{-5}	L
τ^* (s)	213.25	F

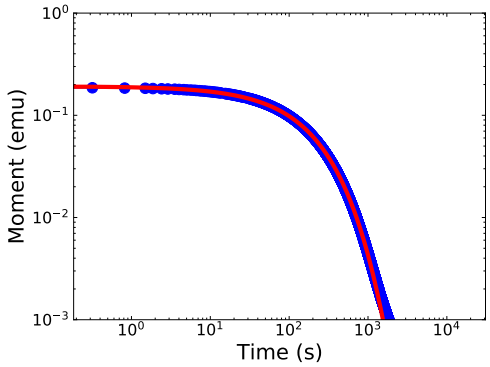

Parameter	Fit result	16 K
M_0 (emu)	0.192	F
β	0.753	F
t_{offset} (s)	0	0
M_{eq} (emu)	3.249×10^{-5}	L
τ^* (s)	169.46	F

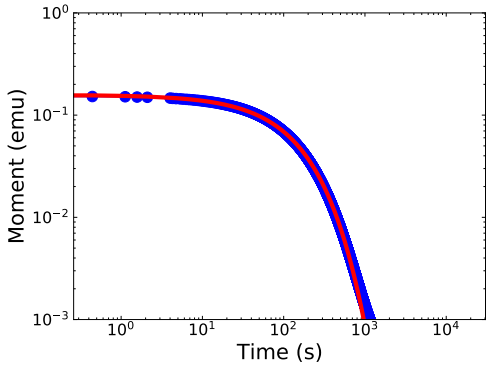

Parameter	Fit result	20 K
M_0 (emu)	0.158	F
β	0.799	F
t_{offset} (s)	0	0
M_{eq} (emu)	1.863×10^{-5}	L
τ^* (s)	126.35	F

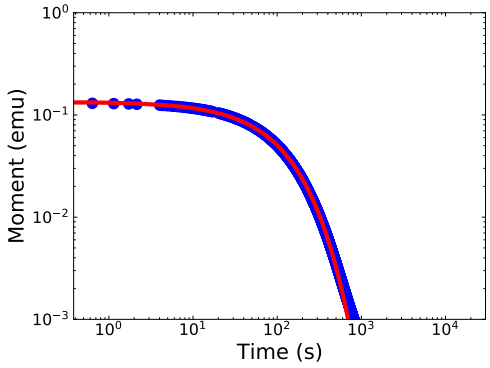

Parameter	Fit result	23 K
M_0 (emu)	0.135	F
β	0.829	F
t_{offset} (s)	0	0
M_{eq} (emu)	1.558×10^{-5}	L
τ^* (s)	102.22	F

Figure S63: Full DC decay curves fitted to Eq. 11 with $t_{\text{offset}} = 0$, M_{eq} set to the last measured values and all other parameters fitted freely.

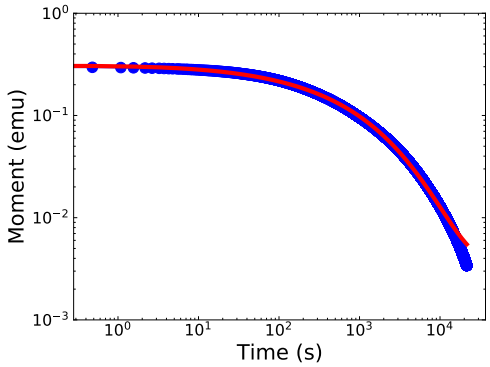

Parameter	Fit result	2 K
M_0 (emu)	0.331	F
β	0.458	F
t_{offset} (s)	2.24	F
M_{eq} (emu)	3.411×10^{-3}	L
τ^* (s)	623.59	F

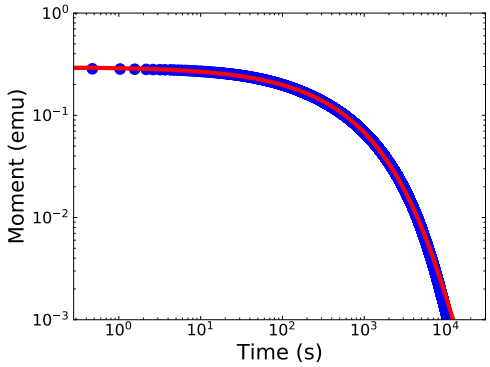

Parameter	Fit result	4 K
M_0 (emu)	0.301	F
β	0.555	F
t_{offset} (s)	0.39	F
M_{eq} (emu)	2.546×10^{-4}	L
τ^* (s)	484.82	F

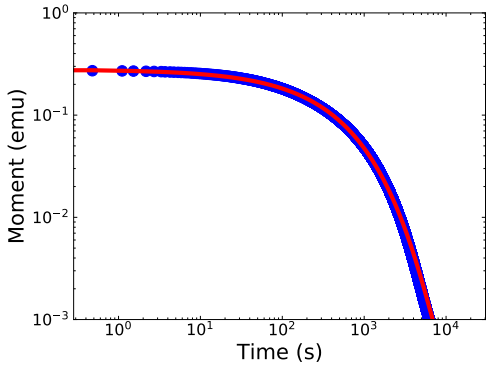

Parameter	Fit result	6 K
M_0 (emu)	0.279	F
β	0.619	F
t_{offset} (s)	1.37×10^{-2}	F
M_{eq} (emu)	1.971×10^{-4}	L
τ^* (s)	394.70	F

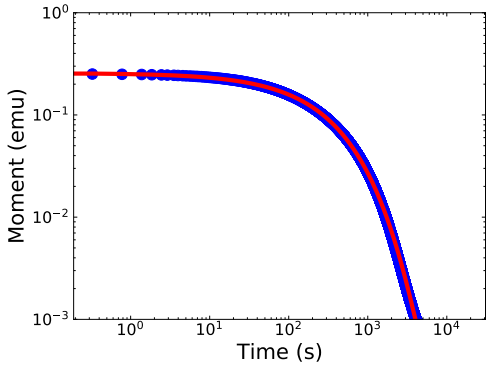

Parameter	Fit result	9 K
M_0 (emu)	0.257	F
β	0.668	F
t_{offset} (s)	3.12×10^{-4}	F
M_{eq} (emu)	1.452×10^{-4}	L
τ^* (s)	295.41	F

Figure S64: Full DC decay curves fitted to Eq. 11 with M_{eq} set to the last measured point and all other parameters fitted freely.

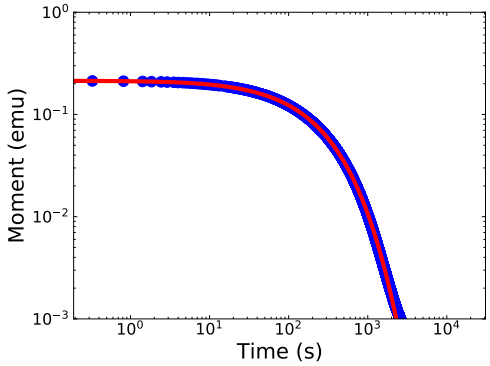

Parameter	Fit result	13K
M_0 (emu)	0.231	F
β	0.702	F
t_{offset} (s)	5.43	F
M_{eq} (emu)	6.649×10^{-5}	L
τ^* (s)	202.56	F

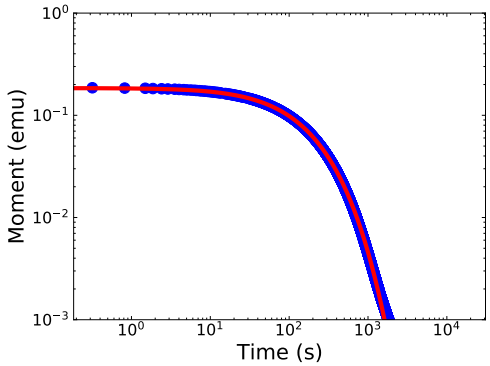

Parameter	Fit result	16 K
M_0 (emu)	0.252	F
β	0.689	F
t_{offset} (s)	25.22	F
M_{eq} (emu)	3.249×10^{-5}	L
τ^* (s)	136.31	F

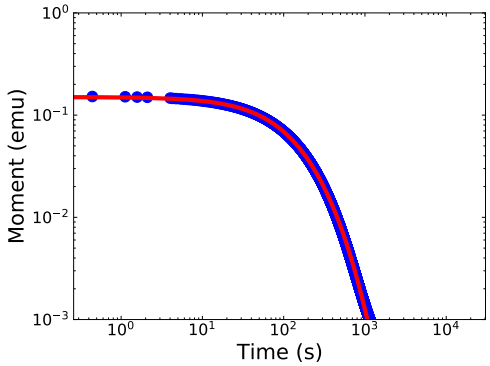

Parameter	Fit result	20 K
M_0 (emu)	1.211	F
β	0.546	F
t_{offset} (s)	126.74	F
M_{eq} (emu)	1.863×10^{-5}	L
τ^* (s)	32.95	F

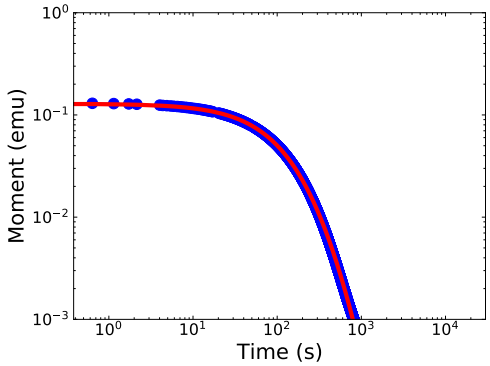

Parameter	Fit result	23 K
M_0 (emu)	7.019×10^{4}	F
β	0.250	F
t_{offset} (s)	314.97	F
M_{eq} (emu)	1.558×10^{-5}	L
τ^* (s)	1.025×10^{-2}	F

Figure S65: Full DC decay curves fitted to Eq. 11 with M_{eq} set to the last measured point and all other parameters fitted freely.

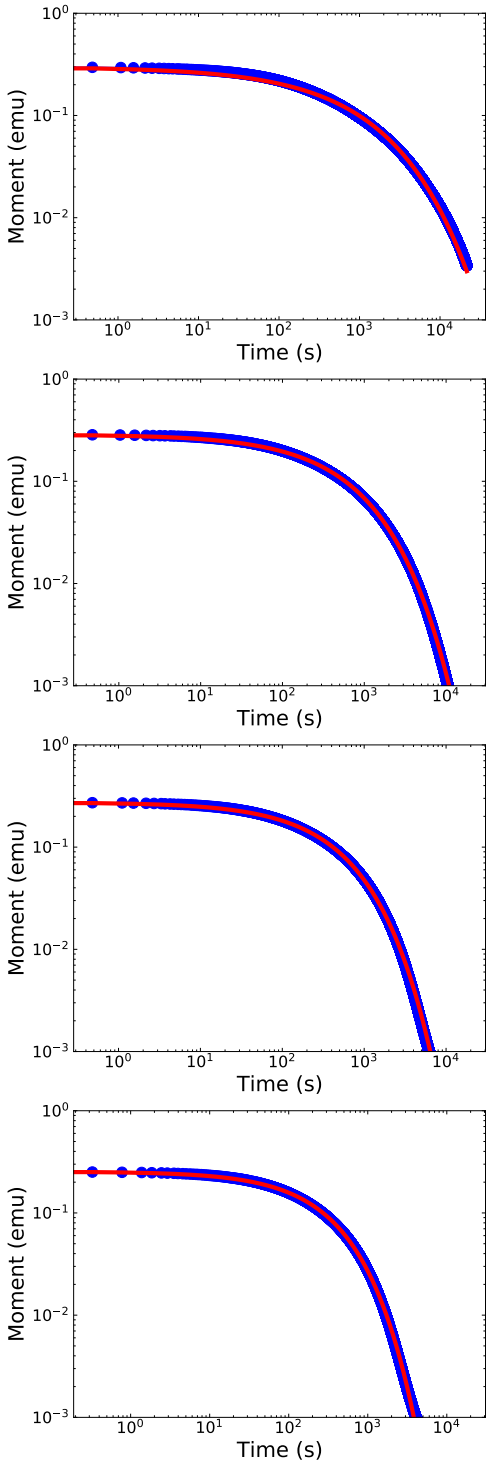

Parameter	Fit result	2 K
M_0 (emu)	0.298	X
β	0.466	F
t_{offset} (s)	0	0
M_{eq} (emu)	0	0
τ^* (s)	814.62	F

Parameter	Fit result	4 K
M_0 (emu)	0.287	X
β	0.575	F
t_{offset} (s)	0	0
M_{eq} (emu)	0	0
τ^* (s)	534.35	F

Parameter	Fit result	2 K
M_0 (emu)	0.273	X
β	0.628	F
t_{offset} (s)	0	0
M_{eq} (emu)	0	0
τ^* (s)	410.98	F

Parameter	Fit result	9 K
M_0 (emu)	0.253	X
β	0.674	F
t_{offset} (s)	0	0
M_{eq} (emu)	0	0
τ^* (s)	302.69	F

Figure S66: Full DC decay curves fitted to Eq. 11 with $M_{\text{eq}} = 0$ set to target magnetisation, M_0 fixed to first measured point at target field, $t_{\text{offset}} = 0$ and α and β fitted freely.

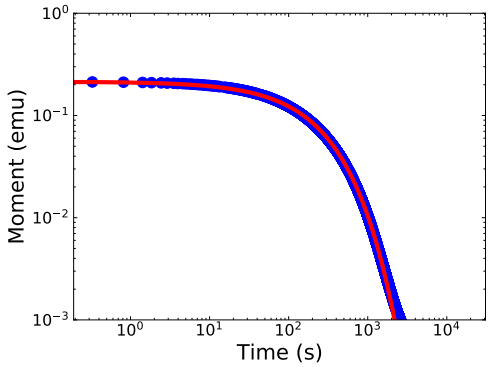

Parameter	Fit result	13 K
M_0 (emu)	0.214	X
β	0.734	F
t_{offset} (s)	0	0
M_{eq} (emu)	0	0
τ^* (s)	222.02	F

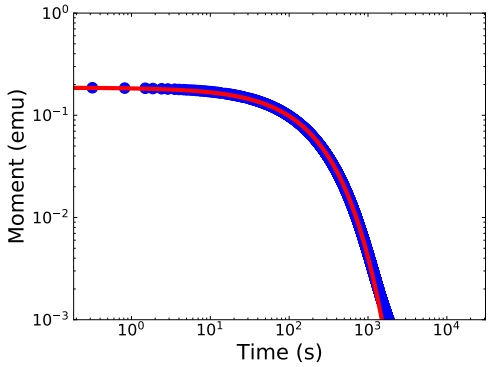

Parameter	Fit result	16 K
M_0 (emu)	0.187	X
β	0.775	F
t_{offset} (s)	0	0
M_{eq} (emu)	0	0
τ^* (s)	177.25	F

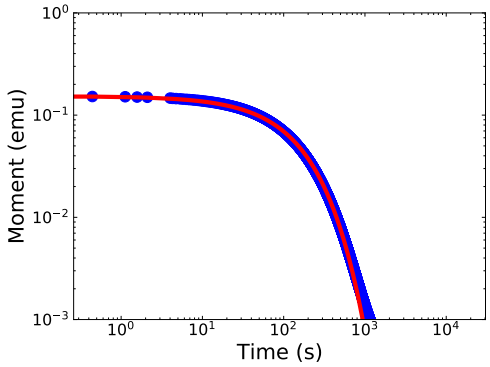

Parameter	Fit result	20 K
M_0 (emu)	0.153	X
β	0.824	F
t_{offset} (s)	0	0
M_{eq} (emu)	0	0
τ^* (s)	132.05	F

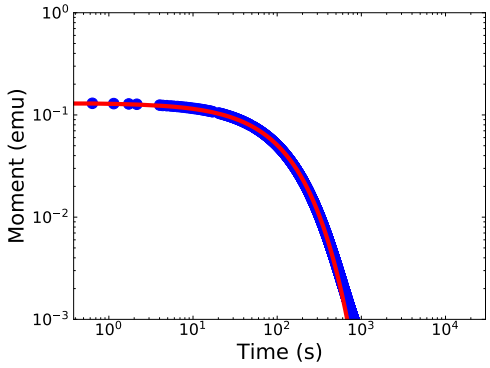

Parameter	Fit result	23 K
M_0 (emu)	0.131	X
β	0.855	F
t_{offset} (s)	0	0
M_{eq} (emu)	0	0
τ^* (s)	106.40	F

Figure S67: Full DC decay curves fitted to Eq. 11 with $M_{\text{eq}} = 0$ set to target magnetisation, M_0 fixed to first measured point at target field, $t_{\text{offset}} = 0$ and α and β fitted freely.

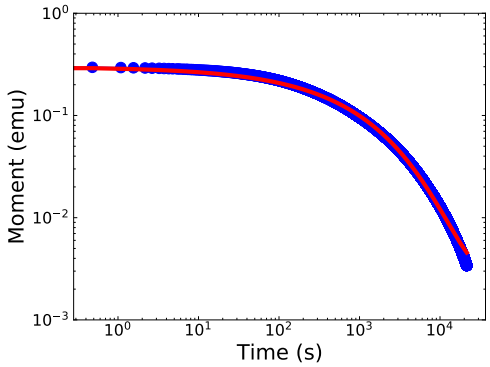

Parameter	Fit result	2 K
M_0 (emu)	0.298	X
β	0.487	F
t_{offset} (s)	0	0
M_{eq} (emu)	2.516×10^{-3}	F
τ^* (s)	796.55	F

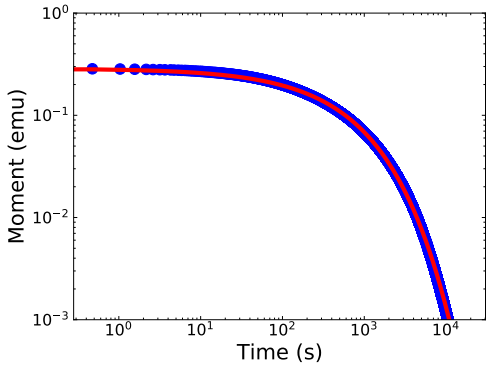

Parameter	Fit result	4 K
M_0 (emu)	0.287	X
β	0.575	F
t_{offset} (s)	0	0
M_{eq} (emu)	6.245×10^{-6}	F
τ^* (s)	534.32	F

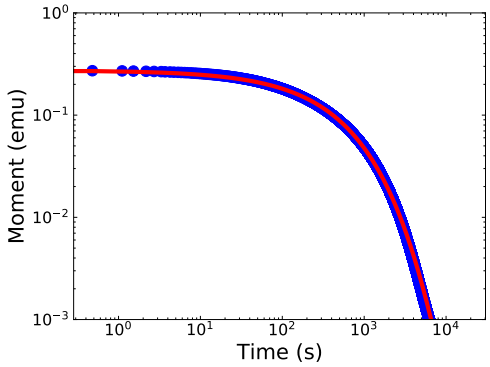

Parameter	Fit result	6 K
M_0 (emu)	0.273	X
β	0.629	F
t_{offset} (s)	0	0
M_{eq} (emu)	1.061×10^{-4}	F
τ^* (s)	410.58	F

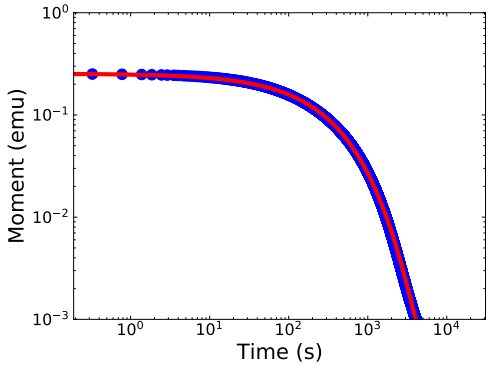

Parameter	Fit result	9 K
M_0 (emu)	0.253	X
β	0.677	F
t_{offset} (s)	0	0
M_{eq} (emu)	2.319×10^{-4}	F
τ^* (s)	301.98	F

Figure S68: Full DC decay curves fitted to Eq. 11 with M_0 fixed to first measured point at target field, $t_{\text{offset}} = 0$ and all other parameters fitted freely.

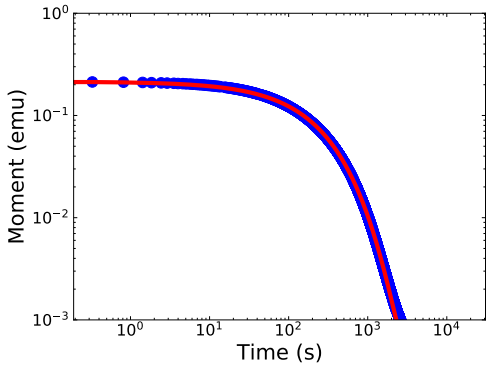

Parameter	Fit result	13 K
M_0 (emu)	0.214	X
β	0.738	F
t_{offset} (s)	0	0
M_{eq} (emu)	2.248×10^{-4}	F
τ^* (s)	221.43	F

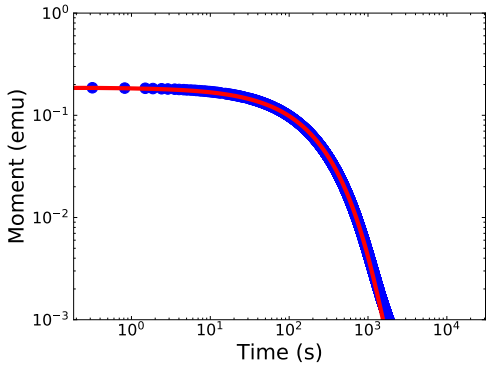

Parameter	Fit result	16 K
M_0 (emu)	0.187	X
β	0.778	F
t_{offset} (s)	0	0
M_{eq} (emu)	1.686×10^{-4}	F
τ^* (s)	176.85	F

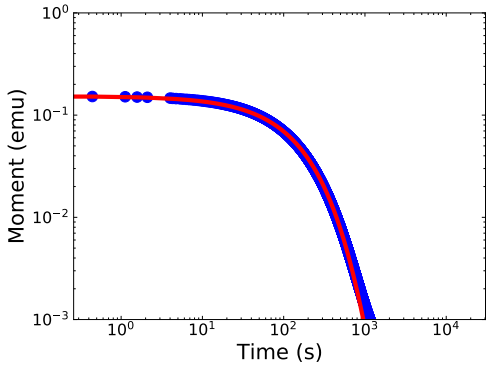

Parameter	Fit result	20 K
M_0 (emu)	0.153	X
β	0.826	F
t_{offset} (s)	0	0
M_{eq} (emu)	1.019×10^{-4}	F
τ^* (s)	131.82	F

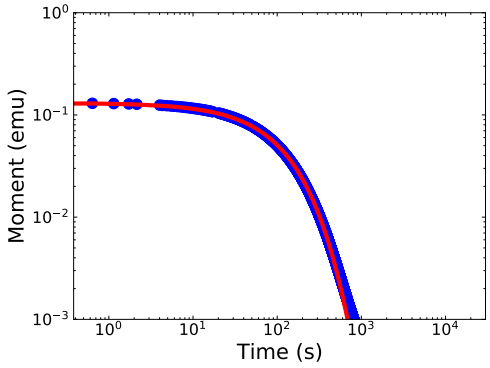

Parameter	Fit result	23 K
M_0 (emu)	0.133	X
β	0.856	F
t_{offset} (s)	0	0
M_{eq} (emu)	6.817×10^{-5}	F
τ^* (s)	106.26	F

Figure S69: Full DC decay curves fitted to Eq. 11 with M_0 fixed to first measured point at target field, $t_{\text{offset}} = 0$ and all other parameters fitted freely.

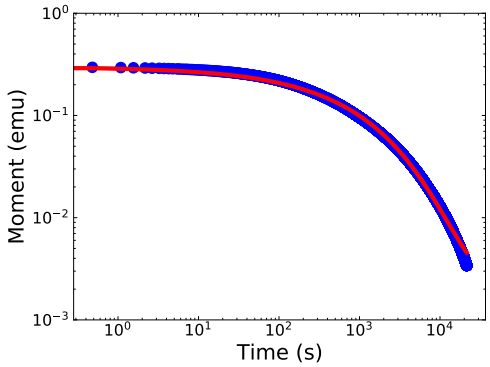

Parameter	Fit result	2 K
M_0 (emu)	0.298	X
β	0.487	F
t_{offset} (s)	1.517×10^{-26}	F
M_{eq} (emu)	2.516×10^{-3}	F
τ^* (s)	796.55	F

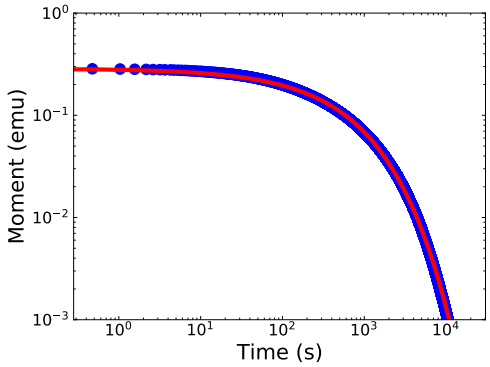

Parameter	Fit result	4 K
M_0 (emu)	0.287	X
β	0.575	F
t_{offset} (s)	6.378×10^{-21}	F
M_{eq} (emu)	6.245×10^{-6}	F
τ^* (s)	534.32	F

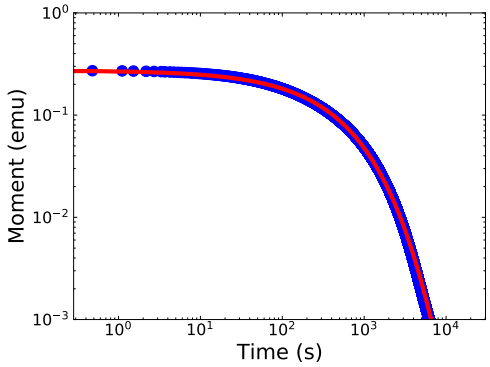

Parameter	Fit result	6 K
M_0 (emu)	0.273	X
β	0.629	F
t_{offset} (s)	3.192×10^{-22}	F
M_{eq} (emu)	1.091×10^{-4}	F
τ^* (s)	410.58	F

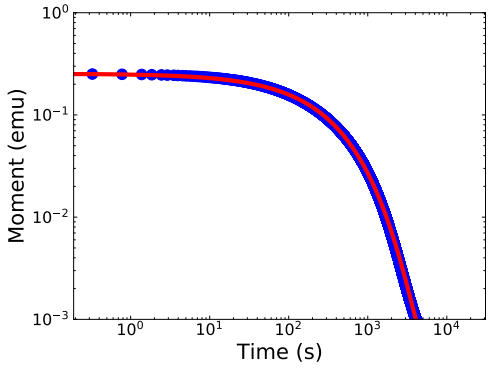

Parameter	Fit result	9 K
M_0 (emu)	0.253	X
β	0.677	F
t_{offset} (s)	3.213×10^{-19}	F
M_{eq} (emu)	2.319×10^{-4}	F
τ^* (s)	301.98	F

Figure S70: Full DC decay curves fitted to Eq. 11 with M_0 fixed to first measured point at target field and all other parameters fitted freely.

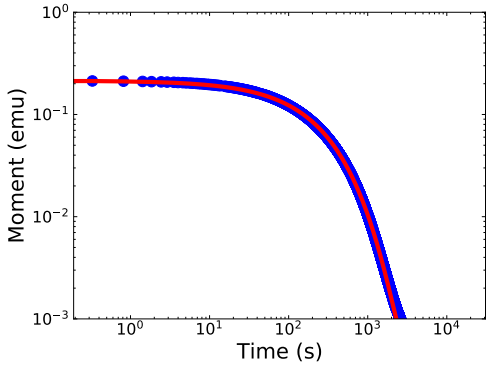

Parameter	Fit result	13 K
M_0 (emu)	0.214	X
β	0.738	F
t_{offset} (s)	8.3454×10^{-24}	F
M_{eq} (emu)	2.248×10^{-4}	F
τ^* (s)	221.43	F

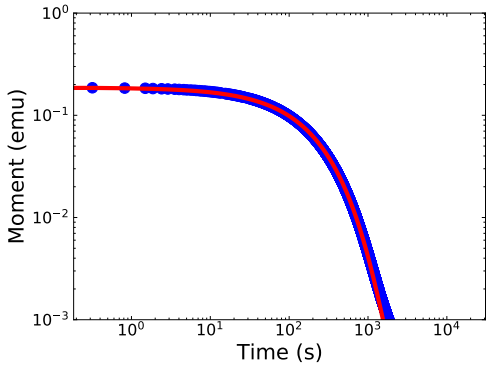

Parameter	Fit result	16 K
M_0 (emu)	0.187	X
β	0.778	F
t_{offset} (s)	4.094×10^{-25}	F
M_{eq} (emu)	1.686×10^{-4}	F
τ^* (s)	176.85	F

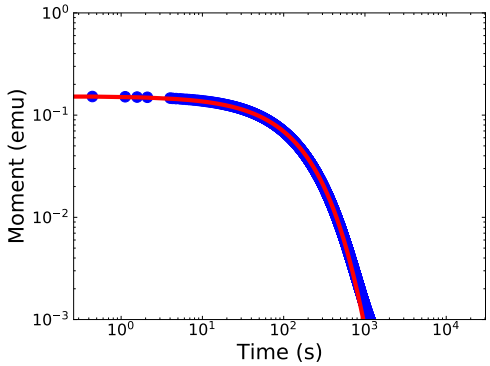

Parameter	Fit result	20 K
M_0 (emu)	0.153	X
β	0.826	F
t_{offset} (s)	1.885×10^{-22}	F
M_{eq} (emu)	1.019×10^{-4}	F
τ^* (s)	131.82	F

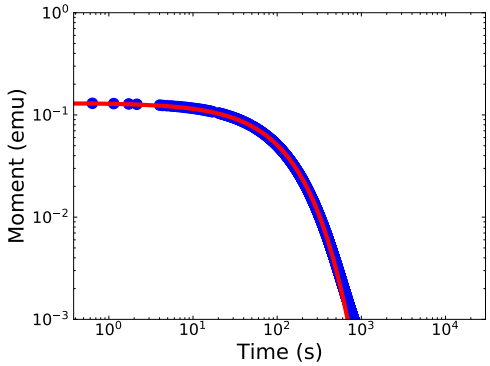

Parameter	Fit result	9 K
M_0 (emu)	0.131	X
β	0.856	F
t_{offset} (s)	3.483×10^{-19}	F
M_{eq} (emu)	6.817×10^{-5}	F
τ^* (s)	106.26	F

Figure S71: Full DC decay curves fitted to Eq. 11 with M_0 fixed to first measured point at target field and all other parameters fitted freely.

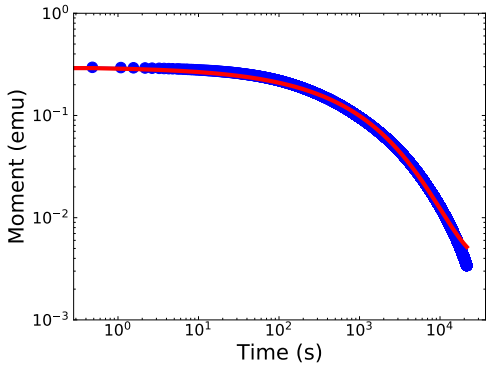

Parameter	Fit result	2 K
M_0 (emu)	0.298	X
β	0.494	F
t_{offset} (s)	2.137×10^{-19}	F
M_{eq} (emu)	3.411×10^{-3}	L
τ^* (s)	793.23	F

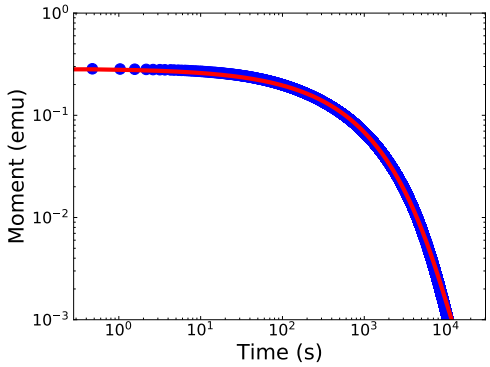

Parameter	Fit result	4 K
M_0 (emu)	0.287	X
β	0.578	F
t_{offset} (s)	1.084×10^{-19}	F
M_{eq} (emu)	2.546×10^{-4}	L
τ^* (s)	533.25	F

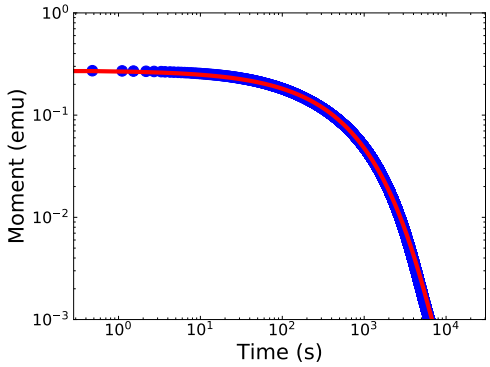

Parameter	Fit result	6 K
M_0 (emu)	0.273	X
β	0.630	F
t_{offset} (s)	1.567×10^{-22}	F
M_{eq} (emu)	1.971×10^{-4}	L
τ^* (s)	410.25	F

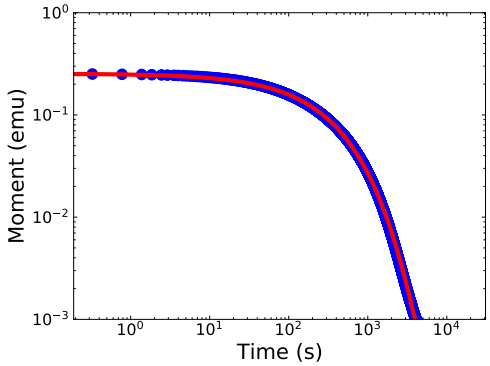

Parameter	Fit result	9 K
M_0 (emu)	0.253	X
β	0.676	F
t_{offset} (s)	4.043×10^{-21}	F
M_{eq} (emu)	1.452×10^{-4}	L
τ^* (s)	302.25	F

Figure S72: Full DC decay curves fitted to Eq. 11 with M_0 fixed to first measured point at target field, M_{eq} set to the last measured point and all other parameters fitted freely.

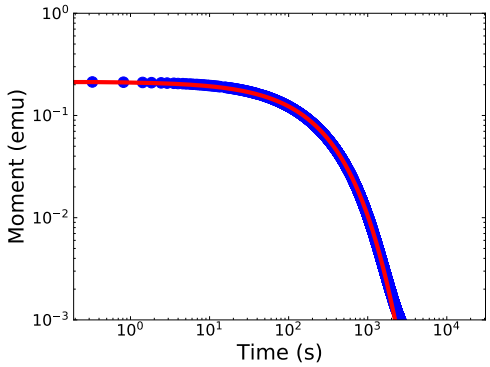

Parameter	Fit result	13 K
M_0 (emu)	0.214	X
β	0.736	F
t_{offset} (s)	1.459×10^{-22}	F
M_{eq} (emu)	6.649×10^{-5}	L
τ^* (s)	221.84	F

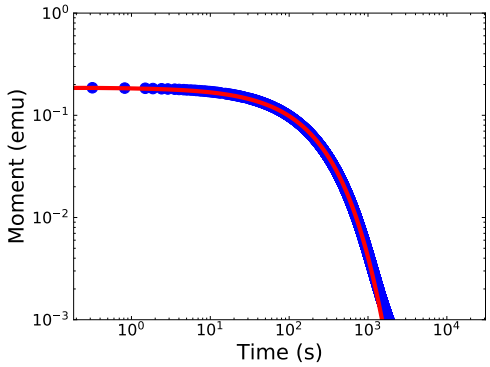

Parameter	Fit result	16 K
M_0 (emu)	0.187	X
β	0.776	F
t_{offset} (s)	1.131×10^{-24}	F
M_{eq} (emu)	3.249×10^{-5}	L
τ^* (s)	177.18	F

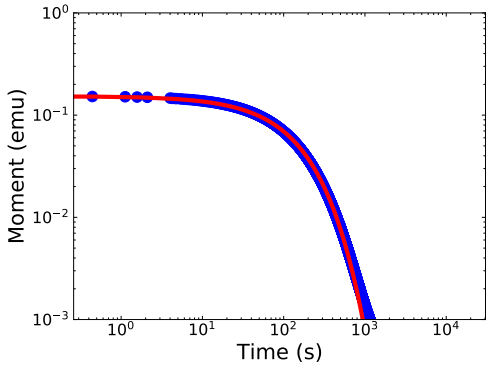

Parameter	Fit result	20 K
M_0 (emu)	0.153	X
β	0.825	F
t_{offset} (s)	3.600×10^{-22}	F
M_{eq} (emu)	1.863×10^{-5}	L
τ^* (s)	132.01	F

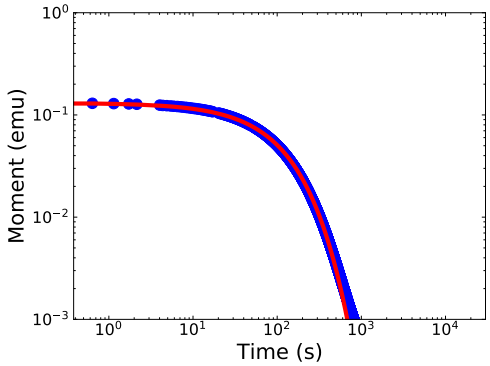

Parameter	Fit result	23 K
M_0 (emu)	0.131	X
β	0.855	F
t_{offset} (s)	3.916×10^{-19}	F
M_{eq} (emu)	1.558×10^{-5}	L
τ^* (s)	106.36	F

Figure S73: Full DC decay curves fitted to Eq. 11 with M_0 fixed to first measured point at target field, M_{eq} set to the last measured point and all other parameters fitted freely.

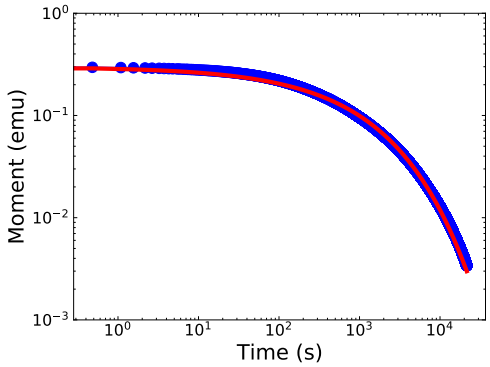

Parameter	Fit result	2 K
M_0 (emu)	0.298	X
β	0.466	F
t_{offset} (s)	8.376×10^{-23}	F
M_{eq} (emu)	0	0
τ^* (s)	814.26	F

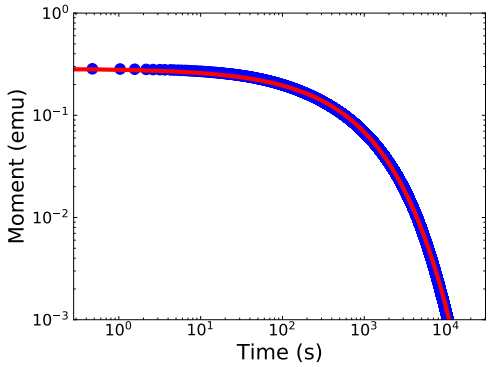

Parameter	Fit result	4 K
M_0 (emu)	0.287	X
β	0.575	F
t_{offset} (s)	1.854×10^{-20}	F
M_{eq} (emu)	0	0
τ^* (s)	534.35	F

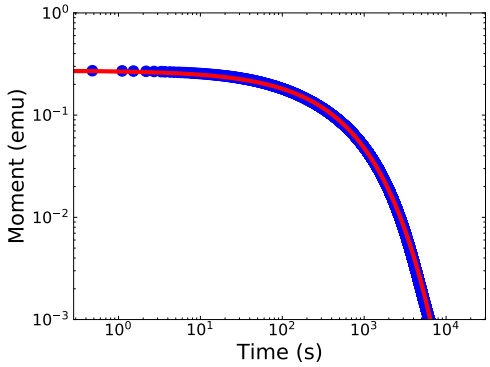

Parameter	Fit result	6 K
M_0 (emu)	0.273	X
β	0.628	F
t_{offset} (s)	2.206×10^{-22}	F
M_{eq} (emu)	0	0
τ^* (s)	410.98	F

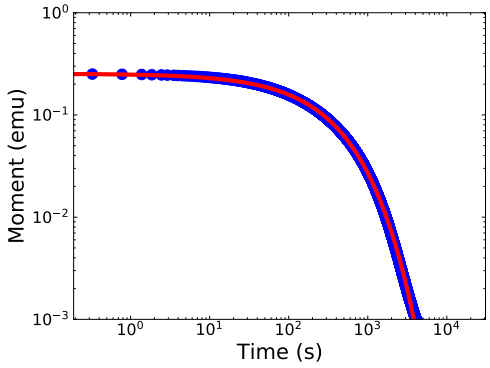

Parameter	Fit result	9 K
M_0 (emu)	0.253	X
β	0.674	F
t_{offset} (s)	3.774×10^{-19}	F
M_{eq} (emu)	0	0
τ^* (s)	302.69	F

Figure S74: Full DC decay curves fitted to Eq. 11 with M_0 fixed to first measured point at target field, M_{eq} set to the target magnetisation and all other parameters fitted freely.

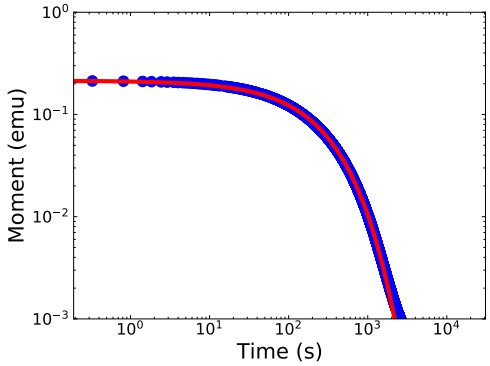

Parameter	Fit result	13 K
M_0 (emu)	0.214	X
β	0.734	F
t_{offset} (s)	3.241×10^{-22}	F
M_{eq} (emu)	0	0
τ^* (s)	222.02	F

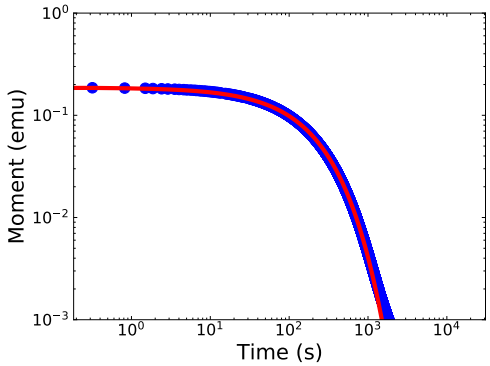

Parameter	Fit result	16 K
M_0 (emu)	0.187	X
β	0.775	F
t_{offset} (s)	1.542×10^{-24}	F
M_{eq} (emu)	0	0
τ^* (s)	177.25	F

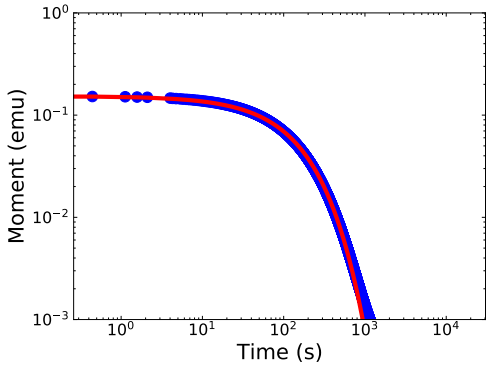

Parameter	Fit result	20 K
M_0 (emu)	0.153	X
β	0.824	F
t_{offset} (s)	4.283×10^{-22}	F
M_{eq} (emu)	0	0
τ^* (s)	132.05	F

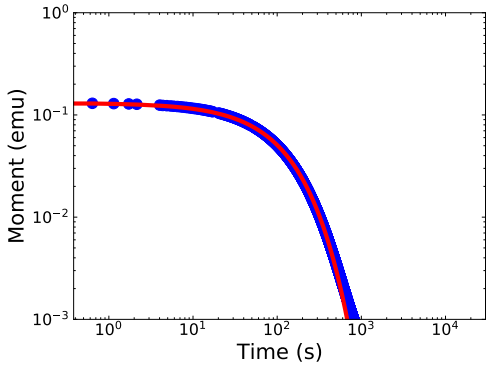

Parameter	Fit result	23 K
M_0 (emu)	0.131	X
β	0.855	F
t_{offset} (s)	4.250×10^{-19}	F
M_{eq} (emu)	0	0
τ^* (s)	106.40	F

Figure S75: Full DC decay curves fitted to Eq. 11 with M_0 fixed to first measured point at target field, M_{eq} set to the target magnetisation and all other parameters fitted freely.

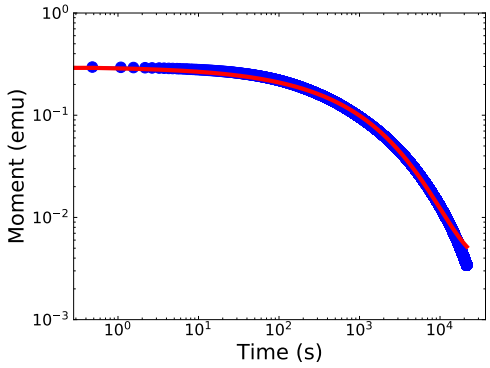

Parameter	Fit result	2 K
M_0 (emu)	0.298	X
β	0.494	F
t_{offset} (s)	0	0
M_{eq} (emu)	3.411×10^{-3}	L
τ^* (s)	790.28	F

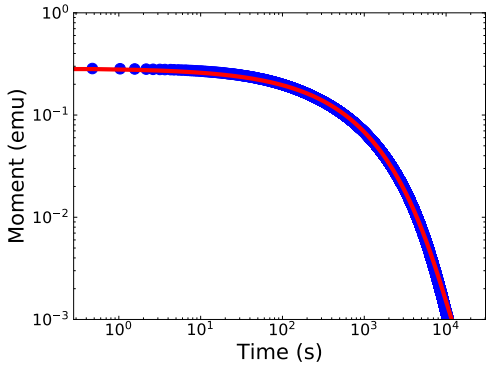

Parameter	Fit result	4 K
M_0 (emu)	0.287	X
β	0.578	F
t_{offset} (s)	0	0
M_{eq} (emu)	2.546×10^{-4}	L
τ^* (s)	533.25	F

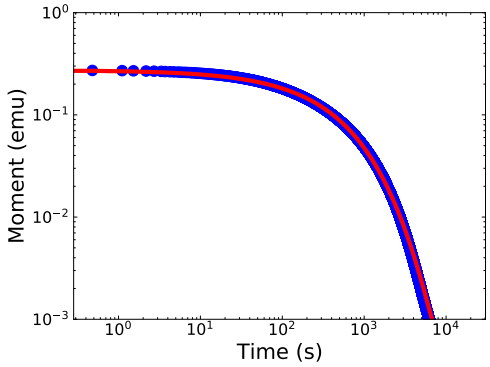

Parameter	Fit result	6 K
M_0 (emu)	0.273	X
β	0.630	F
t_{offset} (s)	0	0
M_{eq} (emu)	1.971×10^{-4}	L
τ^* (s)	410.25	F

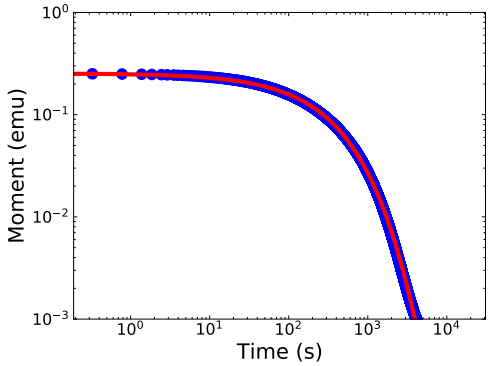

Parameter	Fit result	9 K
M_0 (emu)	0.253	X
β	0.676	F
t_{offset} (s)	0	0
M_{eq} (emu)	1.452×10^{-4}	L
τ^* (s)	302.25	F

Figure S76: Full DC decay curves fitted to Eq. 11 with M_0 fixed to first measured point at target field, M_{eq} set to the last measured point, $t_{\text{offset}} = 0$ and all other parameters fitted freely.

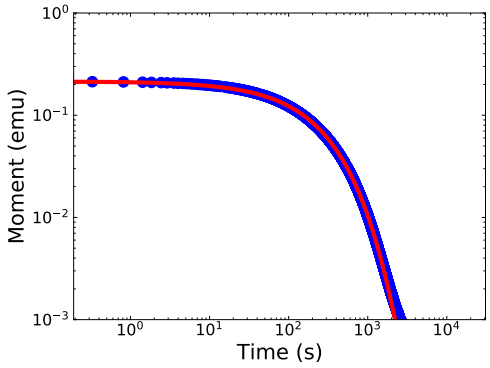

Parameter	Fit result	13 K
M_0 (emu)	0.214	X
β	0.736	F
t_{offset} (s)	0	0
M_{eq} (emu)	6.649×10^{-5}	L
τ^* (s)	221.84	F

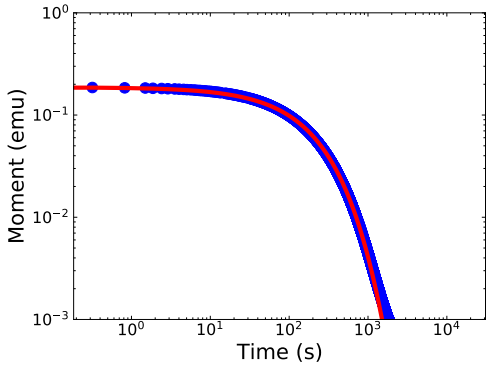

Parameter	Fit result	16 K
M_0 (emu)	0.187	X
β	0.776	F
t_{offset} (s)	0	0
M_{eq} (emu)	3.249×10^{-5}	L
τ^* (s)	177.18	F

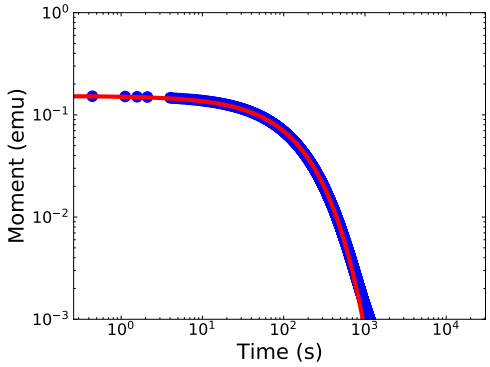

Parameter	Fit result	20 K
M_0 (emu)	0.153	X
β	0.825	F
t_{offset} (s)	0	0
M_{eq} (emu)	1.863×10^{-5}	L
τ^* (s)	132.01	F

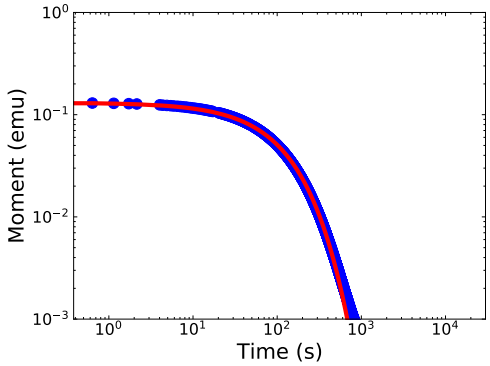

Parameter	Fit result	23 K
M_0 (emu)	0.131	X
β	0.855	F
t_{offset} (s)	0	0
M_{eq} (emu)	1.558×10^{-5}	L
τ^* (s)	106.36	F

Figure S77: Full DC decay curves fitted to Eq. 11 with M_0 fixed to first measured point at target field, M_{eq} set to the last measured point, $t_{\text{offset}} = 0$ and all other parameters fitted freely.

S2.5 DC decays fitting > 1 % M_0

As the data where $M < 0.01 M_0$ does not represent the main relaxation of $[Dy(Dtp)_2][Al\{OC(CF_3)_3\}_4]$ then we cut this data out and refit the remaining DC decay trace to Eq. 11. The resultant decay traces were analysed using Eq. 11 with different constraints on the fitted parameters as shown in Table S15 and described in Section 4.3.1. The τ^* and β parameters extracted from these fits were used to calculate τ_{mode}, $\langle\tau\rangle$ and $e^{\langle \ln[\tau]\rangle}$. These four measures of τ were then compared to the τ_{debye} extracted from Waveform measurements of $[Dy(Dtp)_2][Al\{OC(CF_3)_3\}_4]$ for all ways of fitting Eq. 11 to determine the best method and metric for characterising SMMs using DC decay measurements.

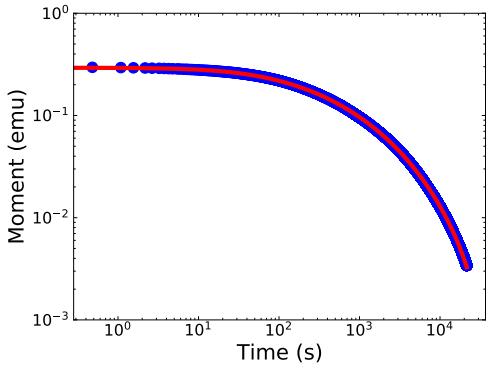

Parameter	Fit result	2 K
M_0 (emu)	0.491	F
β	0.342	F
t_{offset} (s)	36.19	F
M_{eq} (emu)	-1.966×10^{-3}	F
τ^* (s)	256.62	F

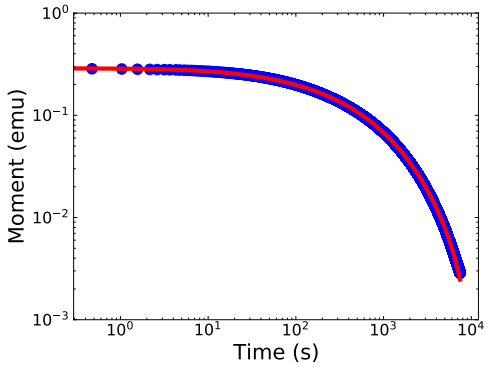

Parameter	Fit result	4 K
M_0 (emu)	0.333	F
β	0.502	F
t_{offset} (s)	8.38	F
M_{eq} (emu)	-2.181×10^{-3}	F
τ^* (s)	411.11	F

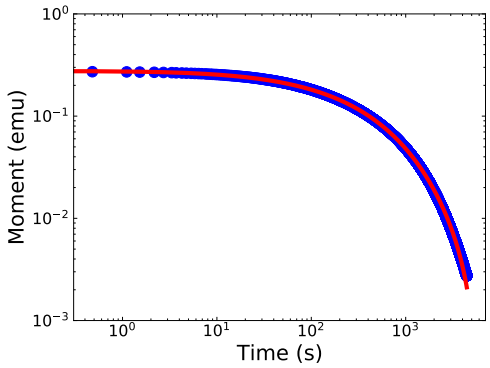

Parameter	Fit result	6 K
M_0 (emu)	0.299	F
β	0.567	F
t_{offset} (s)	4.01	F
M_{eq} (emu)	-2.678×10^{-3}	F
τ^* (s)	361.95	F

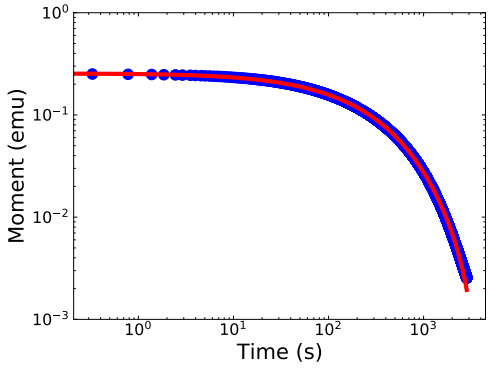

Parameter	Fit result	9 K
M_0 (emu)	0.268	F
β	0.633	F
t_{offset} (s)	2.60	F
M_{eq} (emu)	-1.673×10^{-3}	F
τ^* (s)	283.35	F

Figure S78: DC decay curves fitted for $M > 0.01\ M_0$ to Eq. 11 with all parameters fitted freely.

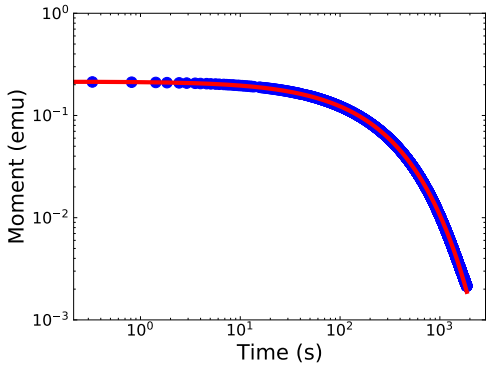

Parameter	Fit result	13 K
M_0 (emu)	0.228	F
β	0.705	F
t_{offset} (s)	4.08	F
M_{eq} (emu)	-1.300×10^{-4}	F
τ^* (s)	205.86	F

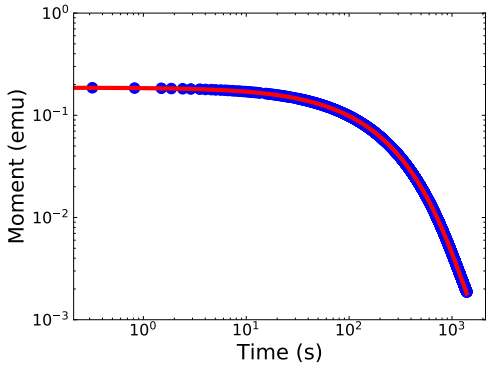

Parameter	Fit result	16 K
M_0 (emu)	0.205	F
β	0.748	F
t_{offset} (s)	6.79	F
M_{eq} (emu)	4.655×10^{-4}	F
τ^* (s)	161.34	F

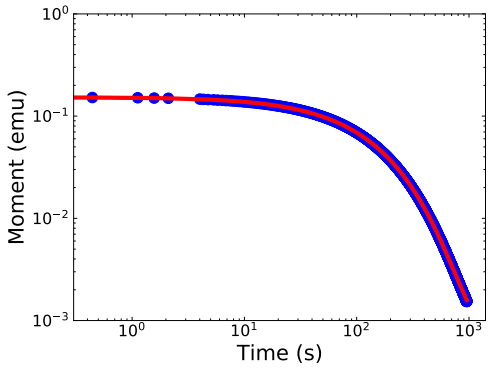

Parameter	Fit result	20 K
M_0 (emu)	0.175	F
β	0.798	F
t_{offset} (s)	10.03	F
M_{eq} (emu)	7.259×10^{-4}	F
τ^* (s)	118.91	F

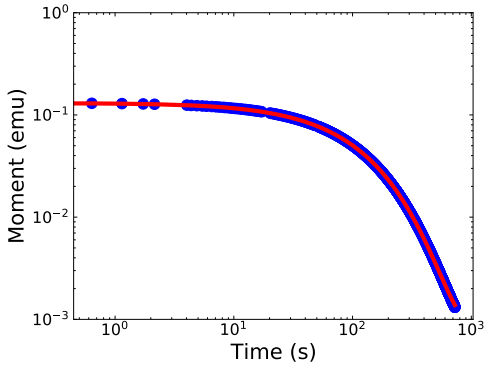

Parameter	Fit result	23 K
M_0 (emu)	0.155	F
β	0.830	F
t_{offset} (s)	11.46	F
M_{eq} (emu)	7.149×10^{-4}	F
τ^* (s)	95.87	F

Figure S79: DC decay curves fitted for $M > 0.01\ M_0$ to Eq. 11 with all parameters fitted freely.

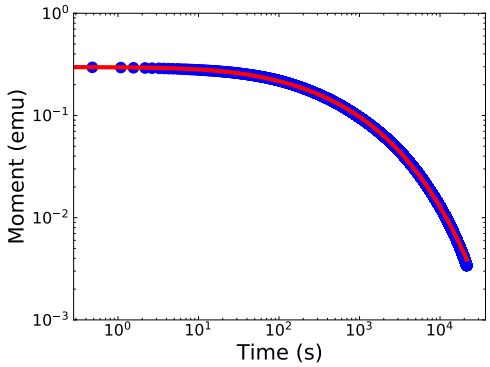

Parameter	Fit result	2 K
M_0 (emu)	0.404	F
β	0.387	F
t_{offset} (s)	18.93	F
M_{eq} (emu)	0	0
τ^* (s)	405.63	F

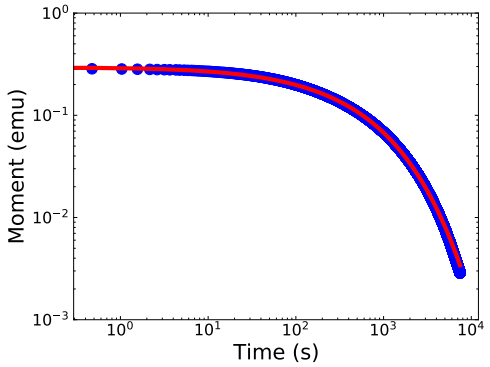

Parameter	Fit result	4 K
M_0 (emu)	0.307	F
β	0.544	F
t_{offset} (s)	1.55	F
M_{eq} (emu)	0	0
τ^* (s)	467.94	F

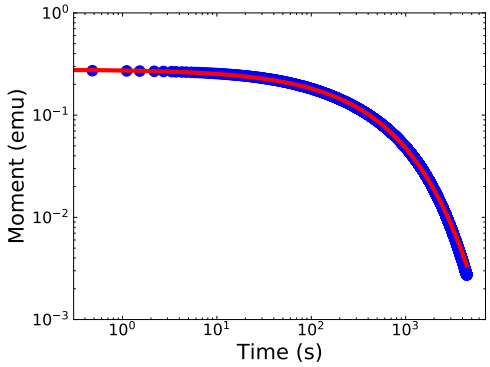

Parameter	Fit result	6 K
M_0 (emu)	0.281	F
β	0.612	F
t_{offset} (s)	7.73×10^{-2}	F
M_{eq} (emu)	0	0
τ^* (s)	390.25	F

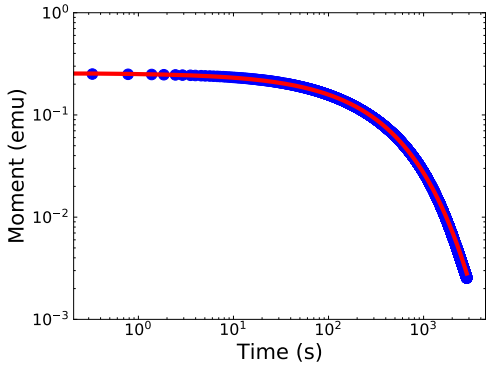

Parameter	Fit result	9 K
M_0 (emu)	0.257	F
β	0.665	F
t_{offset} (s)	5.70×10^{-2}	F
M_{eq} (emu)	0	0
τ^* (s)	295.12	F

Figure S80: DC decay curves fitted for $M > 0.01\ M_0$ to Eq. 11 with $M_{\text{eq}} = 0$ set to target and all other parameters fitted freely.

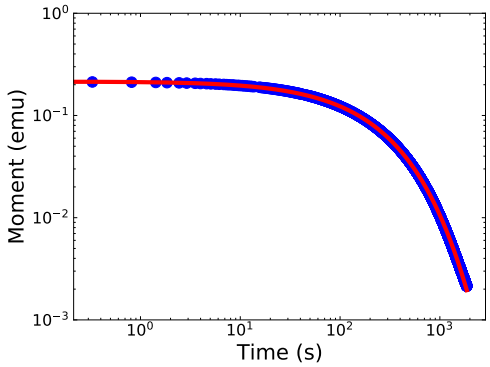

Parameter	Fit result	13 K
M_0 (emu)	0.226	F
β	0.710	F
t_{offset} (s)	3.33	F
M_{eq} (emu)	0	0
τ^* (s)	207.50	F

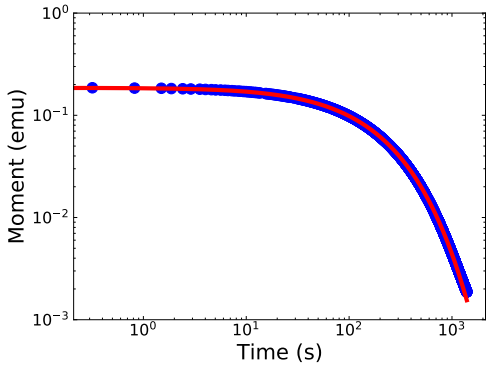

Parameter	Fit result	16 K
M_0 (emu)	0.222	F
β	0.719	F
t_{offset} (s)	13.80	F
M_{eq} (emu)	0	0
τ^* (s)	151.40	F

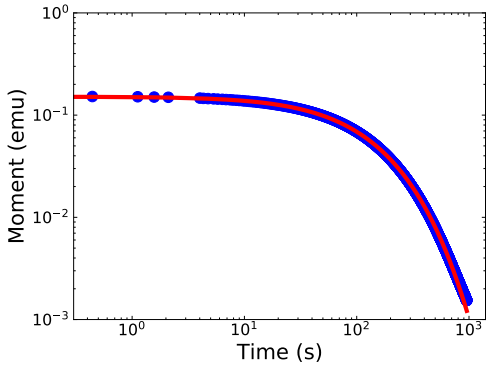

Parameter	Fit result	20 K
M_0 (emu)	0.275	F
β	0.702	F
t_{offset} (s)	42.96	F
M_{eq} (emu)	0	0
τ^* (s)	89.80	F

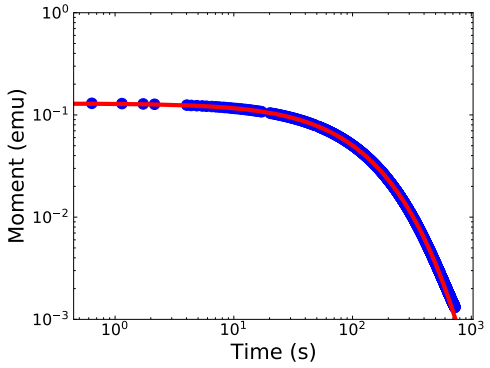

Parameter	Fit result	23 K
M_0 (emu)	0.484	F
β	0.662	F
t_{offset} (s)	78.70	F
M_{eq} (emu)	0	0
τ^* (s)	51.93	F

Figure S81: DC decay curves fitted for $M > 0.01\ M_0$ to Eq. 11 with $M_{\text{eq}} = 0$ set to target and all other parameters fitted freely.

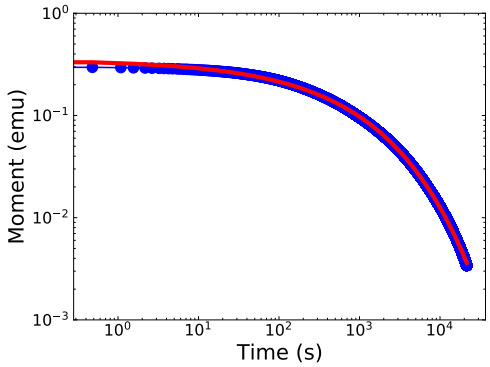

Parameter	Fit result	2 K
M_0 (emu)	0.350	F
β	0.415	F
t_{offset} (s)	0	0
M_{eq} (emu)	0	0
τ^* (s)	553.73	F

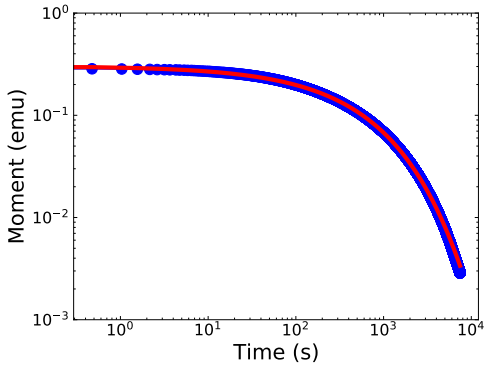

Parameter	Fit result	4 K
M_0 (emu)	0.303	F
β	0.548	F
t_{offset} (s)	0	0
M_{eq} (emu)	0	0
τ^* (s)	477.85	F

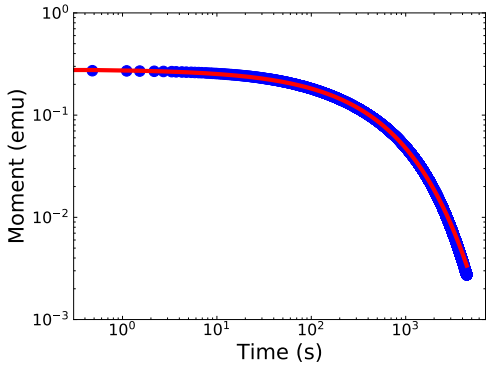

Parameter	Fit result	6 K
M_0 (emu)	0.281	F
β	0.612	F
t_{offset} (s)	0	0
M_{eq} (emu)	0	0
τ^* (s)	390.71	F

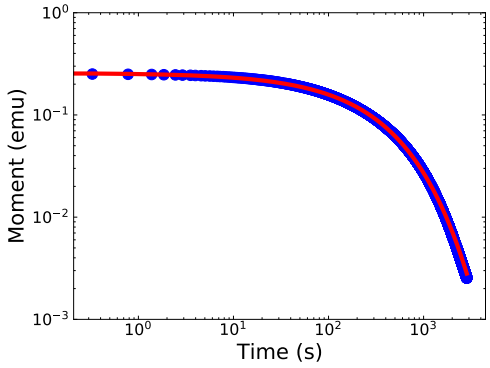

Parameter	Fit result	9 K
M_0 (emu)	0.257	F
β	0.666	F
t_{offset} (s)	0	0
M_{eq} (emu)	0	0
τ^* (s)	295.36	F

Figure S82: DC decay curves fitted for $M > 0.01\ M_0$ to Eq. 11 with $M_{\text{eq}} = 0$ set to target, $t_{\text{offset}} = 0$ and all other parameters fitted freely.

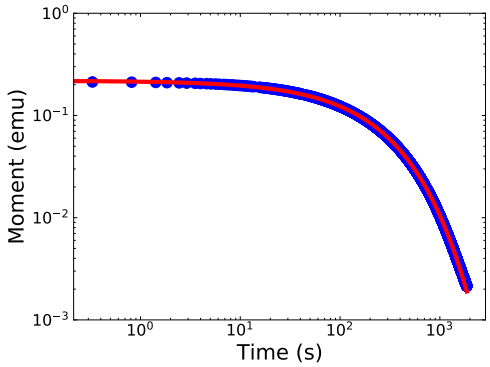

Parameter	Fit result	13 K
M_0 (emu)	0.219	F
β	0.721	F
t_{offset} (s)	0	0
M_{eq} (emu)	0	0
τ^* (s)	214.34	F

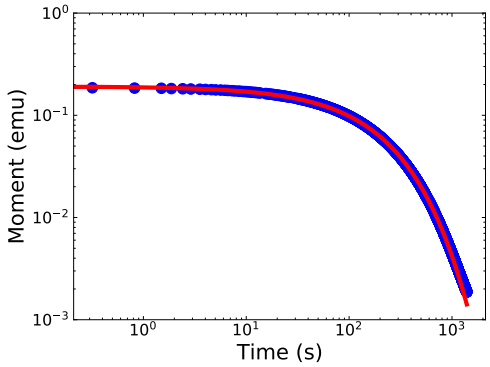

Parameter	Fit result	16 K
M_0 (emu)	0.191	F
β	0.757	F
t_{offset} (s)	0	0
M_{eq} (emu)	0	0
τ^* (s)	170.46	F

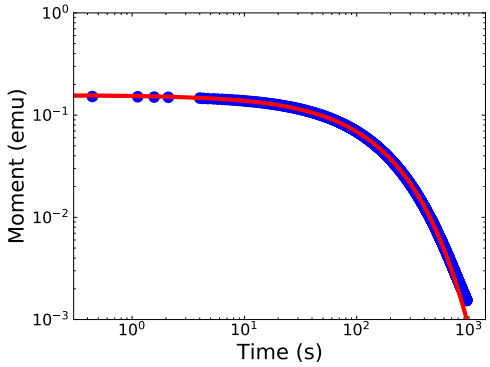

Parameter	Fit result	20 K
M_0 (emu)	0.157	F
β	0.804	F
t_{offset} (s)	0	0
M_{eq} (emu)	0	0
τ^* (s)	127.06	F

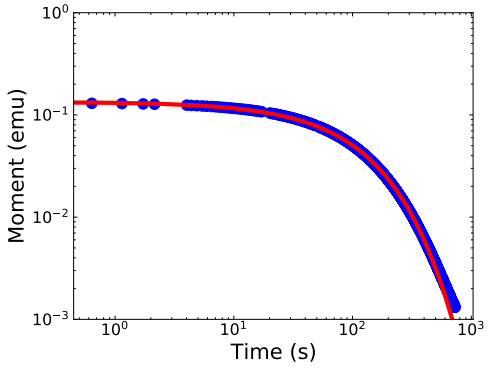

Parameter	Fit result	23 K
M_0 (emu)	0.134	F
β	0.834	F
t_{offset} (s)	0	0
M_{eq} (emu)	0	0
τ^* (s)	102.73	F

Figure S83: DC decay curves fitted for $M > 0.01\ M_0$ to Eq. 11 with $M_{\text{eq}} = 0$ set to target, $t_{\text{offset}} = 0$ and all other parameters fitted freely.

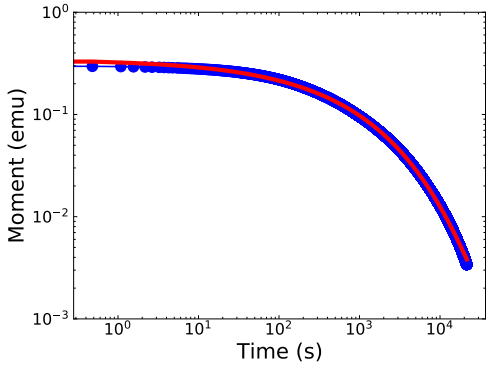

Parameter	Fit result	2 K
M_0 (emu)	0.347	F
β	0.421	F
t_{offset} (s)	0	0
M_{eq} (emu)	4.304×10^{-4}	F
τ^* (s)	565.29	F

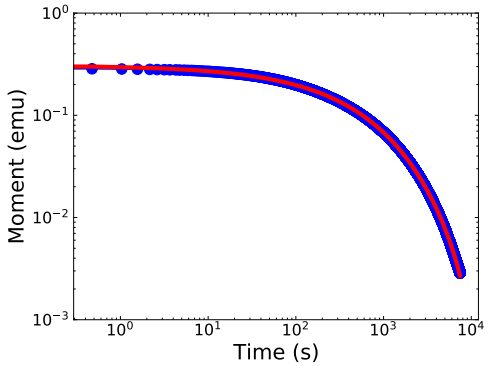

Parameter	Fit result	4 K
M_0 (emu)	0.308	F
β	0.531	F
t_{offset} (s)	0	0
M_{eq} (emu)	-1.309×10^{-3}	F
τ^* (s)	467061	F

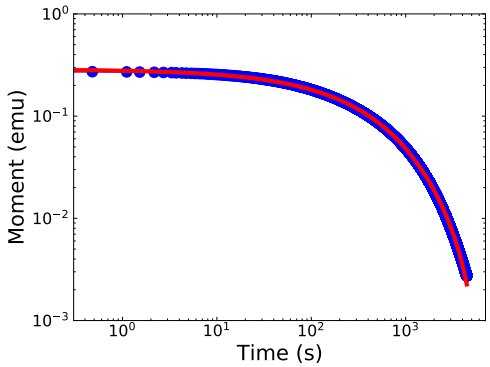

Parameter	Fit result	6 K
M_0 (emu)	0.287	F
β	0.584	F
t_{offset} (s)	0	0
M_{eq} (emu)	-2.154×10^{-3}	F
τ^* (s)	383.15	F

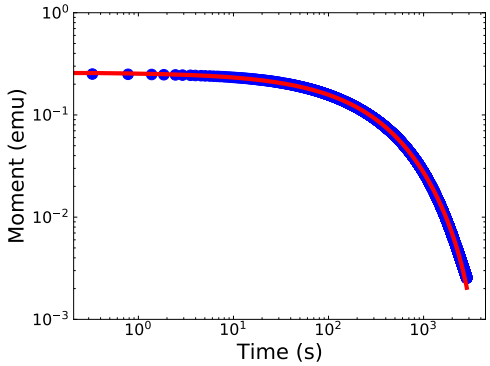

Parameter	Fit result	9 K
M_0 (emu)	0.347	F
β	0.421	F
t_{offset} (s)	0	0
M_{eq} (emu)	-1.365×10^{-3}	F
τ^* (s)	292.98	F

Figure S84: DC decay curves fitted for $M > 0.01\ M_0$ to Eq. 11 with $t_{\text{offset}} = 0$ and all other parameters fitted freely.

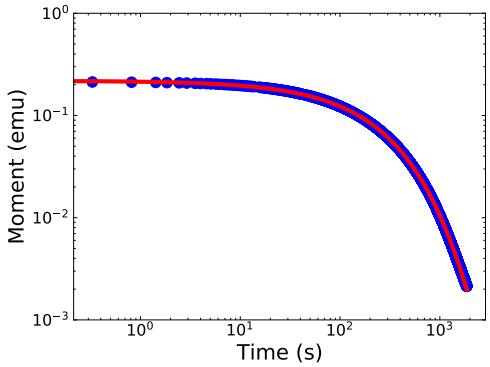

Parameter	Fit result	13 K
M_0 (emu)	0.218	F
β	0.723	F
t_{offset} (s)	0	0
M_{eq} (emu)	1.324×10^{-4}	F
τ^* (s)	214.47	F

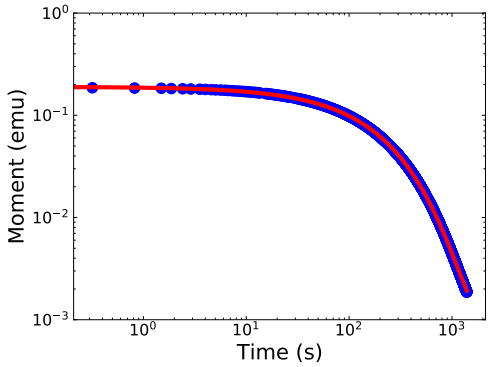

Parameter	Fit result	16 K
M_0 (emu)	0.190	F
β	0.774	F
t_{offset} (s)	0	0
M_{eq} (emu)	7.358×10^{-4}	F
τ^* (s)	170.91	F

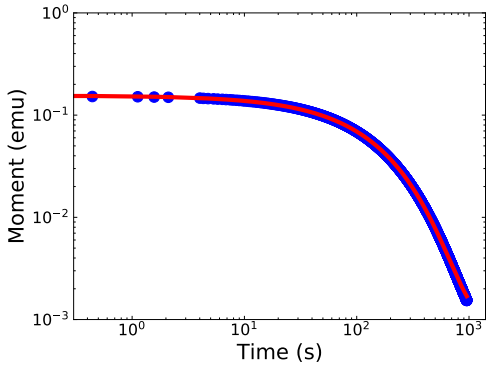

Parameter	Fit result	20 K
M_0 (emu)	0.155	F
β	0.831	F
t_{offset} (s)	0	0
M_{eq} (emu)	9.495×10^{-4}	F
τ^* (s)	127.44	F

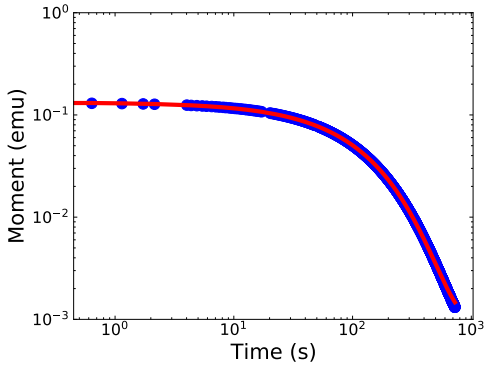

Parameter	Fit result	23 K
M_0 (emu)	0.132	F
β	0.866	F
t_{offset} (s)	0	0
M_{eq} (emu)	8.957×10^{-4}	F
τ^* (s)	102.94	F

Figure S85: DC decay curves fitted for $M > 0.01\ M_0$ to Eq. 11 with $t_{\text{offset}} = 0$ and all other parameters fitted freely.

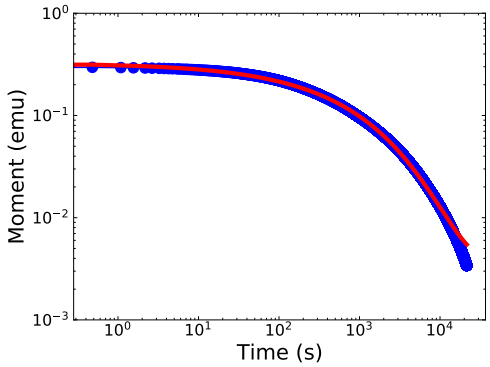

Parameter	Fit result	2 K
M_0 (emu)	0.326	F
β	0.462	F
t_{offset} (s)	0	0
M_{eq} (emu)	3.411×10^{-3}	L
τ^* (s)	645.21	F

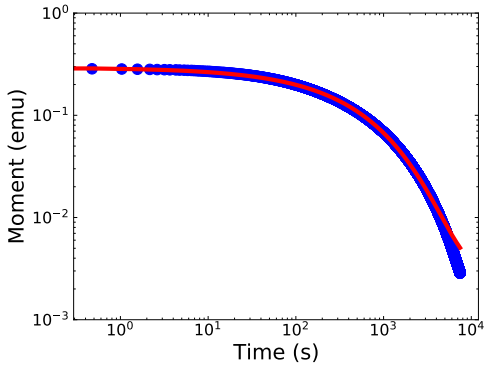

Parameter	Fit result	4 K
M_0 (emu)	0.292	F
β	0.587	F
t_{offset} (s)	0	0
M_{eq} (emu)	2.867×10^{-3}	L
τ^* (s)	498.76	F

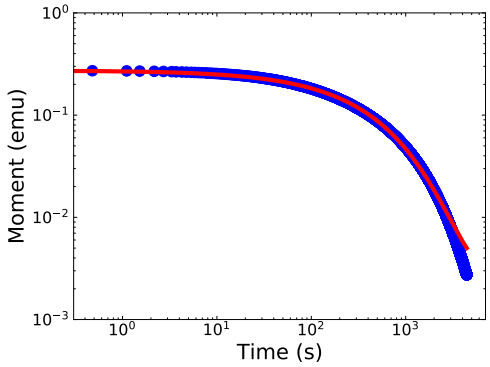

Parameter	Fit result	4 K
M_0 (emu)	0.273	F
β	0.650	F
t_{offset} (s)	0	0
M_{eq} (emu)	2.736×10^{-3}	L
τ^* (s)	399.22	F

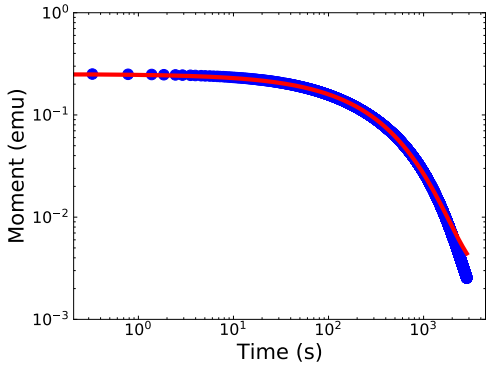

Parameter	Fit result	9 K
M_0 (emu)	0.251	F
β	0.704	F
t_{offset} (s)	0	0
M_{eq} (emu)	2.536×10^{-3}	L
τ^* (s)	299.12	F

Figure S86: DC decay curves fitted for $M > 0.01\ M_0$ to Eq. 11 with $t_{\text{offset}} = 0$, M_{eq} set to the last measured values and all other parameters fitted freely.

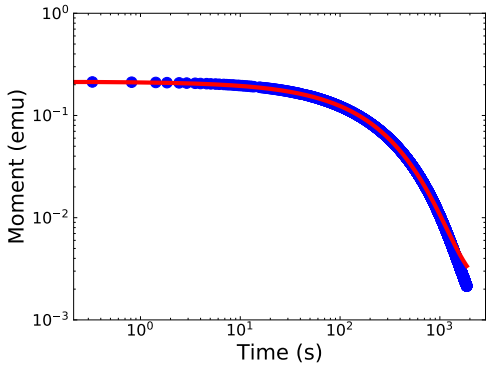

Parameter	Fit result	13 K
M_0 (emu)	0.214	F
β	0.761	F
t_{offset} (s)	0	0
M_{eq} (emu)	2.141×10^{-3}	L
τ^* (s)	216.10	F

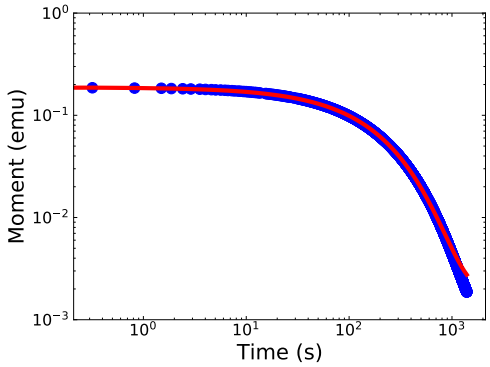

Parameter	Fit result	16 K
M_0 (emu)	0.188	F
β	0.800	F
t_{offset} (s)	0	0
M_{eq} (emu)	1.869×10^{-3}	L
τ^* (s)	171.42	F

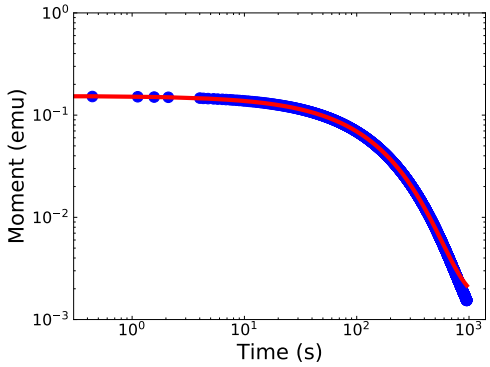

Parameter	Fit result	20 K
M_0 (emu)	0.154	F
β	0.849	F
t_{offset} (s)	0	0
M_{eq} (emu)	1.540×10^{-3}	L
τ^* (s)	127.60	F

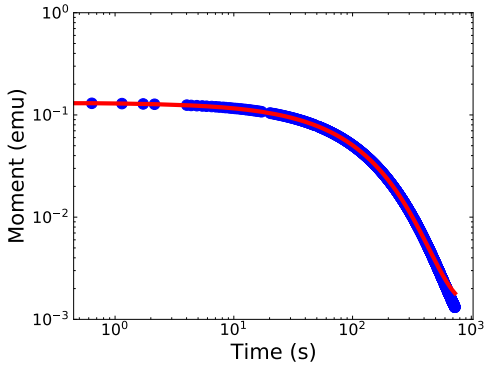

Parameter	Fit result	23 K
M_0 (emu)	0.132	F
β	0.880	F
t_{offset} (s)	0	0
M_{eq} (emu)	1.314×10^{-3}	L
τ^* (s)	102.99	F

Figure S87: DC decay curves fitted for $M > 0.01\ M_0$ to Eq. 11 with $t_{\text{offset}} = 0$, M_{eq} set to the last measured values and all other parameters fitted freely.

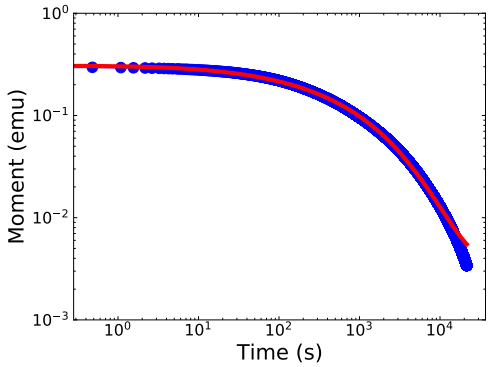

Parameter	Fit result	2 K
M_0 (emu)	0.331	F
β	0.458	F
t_{offset} (s)	2.24	F
M_{eq} (emu)	3.4114×10^{-3}	L
τ^* (s)	623.59	F

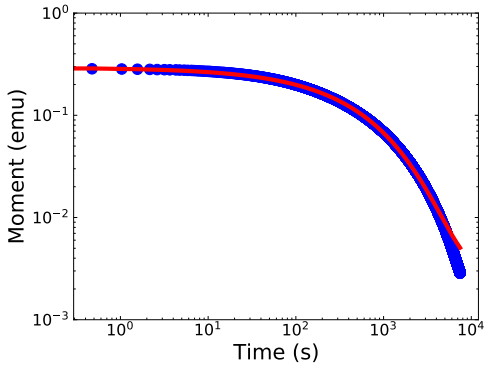

Parameter	Fit result	4 K
M_0 (emu)	0.292	F
β	0.587	F
t_{offset} (s)	4.47×10^{-3}	F
M_{eq} (emu)	2.867×10^{-3}	L
τ^* (s)	498.70	F

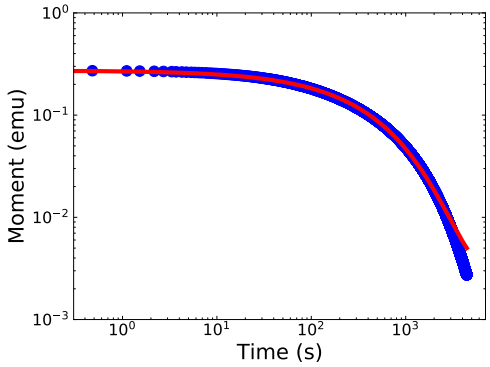

Parameter	Fit result	6 K
M_0 (emu)	0.273	F
β	0.650	F
t_{offset} (s)	8.10×10^{-14}	F
M_{eq} (emu)	2.736×10^{-3}	L
τ^* (s)	399.22	F

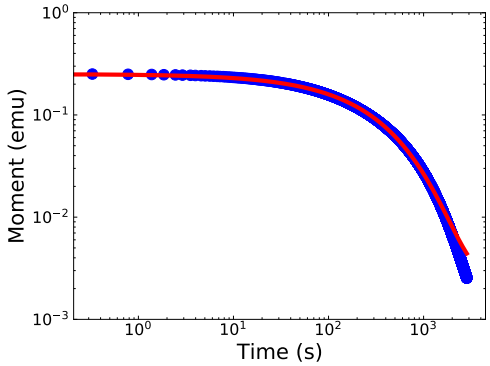

Parameter	Fit result	9 K
M_0 (emu)	0.251	F
β	0.704	F
t_{offset} (s)	1.25×10^{-17}	F
M_{eq} (emu)	2.536×10^{-3}	L
τ^* (s)	299.12	F

Figure S88: DC decay curves fitted for $M > 0.01\ M_0$ to Eq. 11 with M_{eq} set to the last measured point and all other parameters fitted freely.

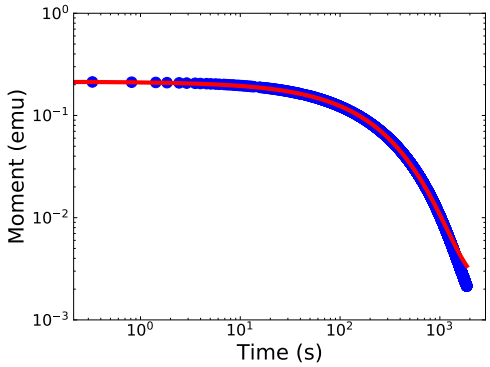

Parameter	Fit result	13 K
M_0 (emu)	0.214	F
β	0.761	F
t_{offset} (s)	9.50×10^{-14}	F
M_{eq} (emu)	2.141×10^{-3}	L
τ^* (s)	216.10	F

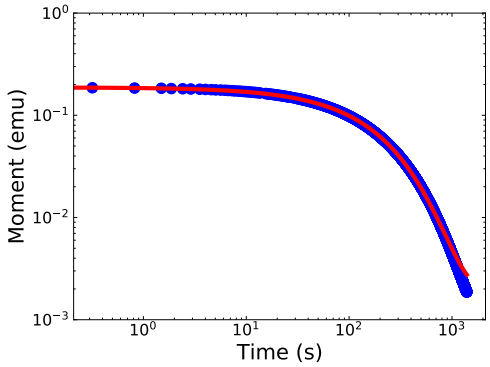

Parameter	Fit result	16 K
M_0 (emu)	0.188	F
β	0.800	F
t_{offset} (s)	1.32×10^{3}	F
M_{eq} (emu)	1.869×10^{-3}	L
τ^* (s)	171.42	F

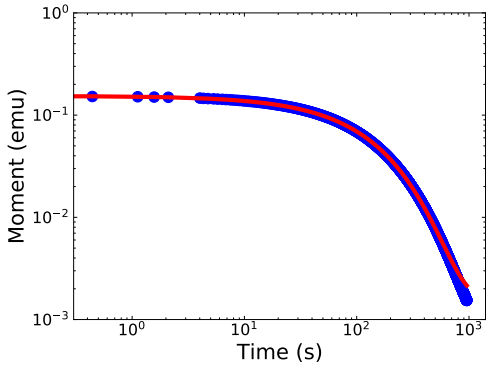

Parameter	Fit result	20 K
M_0 (emu)	0.154	F
β	0.848	F
t_{offset} (s)	0.16	F
M_{eq} (emu)	1.540×10^{-3}	L
τ^* (s)	127.46	F

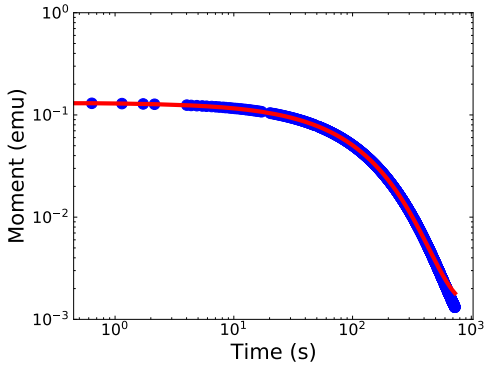

Parameter	Fit result	23 K
M_0 (emu)	0.132	F
β	0.880	F
t_{offset} (s)	0.22	F
M_{eq} (emu)	1.314×10^{-3}	L
τ^* (s)	102.85	F

Figure S89: DC decay curves fitted for $M > 0.01\ M_0$ to Eq. 11 with M_{eq} set to the last measured point and all other parameters fitted freely.

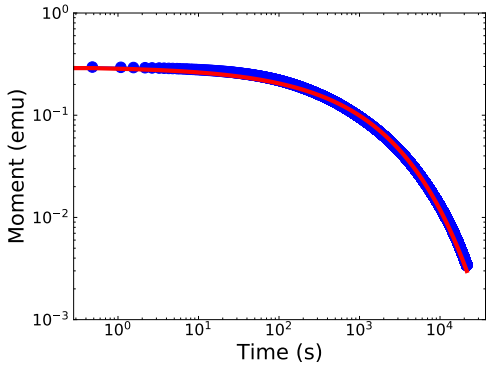

Parameter	Fit result	2 K
M_0 (emu)	0.298	X
β	0.466	F
t_{offset} (s)	0	0
M_{eq} (emu)	0	0
τ^* (s)	814.26	F

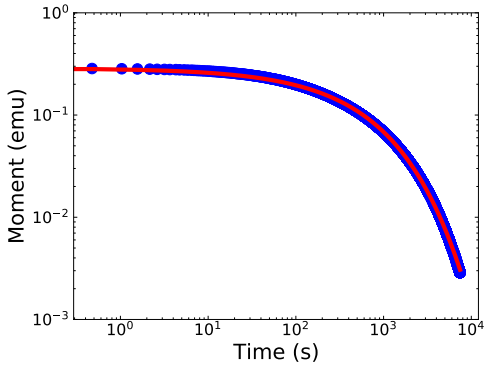

Parameter	Fit result	4 K
M_0 (emu)	0.287	X
β	0.574	F
t_{offset} (s)	0	0
M_{eq} (emu)	0	0
τ^* (s)	534.19	F

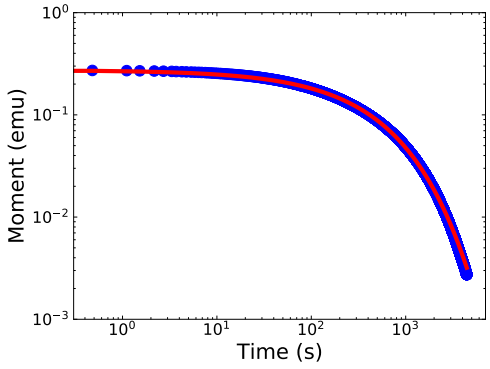

Parameter	Fit result	6 K
M_0 (emu)	0.273	X
β	0.627	F
t_{offset} (s)	0	0
M_{eq} (emu)	0	0
τ^* (s)	410.92	F

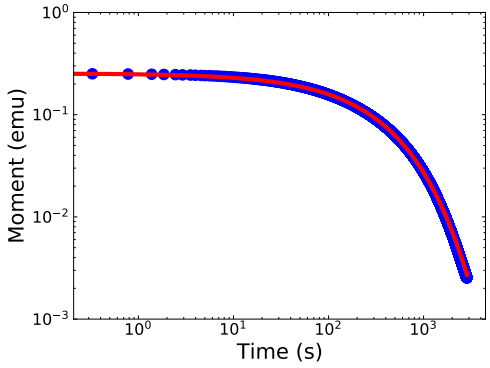

Parameter	Fit result	9 K
M_0 (emu)	0.253	X
β	0.675	F
t_{offset} (s)	0	0
M_{eq} (emu)	0	0
τ^* (s)	302.79	F

Figure S90: DC decay curves fitted for $M > 0.01\ M_0$ to Eq. 11 with $M_{\text{eq}} = 0$ set to target magnetisation, M_0 fixed to first measured point at target field, $t_{\text{offset}} = 0$ and α and β fitted freely.

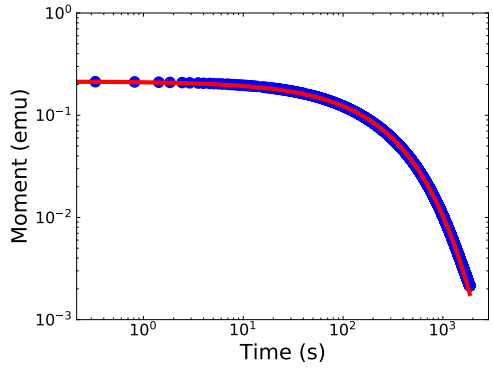

Parameter	Fit result	13 K
M_0 (emu)	0.214	X
β	0.737	F
t_{offset} (s)	0	0
M_{eq} (emu)	0	0
τ^* (s)	222.13	F

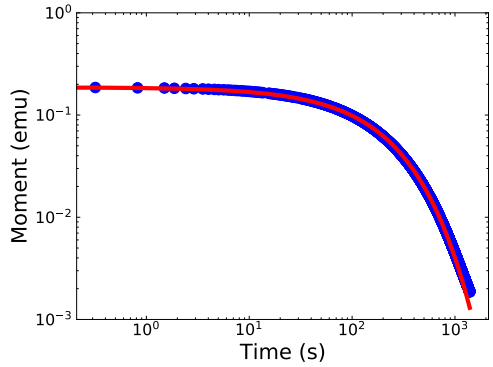

Parameter	Fit result	16 K
M_0 (emu)	0.187	X
β	0.778	F
t_{offset} (s)	0	0
M_{eq} (emu)	0	0
τ^* (s)	177.33	F

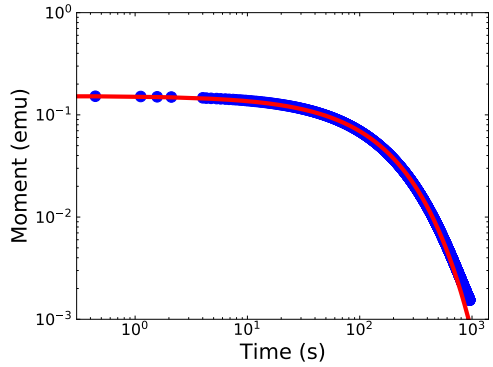

Parameter	Fit result	20 K
M_0 (emu)	0.153	X
β	0.829	F
t_{offset} (s)	0	0
M_{eq} (emu)	0	0
τ^* (s)	132.07	F

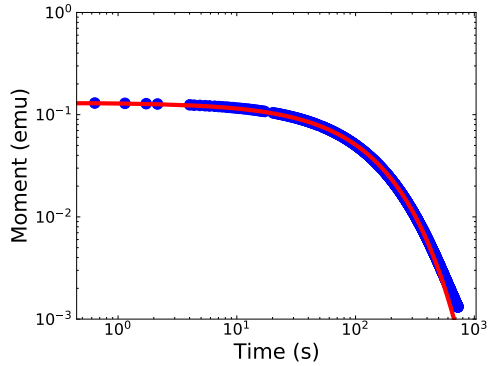

Parameter	Fit result	23 K
M_0 (emu)	0.131	X
β	0.857	F
t_{offset} (s)	0	0
M_{eq} (emu)	0	0
τ^* (s)	106.42	F

Figure S91: DC decay curves fitted for $M > 0.01\ M_0$ to Eq. 11 with $M_{\text{eq}} = 0$ set to target magnetisation, M_0 fixed to first measured point at target field, $t_{\text{offset}} = 0$ and α and β fitted freely.

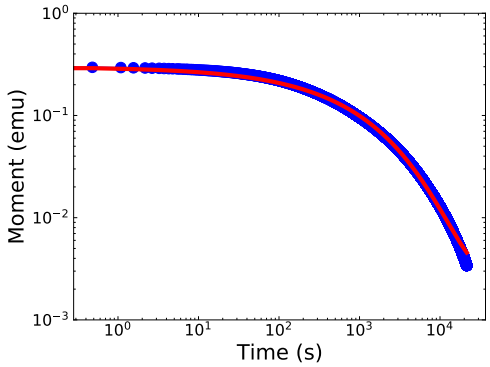

Parameter	Fit result	2 K
M_0 (emu)	0.298	X
β	0.487	F
t_{offset} (s)	0	0
M_{eq} (emu)	2.516×10^{-3}	F
τ^* (s)	796.55	F

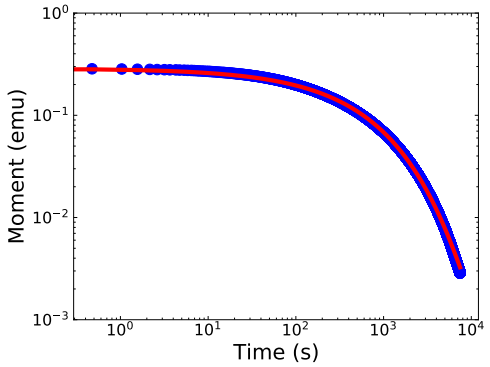

Parameter	Fit result	4 K
M_0 (emu)	0.287	X
β	0.487	F
t_{offset} (s)	0	0
M_{eq} (emu)	3.084×10^{-4}	F
τ^* (s)	532.44	F

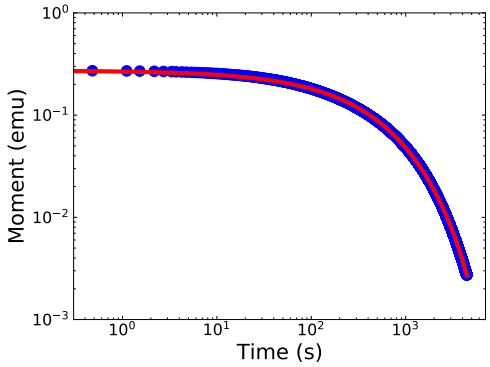

Parameter	Fit result	6 K
M_0 (emu)	0.273	X
β	0.621	F
t_{offset} (s)	0	0
M_{eq} (emu)	-8.001×10^{-4}	F
τ^* (s)	414.59	F

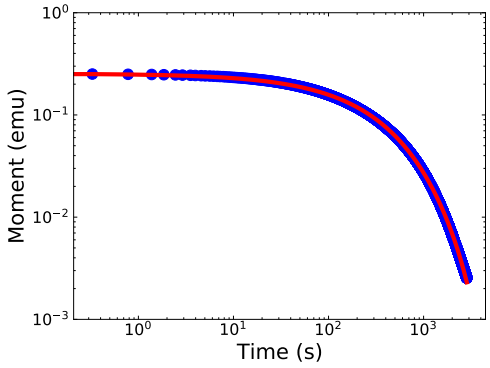

Parameter	Fit result	9 K
M_0 (emu)	0.669	X
β	0.487	F
t_{offset} (s)	0	0
M_{eq} (emu)	-6.411×10^{-4}	F
τ^* (s)	305.04	F

Figure S92: DC decay curves fitted for $M > 0.01\ M_0$ to Eq. 11 with M_0 fixed to first measured point at target field, $t_{\text{offset}} = 0$ and all other parameters fitted freely.

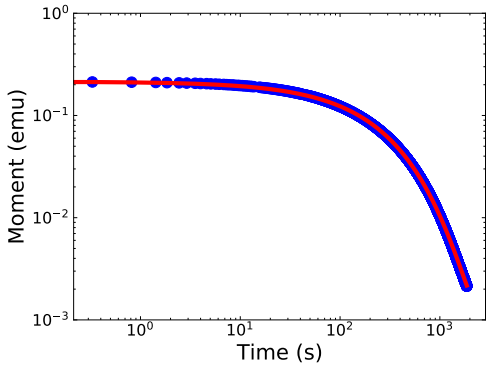

Parameter	Fit result	13 K
M_0 (emu)	0.214	X
β	0.743	F
t_{offset} (s)	0	0
M_{eq} (emu)	5.399×10^{-3}	F
τ^* (s)	220.60	F

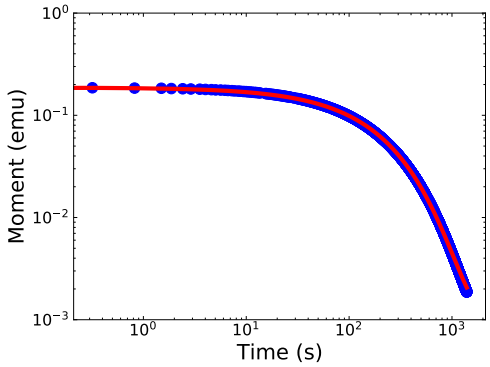

Parameter	Fit result	16 K
M_0 (emu)	0.187	X
β	0.792	F
t_{offset} (s)	0	0
M_{eq} (emu)	1.013×10^{-3}	F
τ^* (s)	174.80	F

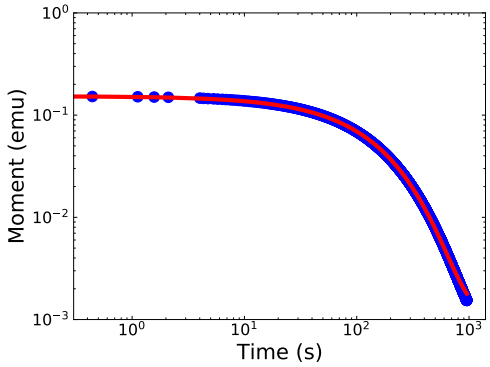

Parameter	Fit result	20 K
M_0 (emu)	0.153	X
β	0.847	F
t_{offset} (s)	0	0
M_{eq} (emu)	1.124×10^{-3}	F
τ^* (s)	129.58	F

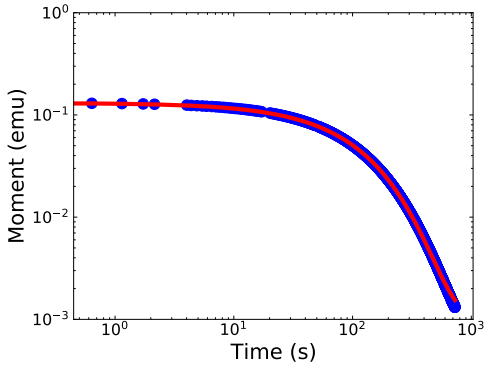

Parameter	Fit result	23 K
M_0 (emu)	0.131	X
β	0.880	F
t_{offset} (s)	0	0
M_{eq} (emu)	1.022×10^{-3}	F
τ^* (s)	104.37	F

Figure S93: DC decay curves fitted for $M > 0.01\ M_0$ to Eq. 11 with M_0 fixed to first measured point at target field, $t_{\text{offset}} = 0$ and all other parameters fitted freely.

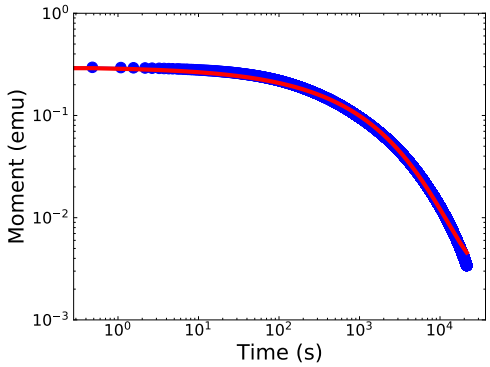

Parameter	Fit result	2 K
M_0 (emu)	0.298	X
β	0.487	F
t_{offset} (s)	1.518×10^{-26}	F
M_{eq} (emu)	2.516×10^{-3}	F
τ^* (s)	796.55	F

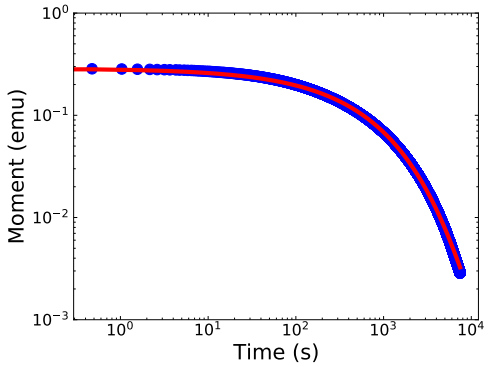

Parameter	Fit result	4 K
M_0 (emu)	0.287	X
β	0.577	F
t_{offset} (s)	9.014×10^{-23}	F
M_{eq} (emu)	3.084×10^{-4}	F
τ^* (s)	532.44	F

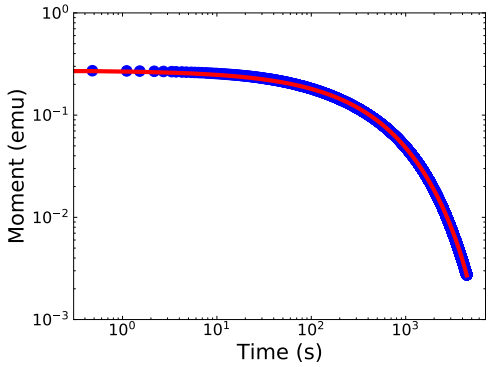

Parameter	Fit result	6 K
M_0 (emu)	0.273	X
β	0.621	F
t_{offset} (s)	7.560×10^{-21}	F
M_{eq} (emu)	-8.001×10^{-4}	F
τ^* (s)	414.59	F

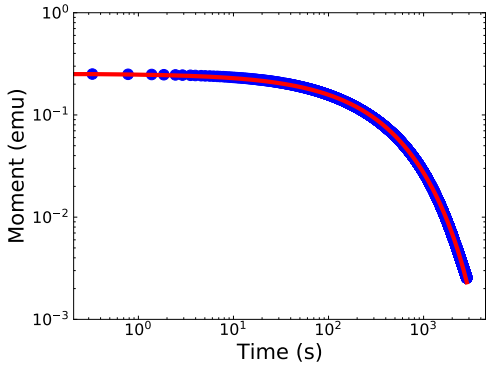

Parameter	Fit result	9 K
M_0 (emu)	0.253	X
β	0.669	F
t_{offset} (s)	9.235×10^{-23}	F
M_{eq} (emu)	-6.411×10^{-4}	F
τ^* (s)	305.04	F

Figure S94: DC decay curves fitted for $M > 0.01\ M_0$ to Eq. 11 with M_0 fixed to first measured point at target field and all other parameters fitted freely.

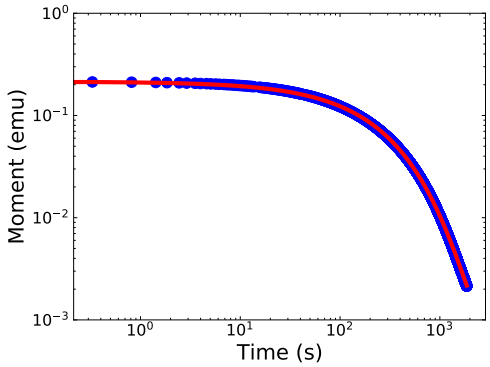

Parameter	Fit result	13 K
M_0 (emu)	0.214	X
β	0.743	F
t_{offset} (s)	1.957×10^{-21}	F
M_{eq} (emu)	5.399×10^{-4}	F
τ^* (s)	220.60	F

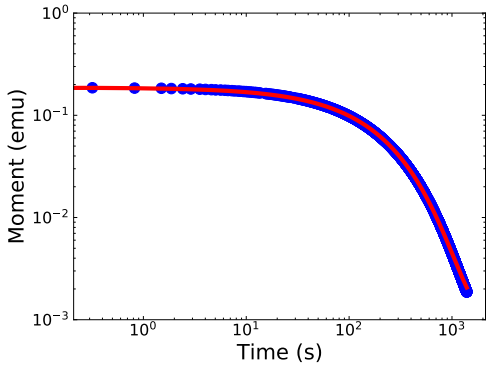

Parameter	Fit result	16 K
M_0 (emu)	0.187	X
β	0.792	F
t_{offset} (s)	1.073×10^{-18}	F
M_{eq} (emu)	1.013×10^{-3}	F
τ^* (s)	174.80	F

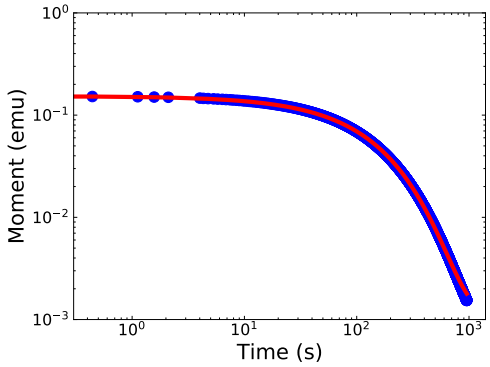

Parameter	Fit result	20 K
M_0 (emu)	0.153	X
β	0.847	F
t_{offset} (s)	5.505×10^{-14}	F
M_{eq} (emu)	1.124×10^{-3}	F
τ^* (s)	129.58	F

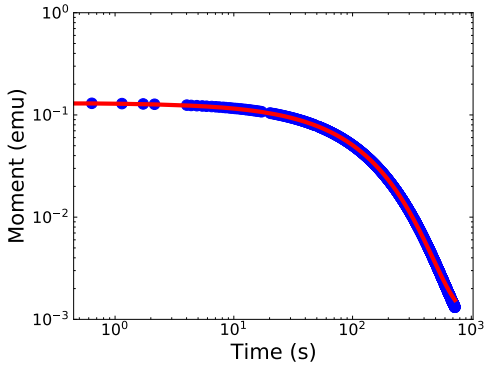

Parameter	Fit result	23 K
M_0 (emu)	0.131	X
β	0.880	F
t_{offset} (s)	4.602×10^{-17}	F
M_{eq} (emu)	1.022×10^{-3}	F
τ^* (s)	104.37	F

Figure S95: DC decay curves fitted for $M > 0.01\ M_0$ to Eq. 11 with M_0 fixed to first measured point at target field and all other parameters fitted freely.

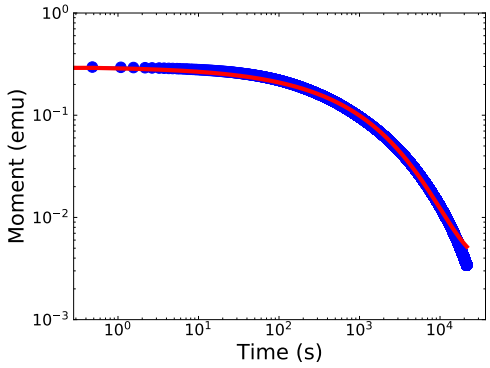

Parameter	Fit result	2 K
M_0 (emu)	0.298	X
β	0.494	F
t_{offset} (s)	2.137×10^{-19}	F
M_{eq} (emu)	3.411×10^{-3}	L
τ^* (s)	790.23	F

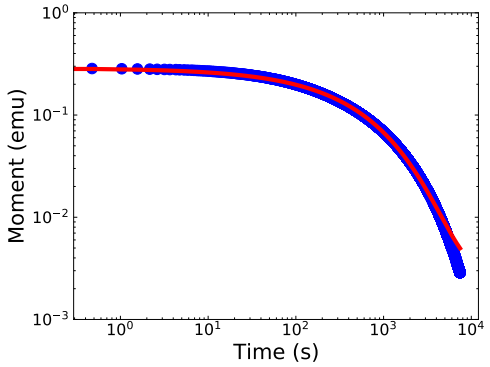

Parameter	Fit result	4 K
M_0 (emu)	0.287	X
β	0.597	F
t_{offset} (s)	3.044×10^{-19}	F
M_{eq} (emu)	2.867×10^{-3}	L
τ^* (s)	518.15	F

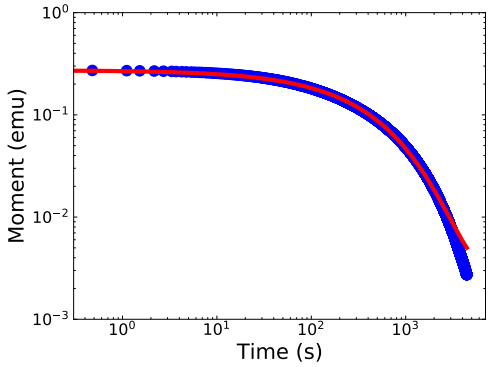

Parameter	Fit result	6 K
M_0 (emu)	0.273	X
β	0.649	F
t_{offset} (s)	4.573×10^{-21}	F
M_{eq} (emu)	2.736×10^{-3}	L
τ^* (s)	398.67	F

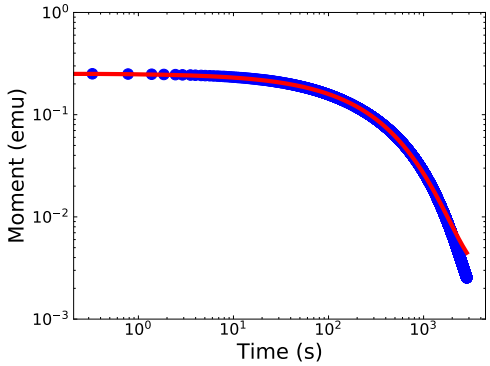

Parameter	Fit result	9 K
M_0 (emu)	0.253	X
β	0.698	F
t_{offset} (s)	0.14	F
M_{eq} (emu)	2.536×10^{-3}	L
τ^* (s)	294.30	F

Figure S96: DC decay curves fitted for $M > 0.01\ M_0$ to Eq. 11 with M_0 fixed to first measured point at target field, M_{eq} set to the last measured point and all other parameters fitted freely.

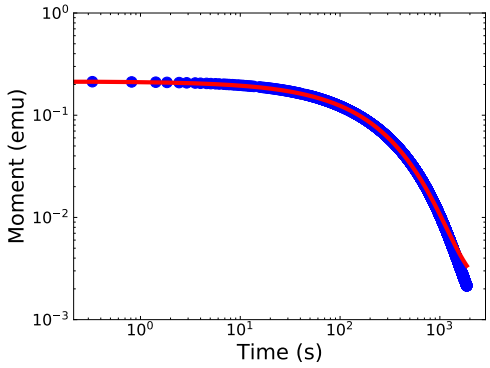

Parameter	Fit result	13 K
M_0 (emu)	0.214	X
β	0.762	F
t_{offset} (s)	1.815×10^{-16}	F
M_{eq} (emu)	2.141×10^{-3}	L
τ^* (s)	216.15	F

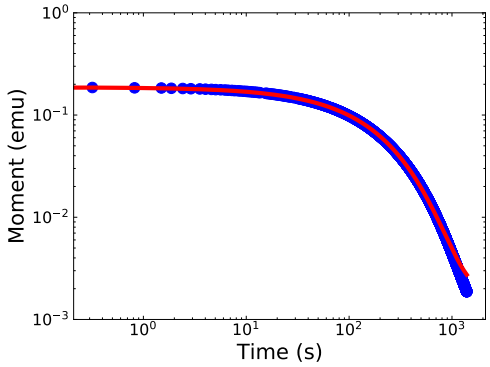

Parameter	Fit result	16 K
M_0 (emu)	0.187	X
β	0.804	F
t_{offset} (s)	3.397×10^{-19}	F
M_{eq} (emu)	1.869×10^{-3}	L
τ^* (s)	172.70	F

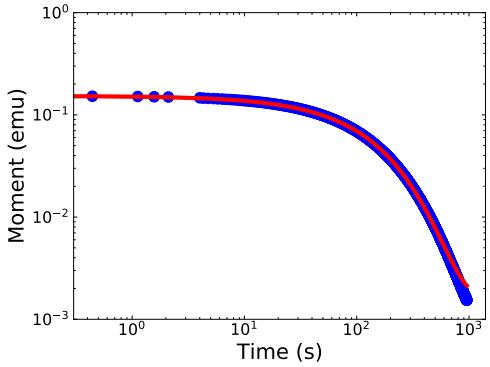

Parameter	Fit result	20 K
M_0 (emu)	0.153	X
β	0.854	F
t_{offset} (s)	7.530×10^{-14}	F
M_{eq} (emu)	1.540×10^{-3}	L
τ^* (s)	128.68	F

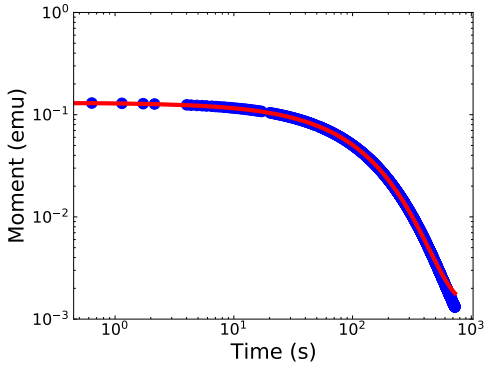

Parameter	Fit result	23 K
M_0 (emu)	0.131	X
β	0.886	F
t_{offset} (s)	1.155×10^{-14}	F
M_{eq} (emu)	1.314×10^{-3}	L
τ^* (s)	103.80	F

Figure S97: DC decay curves fitted for $M > 0.01\ M_0$ to Eq. 11 with M_0 fixed to first measured point at target field, M_{eq} set to the last measured point and all other parameters fitted freely.

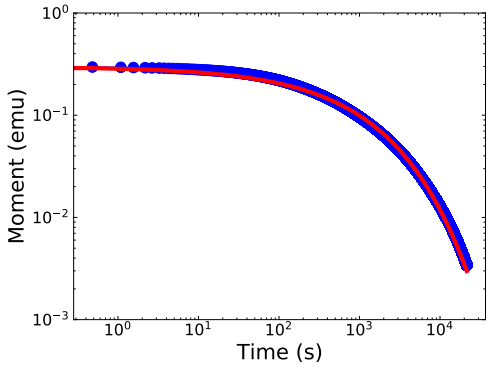

Parameter	Fit result	2 K
M_0 (emu)	0.298	X
β	0.466	F
t_{offset} (s)	8.376×10^{-23}	F
M_{eq} (emu)	0	0
τ^* (s)	814.26	F

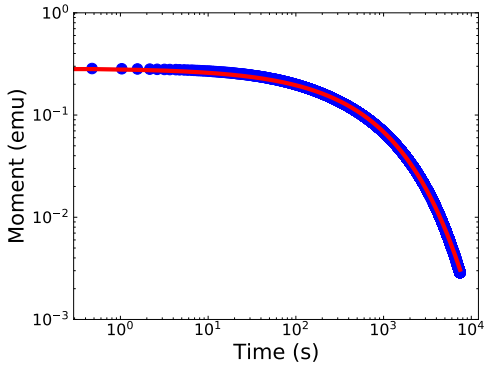

Parameter	Fit result	4 K
M_0 (emu)	0.287	X
β	0.574	F
t_{offset} (s)	2.491×10^{-21}	F
M_{eq} (emu)	0	0
τ^* (s)	534.19	F

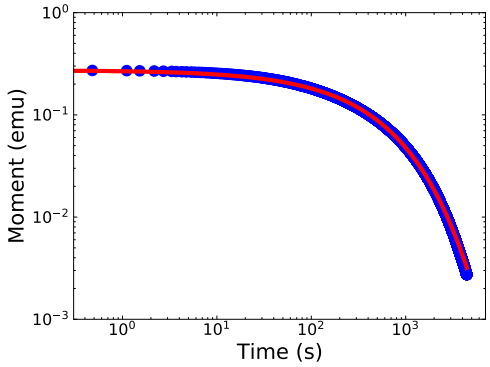

Parameter	Fit result	6 K
M_0 (emu)	0.273	X
β	0.627	F
t_{offset} (s)	4.871×10^{-23}	F
M_{eq} (emu)	0	0
τ^* (s)	410.92	F

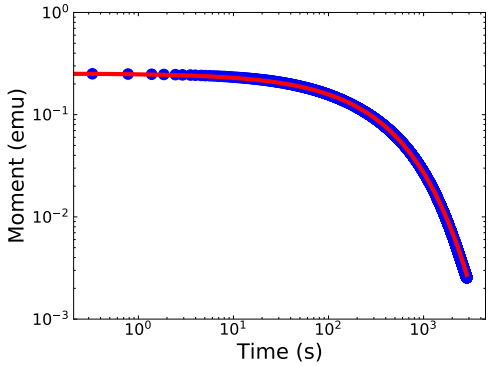

Parameter	Fit result	9 K
M_0 (emu)	0.253	X
β	0.675	F
t_{offset} (s)	1.044×10^{-19}	F
M_{eq} (emu)	0	0
τ^* (s)	302.79	F

Figure S98: DC decay curves fitted for $M > 0.01\ M_0$ to Eq. 11 with M_0 fixed to first measured point at target field, M_{eq} set to the target magnetisation and all other parameters fitted freely.

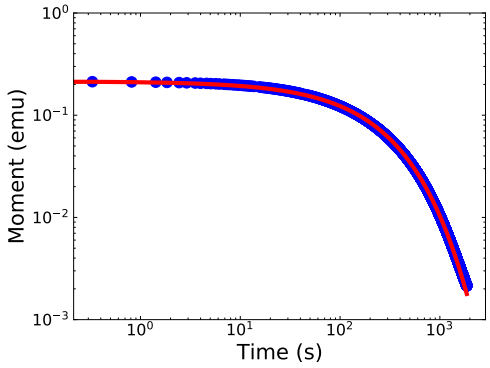

Parameter	Fit result	13 K
M_0 (emu)	0.214	X
β	0.737	F
t_{offset} (s)	2.656×10^{-23}	F
M_{eq} (emu)	0	0
τ^* (s)	222.13	F

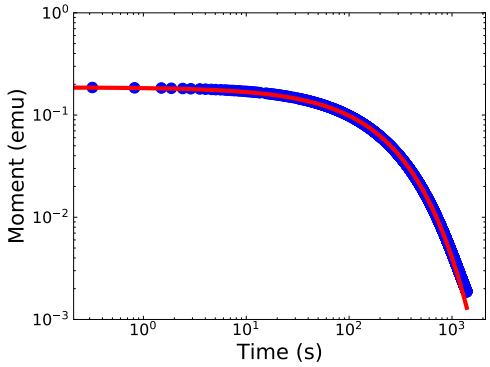

Parameter	Fit result	16 K
M_0 (emu)	0.187	X
β	0.778	F
t_{offset} (s)	3.666×10^{-23}	F
M_{eq} (emu)	0	0
τ^* (s)	177.33	F

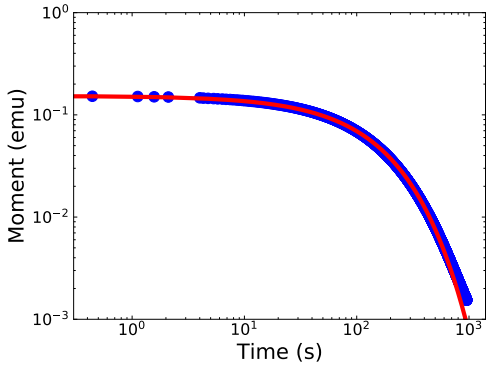

Parameter	Fit result	20 K
M_0 (emu)	0.153	X
β	0.827	F
t_{offset} (s)	9.326×10^{-24}	F
M_{eq} (emu)	0	0
τ^* (s)	132.07	F

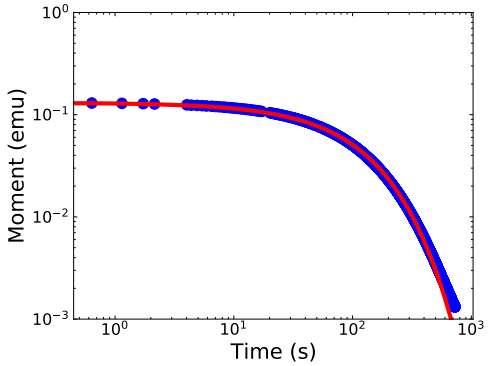

Parameter	Fit result	23 K
M_0 (emu)	0.131	X
β	0.857	F
t_{offset} (s)	2.609×10^{-20}	F
M_{eq} (emu)	0	0
τ^* (s)	106.42	F

Figure S99: DC decay curves fitted for $M > 0.01\ M_0$ to Eq. 11 with M_0 fixed to first measured point at target field, M_{eq} set to the target magnetisation and all other parameters fitted freely.

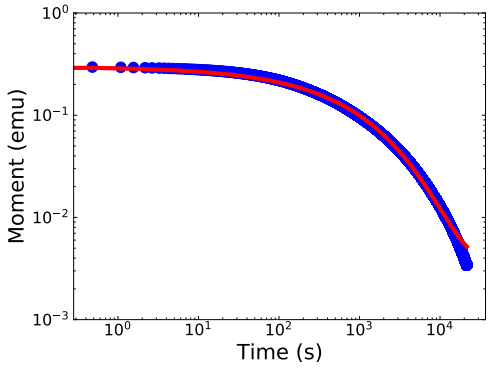

Parameter	Fit result	2 K
M_0 (emu)	0.298	X
β	0.494	F
t_{offset} (s)	0	0
M_{eq} (emu)	3.411×10^{-3}	L
τ^* (s)	790.23	F

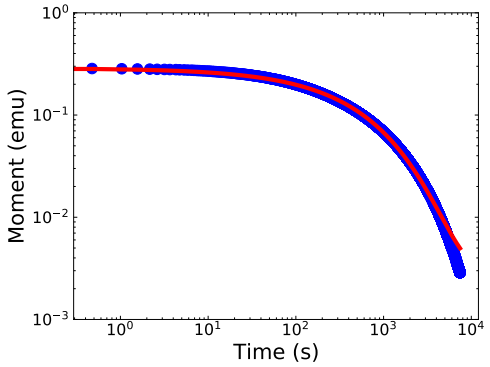

Parameter	Fit result	4 K
M_0 (emu)	0.287	X
β	0.597	F
t_{offset} (s)	0	0
M_{eq} (emu)	2.867×10^{-3}	L
τ^* (s)	518.15	F

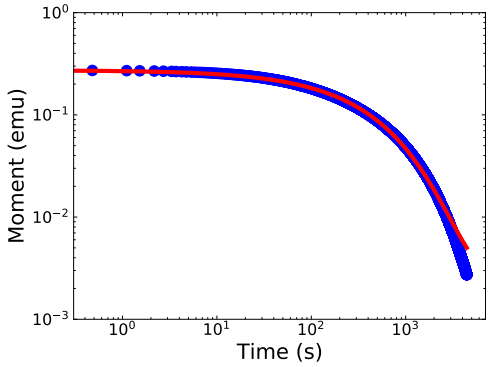

Parameter	Fit result	6 K
M_0 (emu)	0.273	X
β	0.649	F
t_{offset} (s)	0	0
M_{eq} (emu)	2.736×10^{-3}	L
τ^* (s)	398.67	F

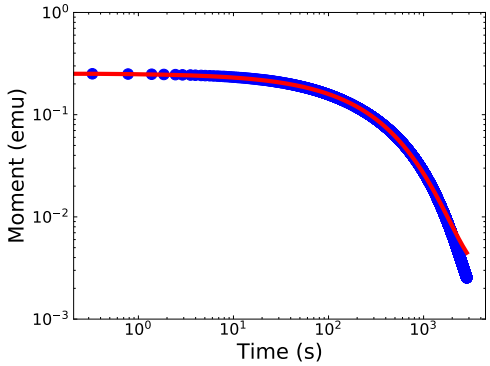

Parameter	Fit result	9 K
M_0 (emu)	0.253	X
β	0.697	F
t_{offset} (s)	0	0
M_{eq} (emu)	2.536×10^{-3}	L
τ^* (s)	294.08	F

Figure S100: DC decay curves fitted for $M > 0.01\ M_0$ to Eq. 11 with M_0 fixed to first measured point at target field, M_{eq} set to the target magnetisation and all other parameters fitted freely.

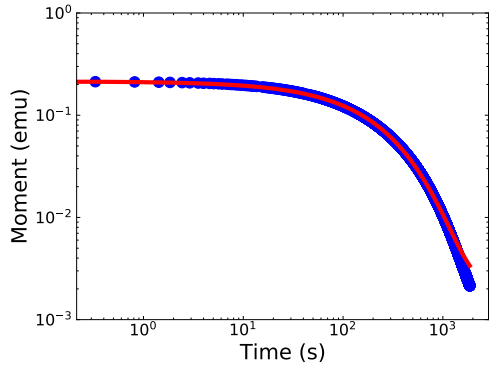

Parameter	Fit result	13 K
M_0 (emu)	0.214	X
β	0.762	F
t_{offset} (s)	0	0
M_{eq} (emu)	2.141×10^{-3}	L
τ^* (s)	216.15	F

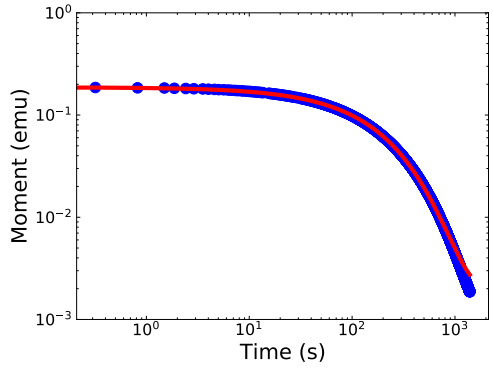

Parameter	Fit result	16 K
M_0 (emu)	0.187	X
β	0.804 m	F
t_{offset} (s)	0	0
M_{eq} (emu)	1.869×10^{-3}	L
τ^* (s)	172.70	F

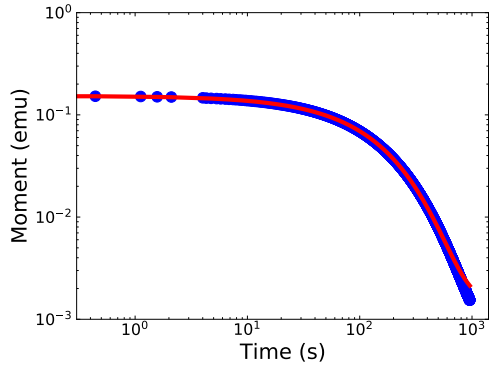

Parameter	Fit result	20 K
M_0 (emu)	0.153	X
β	0.854	F
t_{offset} (s)	0	0
M_{eq} (emu)	1.540×10^{-3}	L
τ^* (s)	128.68	F

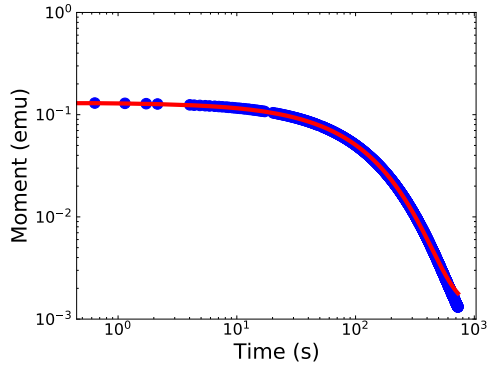

Parameter	Fit result	23 K
M_0 (emu)	0.131	X
β	0.886	F
t_{offset} (s)	0	0
M_{eq} (emu)	1.314×10^{-3}	L
τ^* (s)	103.80	F

Figure S101: DC decay curves fitted for $M > 0.01\ M_0$ to Eq. 11 with M_0 fixed to first measured point at target field, M_{eq} set to the target magnetisation and all other parameters fitted freely.

S2.6 Comparison of relaxation rates

We compare the extracted τ^* from fitting DC decay measurements of $[Dy(Dtp)_2][Al\{OC(CF_3)_3\}_4]$ without the data corresponding to $M < 0.01M_0$ to Eq. 11, and associated τ_{mode}, $\langle\tau\rangle$ and $e^{\langle \ln[\tau]\rangle}$ values to the τ_{debye} obtained from the Waveform measurements.

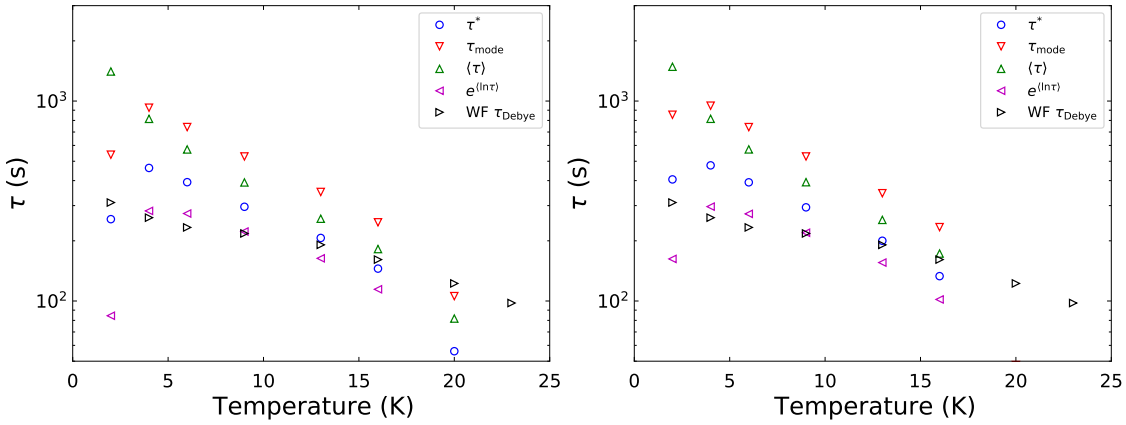

(a) FFFFF (b) FFF0F

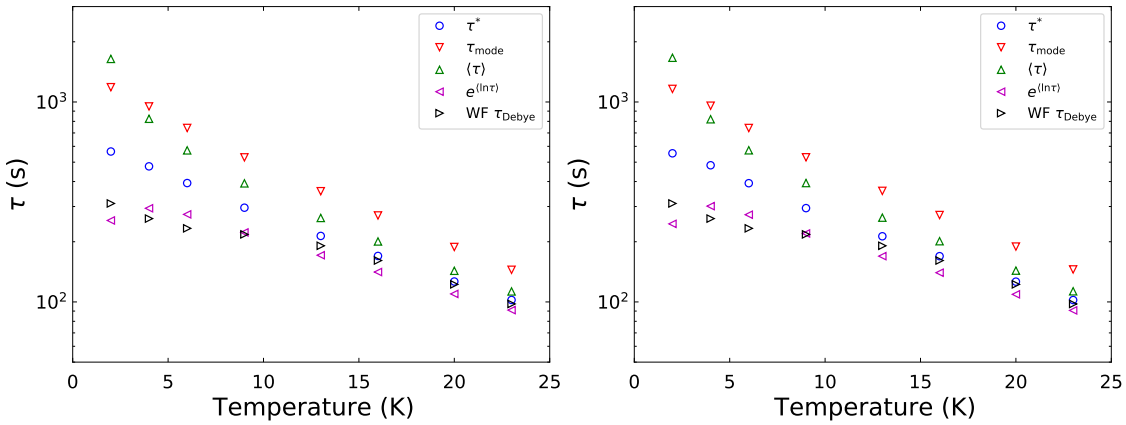

(c) FF0FF (d) FF00F

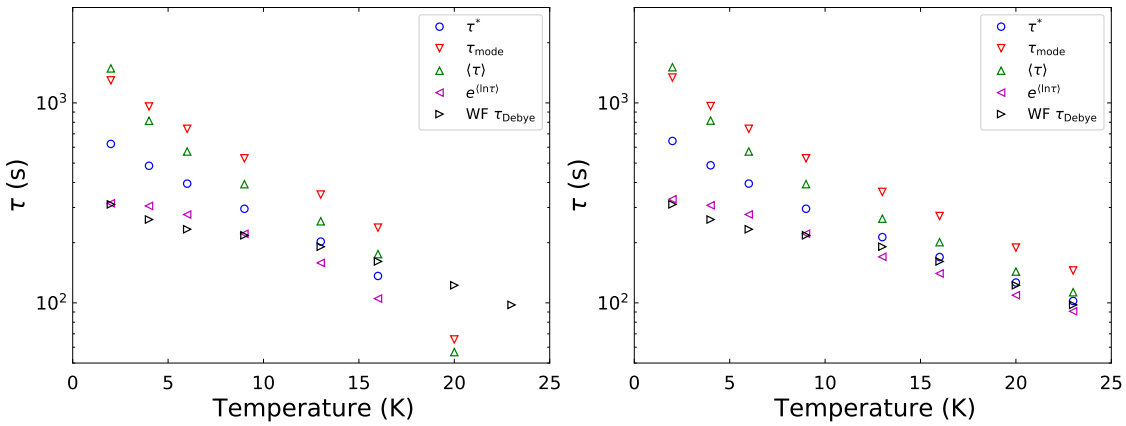

(e) FFFLF (f) FF0LF

Figure S102: Comparison of relaxation rate extracted from waveform measurements of $[Dy(Dtp)_2][Al\{OC(CF_3)_3\}_4]$ to the four metrics of the rate that were obtained from fitting the full DC decay data. M_0 is freely fitted. The sub-figure caption labelling scheme is described in Table S15.

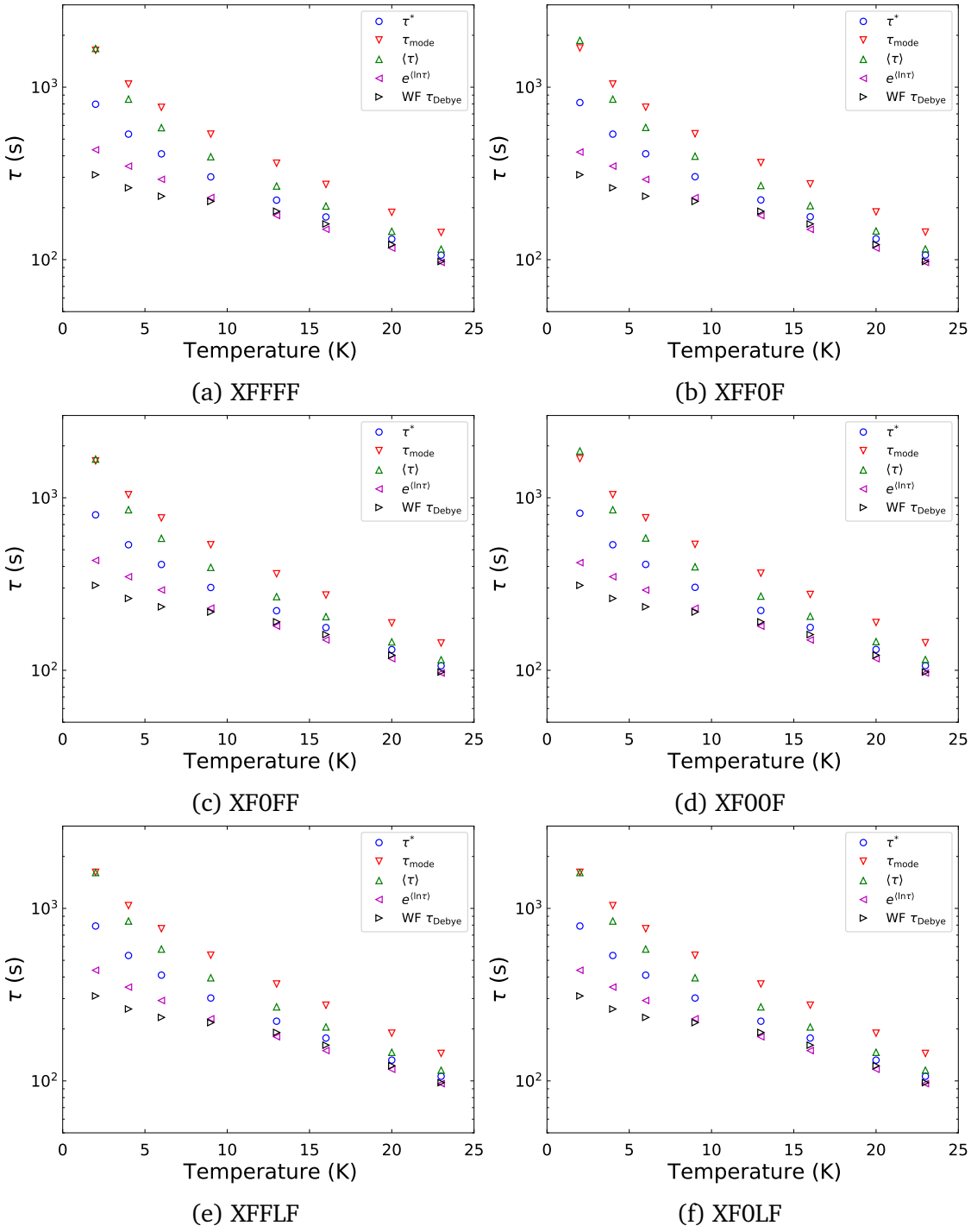

(a) XFFFF (b) XFF0F

(c) XF0FF (d) XF00F

(e) XFFLF (f) XF0LF

Figure S103: Comparison of relaxation rate extracted from waveform measurements of $[Dy(Dtp)_2][Al\{OC(CF_3)_3\}_4]$ to the four metrics of the rate that were obtained from fitting the full DC decay data. M_0 is fixed to the first measured point. The sub-figure labelling scheme is described in Table S15.

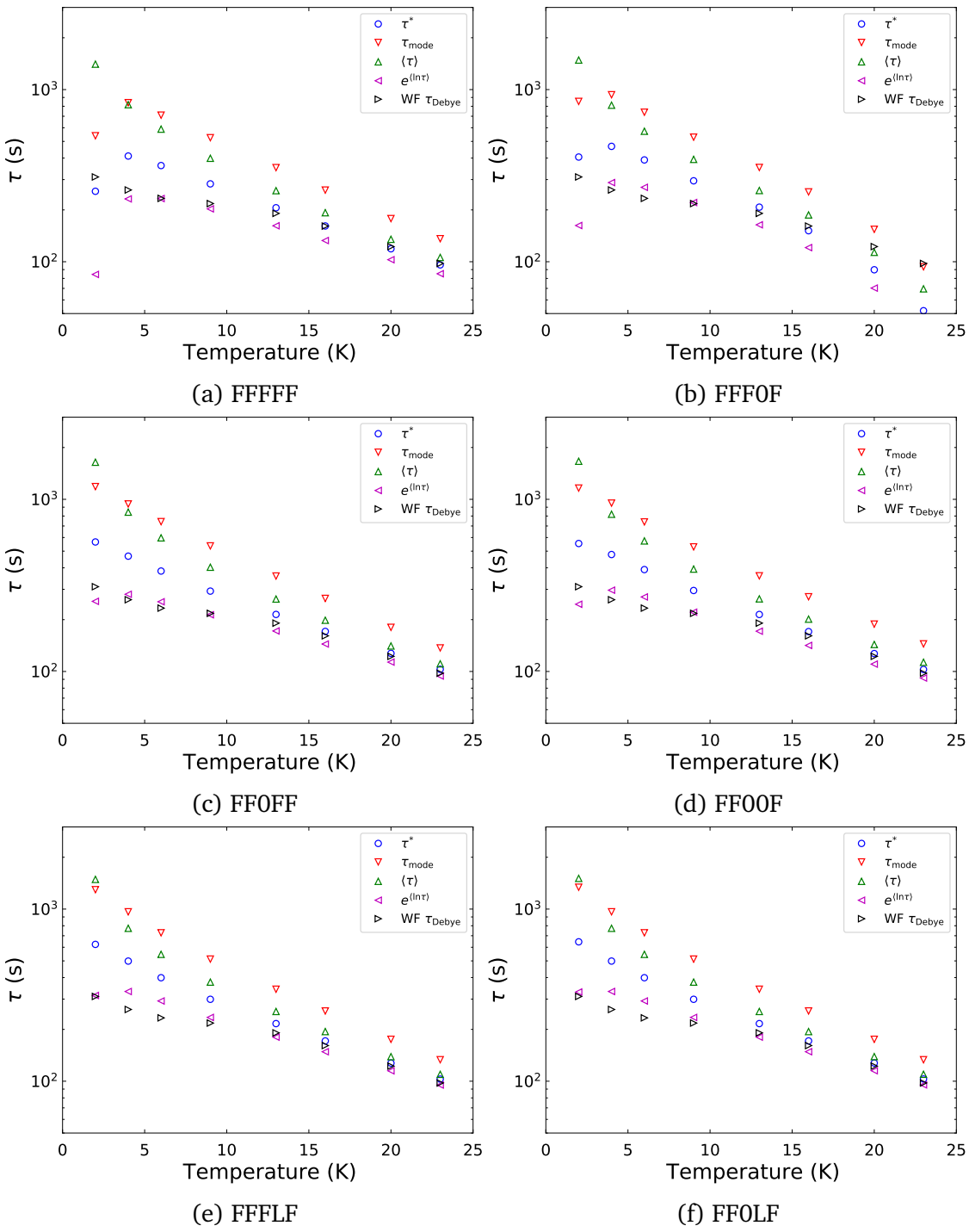

Figure S104: Comparison of relaxation rate extracted from waveform measurements of $[Dy(Dtp)_2][Al\{OC(CF_3)_3\}_4]$ to the four metrics of the rate that were obtained from fitting $> 1\%$ M_0 of the DC decay data. M_0 is freely fitted. The sub-figure labelling scheme is described in Table S15.

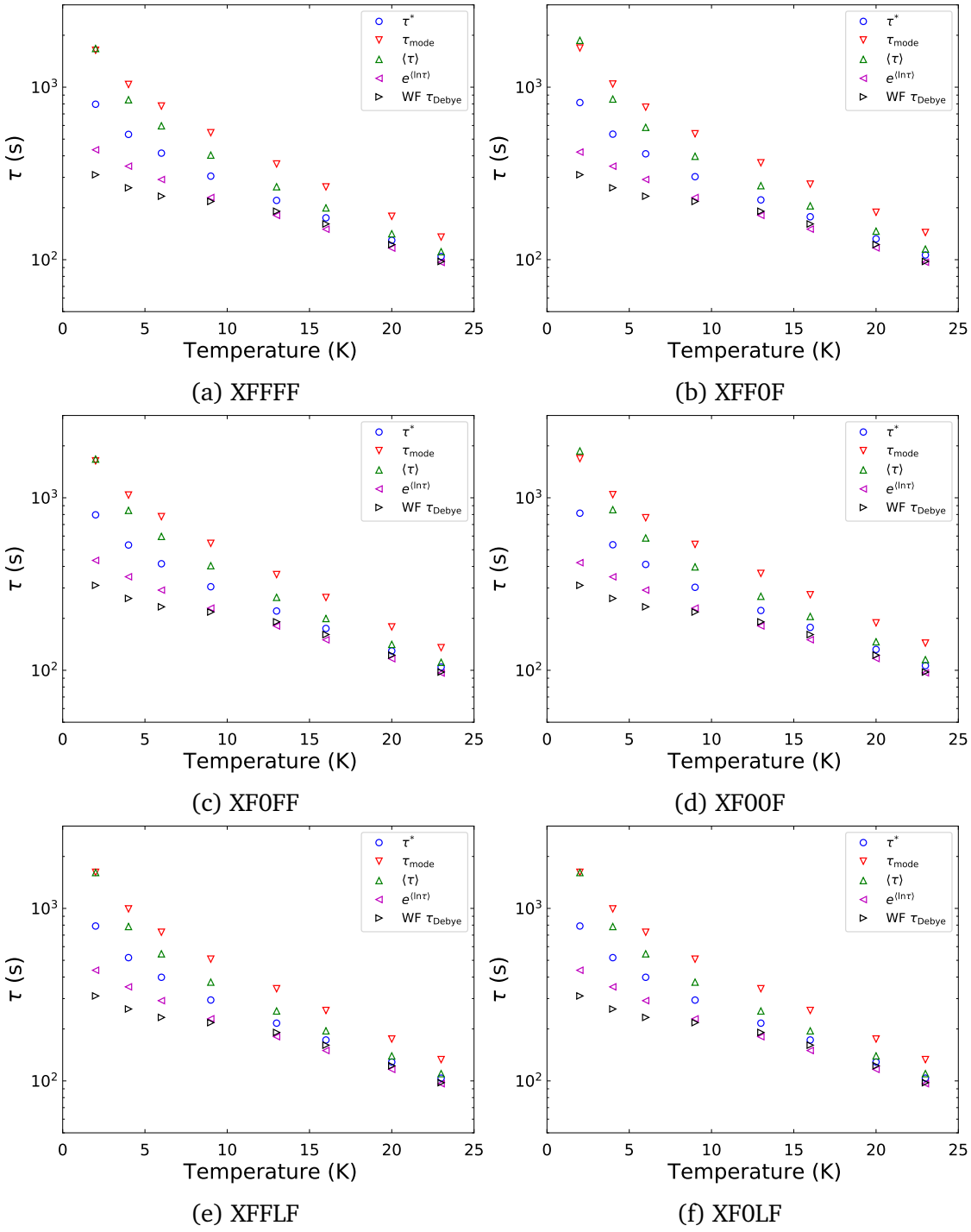

(a) XFFFF (b) XFF0F

(c) XF0FF (d) XF00F

(e) XFFLF (f) XF0LF

Figure S105: Comparison of relaxation rate extracted from waveform measurements of $[Dy(Dtp)_2][Al\{OC(CF_3)_3\}_4]$ to the four metrics of the rate that were obtained from fitting $> 1\%$ M_0 of the DC decay data. M_0 is fixed to the first measured point. The sub-figure labelling scheme is described in Table S15.

S2.7 Fitting of relaxation dynamics

Fitting of relaxation dynamics of $[Dy(Dtp)_2][Al\{OC(CF_3)_3\}_4]$ were performed using the relaxation module in CCFIT2, using the models described in Eq. 10 and Eq. S1.

$$\log\left[\tau^{-1}\right] = \log\left[10^{-A}\mathrm{e}^{-U_{\mathrm{eff}}/T} + 10^{R}T^{n}\right] \tag{S1}$$

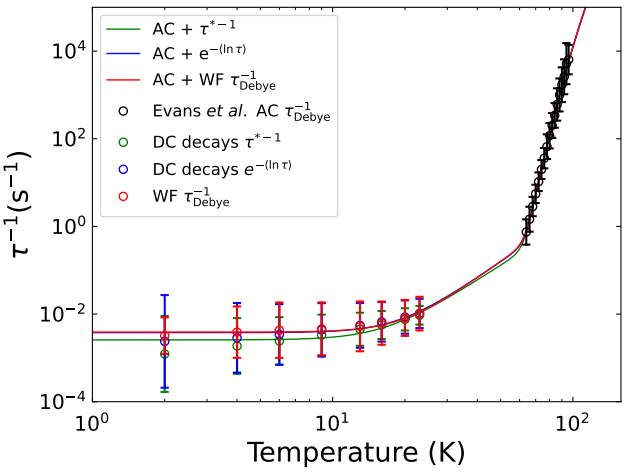

Figure S106: Relaxation rates τ^* (green), $e^{\langle \ln[\tau]\rangle}$ (blue) and τ_{debye} (red) extracted from DC Decay and AC susceptibility[3] measurements of $[Dy(Dtp)_2][Al\{OC(CF_3)_3\}_4]$ fitted to Eq. 10. Parameters are given in Table 2.

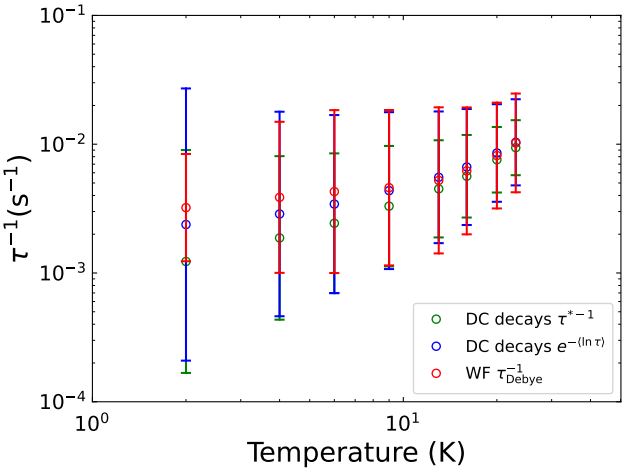

Figure S107: Comparison of τ_{debye} and $e^{\langle \ln[\tau]\rangle}$ extracted from Waveform and DC decay measurements of $[Dy(Dtp)_2][Al\{OC(CF_3)_3\}_4]$ to τ^*.

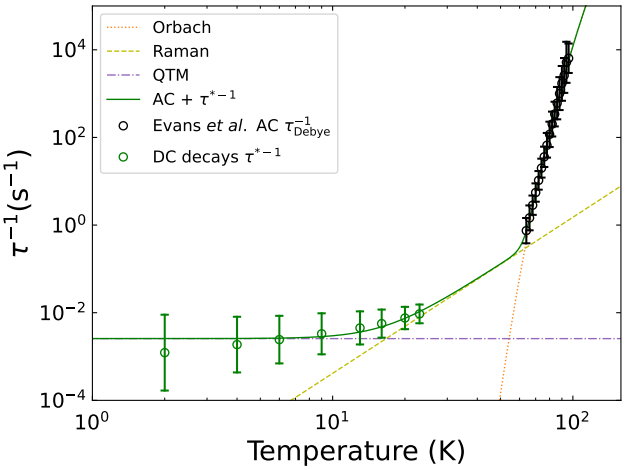

Figure S108: Relaxation rates τ^{*-1} and τ_{debye} extracted from DC decay and AC susceptibility[3] measurements of $[Dy(Dtp)_2][Al\{OC(CF_3)_3\}_4]$ fitted to Eq. 10. Parameters are given in Table 2 (τ^* column).

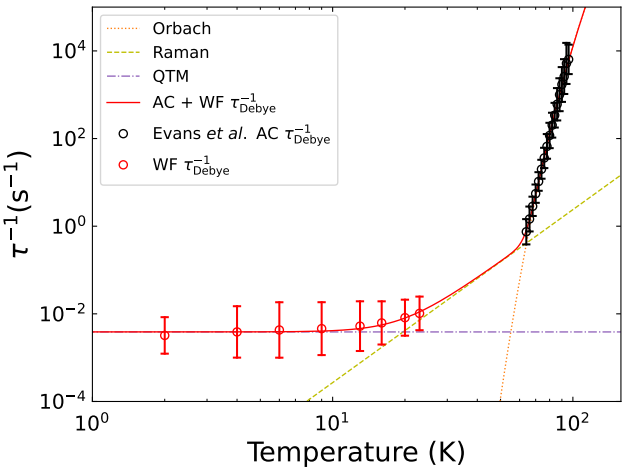

Figure S109: Relaxation rates τ_{debye} extracted from Waveform and AC susceptibility[3] measurements of $[Dy(Dtp)_2][Al\{OC(CF_3)_3\}_4]$ fitted to Eq. 10. Parameters are given in Table 2 (τ_{debye} column).

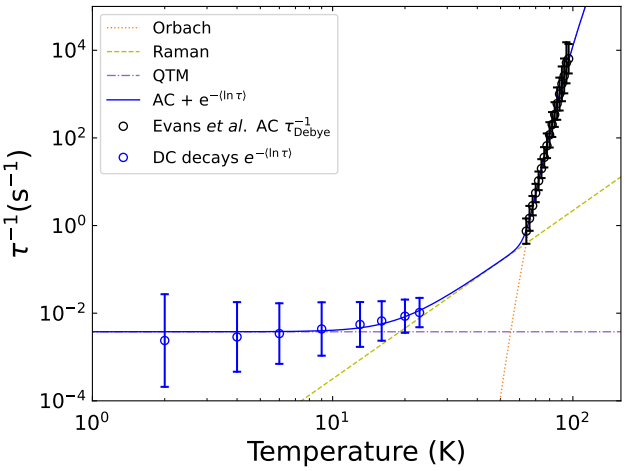

Figure S110: Relaxation rates $e^{\langle \ln[\tau] \rangle}$ and τ_{debye} extracted from DC Decay and AC susceptibility[3] measurements of $[Dy(Dtp)_2][Al\{OC(CF_3)_3\}_4]$ fitted to Eq. 10. Parameters are given in Table 2 ($e^{\langle \ln[\tau] \rangle}$ column).

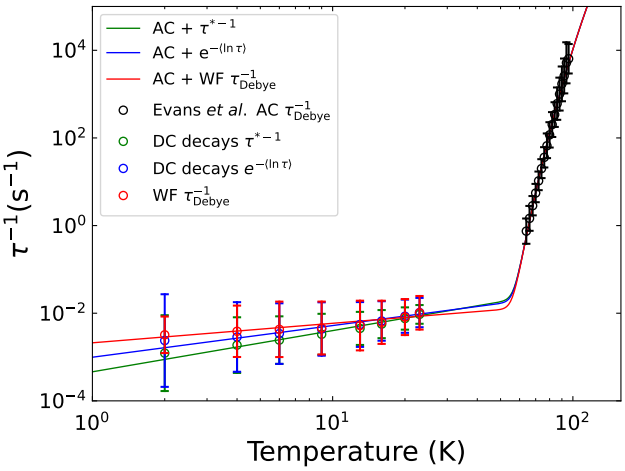

Figure S111: Comparison of τ_{debye} (red), τ^* (green) and $e^{\langle \ln[\tau] \rangle}$ (blue) extracted from Waveform and DC decay measurements of $[Dy(Dtp)_2][Al\{OC(CF_3)_3\}_4]$. The data was fitted to Eq. S1 including the relaxation rates obtained from AC susceptibility measurements of $[Dy(Dtp)_2][Al\{OC(CF_3)_3\}_4]$.[3] Parameters are given in Table S16.

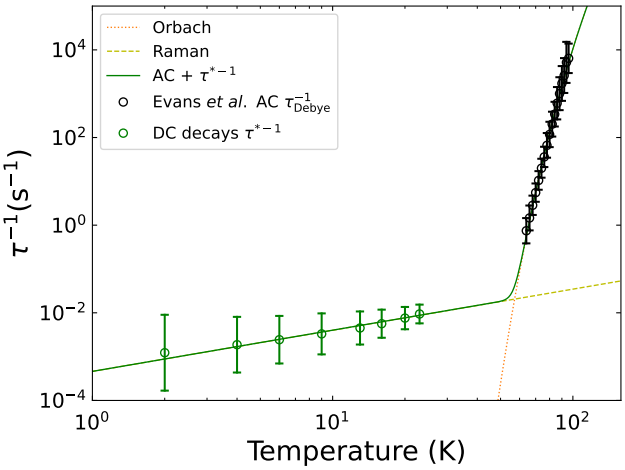

Figure S112: Relaxation rates τ^{*-1} and τ_{debye} extracted from DC decay and AC susceptibility[3] measurements of $[Dy(Dtp)_2][Al\{OC(CF_3)_3\}_4]$ fitted to Eq. S1. Parameters are given in Table S16 (τ^* column).

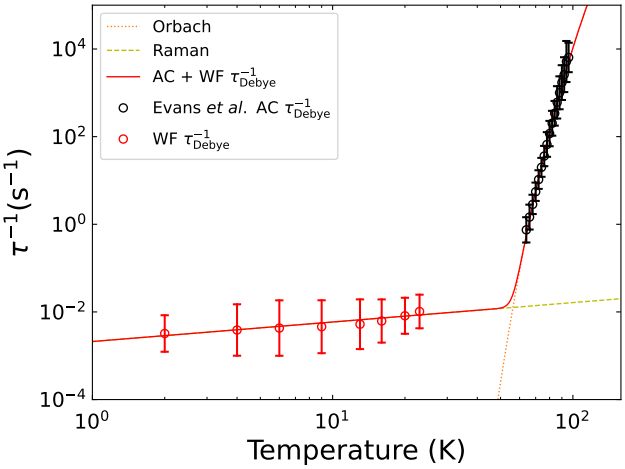

Figure S113: Relaxation rates τ_{debye} extracted from Waveform and AC susceptibility[3] measurements of $[Dy(Dtp)_2][Al\{OC(CF_3)_3\}_4]$ fitted to Eq. S1. Parameters are given in Table S16 (τ_{debye} column).

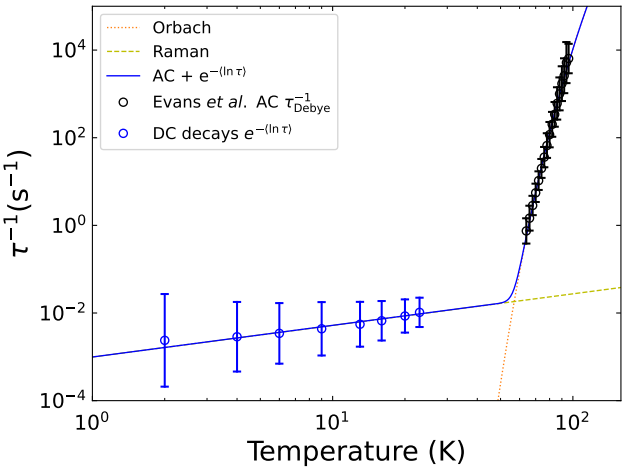

Figure S114: Relaxation rates $e^{\langle \ln[\tau] \rangle}$ and τ_{debye} extracted from DC Decay and AC susceptibility[3] measurements of $[Dy(Dtp)_2][Al\{OC(CF_3)_3\}_4]$ fitted to Eq. S1. Parameters are given in Table S16 ($e^{\langle \ln[\tau] \rangle}$ column).

Table S16: Parameters obtained from fitting relaxation rates obtained from AC susceptibility measurements[3] along with those extracted from Waveform and DC decay measurements performed here to Eq. S1. The resultant fits are shown graphically in Fig. S111.

	DC decays		Waveform	Evans *et al.* Parameters[3]
Parameter	τ^*	$e^{\langle \ln[\tau] \rangle}$	τ_{debye}	
U_{eff} (K)	1758(22)	1758(21)	1756(23)	1761(19)
$A\left(\tau_0 = 10^A/\text{s}\right)$	-11.66(0.13)	-11.66(0.13)	-11.65(0.13)	-11.67(0.11)
$R\left(C = 10^R/\text{s}^{-1}\text{K}^{-n}\right)$	-3.34(0.13)	-3.00(0.16)	-2.675(0.098)	-3.460(0.058)
n	0.94(0.11)	0.72(0.14)	0.444(0.093)	1.096(0.058)

S3 Reanalysis of reported data

S3.1 Standard deviations

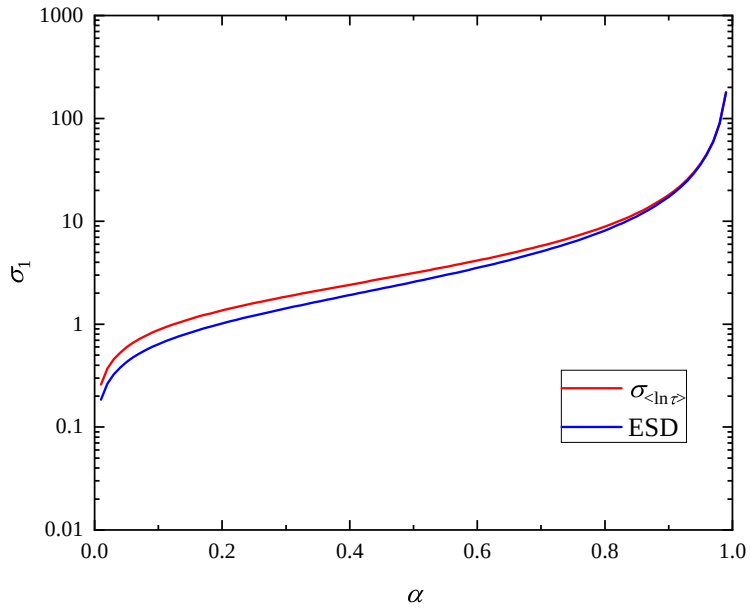

Figure S115: Comparison of the standard deviation of the Generalised Debye model $\sigma_{\langle \ln \tau \rangle}$ [4] to the ESD calculated by Reta and Chilton (ESD)[5] as a function of α. There is good agreement over the whole range of α.

S3.2 $[Dy(C_5{}^iPr_5)(C_5Me_5)][B(C_6F_5)_4]$

We take the raw DC decay curve recorded in zero field at 2 K of $[Dy(C_5{}^iPr_5)(C_5Me_5)][B(C_6F_5)_4]$ as reported by Guo *et al.*[6] The original fit (Fig. S116 and Fig S117 - blue) using Eq. 11 was obtained using the method where $t_{offset} = 0$ and all other parameters were freely fitted. We refitted the DC decay curve using our measurement protocol; M_0 fixed to the value of the first measured point, $t_{offset} = 0$ and M_{eq} fixed to target (in this case $M_{eq} = 0$). τ^* and β are left to fit freely. The results of the new fit are shown in green in Fig. S116 and Fig. S117. The new fit encapsulates much more of the early decay compared to that performed by Guo *et al.*, but has less agreement around the middle before converging at long timescales. The parameters extracted from the new fit show an increase of $\approx 16\%$ in τ^* and $\approx 5\%$ in β compared with Guo *et al.*, significantly altering $e^{\langle \ln[\tau] \rangle}$.

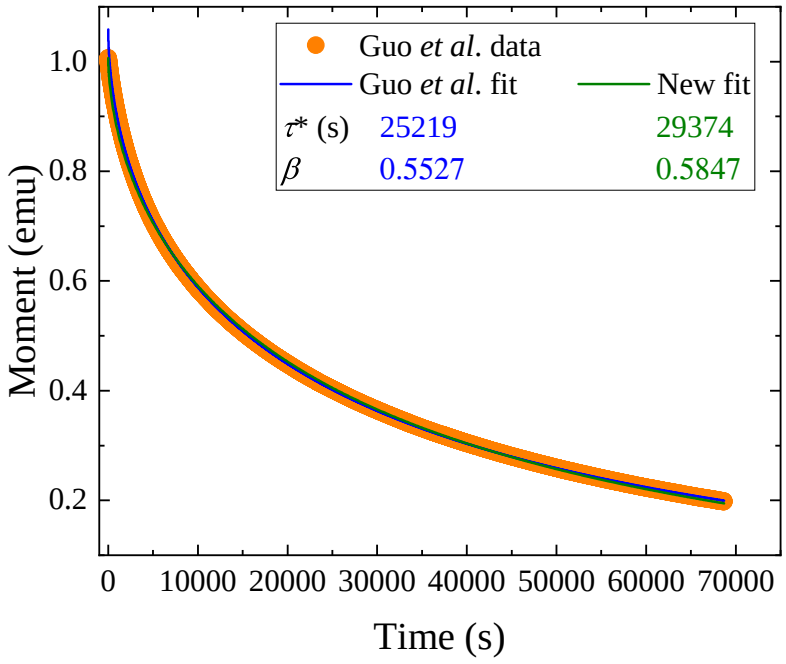

Figure S116: Plot of the 2 K decay curve of $[Dy(C_5{}^iPr_5)(C_5Me_5)][B(C_6F_5)_4]$ on a linear scale and overlaid by the fit to Eq. 11 performed by Guo *et al.* (blue) with $t_{offset} = 0$ and all other parameters freely fitted.[6] We perform a fit fixing M_0 to the first measured data point, M_{eq} fixed to target (in this case zero), $t_{offset} = 0$, with τ^* and β freely fitted.

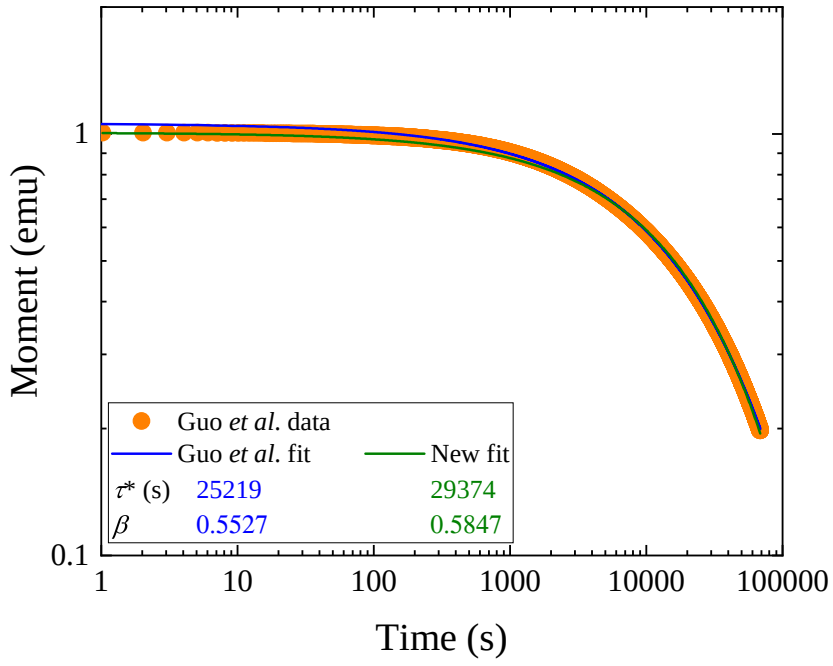

Figure S117: Plot of the 2 K decay curve of $[Dy(C_5{}^iPr_5)(C_5Me_5)][B(C_6F_5)_4]$ on a logarithmic scale and overlaid by the fit to Eq. 11 performed by Guo *et al.* (blue) with $t_{offset} = 0$ and all other parameters freely fitted.[6] We perform a fit fixing M_0 to the first measured data point, M_{eq} fixed to target (in this case zero), $t_{offset} = 0$, with τ^* and β freely fitted.

Notes and references

(1) Spree, L.; Liu, F.; Neu, V.; Rosenkranz, M.; Velkos, G.; Wang, Y.; Schiemenz, S.; Dreiser, J.; Gargiani, P.; Valvidares, M.; Chen, C. H.; Büchner, B.; Avdoshenko, S. M.; Popov, A. A. Robust Single Molecule Magnet Monolayers on Graphene and Graphite with Magnetic Hysteresis up to 28 K. *Advanced Functional Materials* **2021**, *31*, 2105516.

(2) Ding, Y.-S.; Blackmore, W. J. A.; Zhai, Y.-Q.; Giansiracusa, M. J.; Reta, D.; Vitorica-Yrezabal, I.; Winpenny, R. E. P.; Chilton, N. F.; Zheng, Y.-Z. Studies of the Temperature Dependence of the Structure and Magnetism of a Hexagonal-Bipyramidal Dysprosium(III) Single-Molecule Magnet. *Inorganic Chemistry* **2022**, *61*, 227–235.

(3) Evans, P.; Reta, D.; Whitehead, G. F.; Chilton, N. F.; Mills, D. P. Bis-Monophospholyl Dysprosium Cation Showing Magnetic Hysteresis at 48 K. *Journal of the American Chemical Society* **2019**, *141*, 19935–19940.

(4) Zorn, R. Logarithmic moments of relaxation time distributions. *The Journal of Chemical Physics* **2002**, *116*, 3204–3209.

(5) Reta, D.; Chilton, N. F. Uncertainty estimates for magnetic relaxation times and magnetic relaxation parameters. *Physical Chemistry Chemical Physics* **2019**, *21*, 23567–23575.

(6) Guo, F.-S.; Day, B. M.; Chen, Y.-C.; Tong, M.-L.; Mansikkamäki, A.; Layfield, R. A. Magnetic hysteresis up to 80 kelvin in a dysprosium metallocene single-molecule magnet. *Science* **2018**, *362*, 1400–1403.